Doctoral Dissertation
Doctoral Program in Energy Engineering (32nd Cycle)

Flexible calculation approaches to support the European CO₂ emissions regulatory scheme for road vehicles

Alessandro Tansini
* * * * * *

Supervisors
Prof. Federico Millo, Supervisor
Georgios Fontaras PhD, Co-Supervisor
Biagio Ciuffo PhD, Co-Supervisor

Doctoral Examination Committee:
Gilles Corde PhD, IFP Energies nouvelles
Dimitrios Tsokolis PhD, Toyota Motor Europe
Prof. Angelo Onorati, Politecnico di Milano
Prof. Ezio Spessa, Politecnico di Torino
Prof. Stefano d'Ambrosio, Politecnico di Torino

Politecnico di Torino
March 18, 2020

I hereby declare that, the contents and organisation of this dissertation constitute my own original work and does not compromise in any way the rights of third parties, including those relating to the security of personal data.
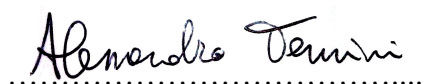
....

Alessandro Tansini

Turin, March 18, 2020

Summary

Climate change is a concern, and the actions undertaken in Europe for the reduction of the carbon footprint are growing interest towards the evaluation of the CO_2 emissions from human activities. Transport sector, which accounts for approximately 30% of the total CO_2 emissions in Europe, is the only sector that did not reduce the carbon footprint with respect to 1990 level [1]. The activities presented in this thesis were carried out in collaboration with the Sustainable Transport Unit (STU) of the European Commission's Joint Research Centre (JRC). The objective was the development and validation of calculation tools to quantify the CO_2 emissions from road vehicles, both Light-Duty Vehicles (LDVs) and Heavy-Duty Vehicles (HDVs), to support the actions undertaken by the European Commission in the path to a more sustainable transportation system. Calculation tools are needed for multiple reasons. The measurement-based determination of the CO_2 emissions is not always the most appropriate and feasible solution, either for technical reasons or for other limitations making it not sustainable under the economic or regulatory point of view. Additionally, when a virtual environment is used to perform assessments, more flexibility is provided concerning the different conditions to be analysed and the aspects that can be quantified; another benefit is the full repeatability of the assessment due to the complete control over the initial conditions. In Europe, calculation tools take part in the certification process of CO_2 emissions from road vehicles. Additionally, calculation tools are used to support studies that might have a direct impact on the developments on Europeans regulations. The Vehicle Energy Consumption calculation Tool (VECTO) was adopted in Europe to quantify the CO_2 emissions from HDVs (only trucks currently, buses and coaches to be included in the future). The CO_2 Model for PAssenger and commercial vehicles Simulation (CO2MPAS) was adopted to handle the so-called correlation process, calculating the NEDC-equivalent CO_2 emissions for all the

LDVs certified in Europe in the transition period between the NEDC and WLTP procedures (2017-2020). These two calculation tools constituted the foundations of the research activities of the PhD Programme, on top of which further assessments, validations and developments were carried out. Additionally, other CO_2 emissions evaluation approaches were derived based the two calculation tools. The first activity regarded extension of the VECTO-based certification procedure. Following the adoption of Commission Regulation (EU) 2017/2400 [2] regarding the CO_2 determination methodology for trucks, DG CLIMA and DG GROW requested to launch a test-campaign to investigate the validity, accuracy and plausibility of the application of the methodology to buses and coaches. Experiments were conducted on one interurban bus and one coach, both on the chassis dynamometer and on the road. The activity was performed in two phases, the experimental phase and the simulation phase. The experimental phase was further divided into multiple phases: chassis dynamometer, on-road and proving ground testing. Vehicle air drag physical determination through experiments, and the use of the specific calculation tool (VECTO Air Drag), were the aspects for which this PhD Programme gave substantial contribution. Air resistance, which is one of the aspects with higher impact on fuel consumption for HDVs, is evaluated through the constant speed test as described in Commission Regulation (EU) 2017/2400 and is mandatory to produce VECTO input data. The constant speed test is performed on a proving ground and it requires specific instruments, atmospheric conditions and careful execution. The data collected during the test is processed through VECTO Air Drag, which performs checks on input data quality and completeness; finally, it calculates the vehicle drag area corrected for side wind. Despite the technical issues encountered during the experiment, that required some data manipulation and the relaxation of some of the calculation tolerances, the results matched very closely the suggested values from the OEMs. Therefore, the study confirmed the accuracy and applicability of the methodology for air drag evaluation to buses and coaches.

During year 2017, DG CLIMA asked the STU to create a baseline of CO_2 emissions for the regulated vehicles of the HDVs fleet (groups 4, 5, 9 and 10). There are two reasons behind this request: a picture of the HDVs fleet fuel efficiency was still missing, and additionally the Commission wanted to develop a methodology to assess the quality of the input data and its impact on VECTO calculated CO_2 emissions for possible normalisation. The activity provided valuable input for drafting the regulation on HDVs CO_2 emissions standards (EU 2019/1242).

For this purpose, the STU was provided with VECTO simulation data of vehicles registered in the year 2016. The exercise produced a database of about 1.7 million rows and 120 columns. The activity included four main phases:

1. Database preparation
2. Statistical market analysis
3. Input data quality analysis and components losses characterisation
4. Creation of the HDVs CO_2 emissions baseline

The main outcome of the activity consists of the distributions of CO_2 emissions per vehicle group and cycle-loading combination. Furthermore, the approach developed for obtaining the fleet CO_2 emissions, normalised for input data quality, constitutes a solution for controlling and possibly normalise the data obtained from manufacturers through the monitoring and reporting scheme. Based on this approach, a new fleet normalisation approach is being developed by the STU for the creation of the baseline for year 2020 that will be used to check CO_2 emissions compliance in the years 2025 and 2030.

In addition to the normalisation approach, other two CO_2 emissions calculation methodologies were developed that can be used for verification purposes. The first one consists of an input-data generation model (components losses maps and engine fuel consumption map) that produces fleet-representative cases for VECTO simulation. The second one rather relies on correlation formulas, derived from VECTO data, to calculate directly the overall energy consumption with no use of simulation.

The activities carried out in the framework of LDVs CO_2 emissions regarded Hybrid Electric Vehicles (HEVs) exclusively. Due to the uptake of electrified vehicle powertrains, CO_2MPAS needed to be extended in order to capture the operation and the associated fuel savings. For this reason, a generic simulation strategy needed to be developed and implemented into the model of CO_2MPAS. A generic simulation strategy for HEVs was also needed for other applications, e.g. traffic simulations or studies (impact assessments, creation of scenarios, etc.).

To increase the level of understanding and create a database for validation, several vehicles with different hybrid powertrain architectures (serial, parallel and power-split) and electrification levels (mild, full, plug-in and range extender) were tested. The tests were carried out at vehicle-level, without tearing down the vehicle to test the components for their characterisation. A combination of vehicle signal logging and physical measurements was adopted to obtain a detailed picture of the powertrain operation and reconstruct the energy flow. Lastly, a generic simulation strategy was developed, consisting of three layers: Supervisor, ICE Manager and Optimiser. The Supervisor has the ability to impose specific operating conditions to prioritise the driving dynamics or the self-sustainment of the system (e.g. restoring the battery state of charge when low). The ICE Manager deals with the physical limitations of the internal combustion engine (ICE), defines some

boundaries for the stop&start operation and handles the warm-up. The Optimiser finds the optimal solution within the set of solutions inherited from the upper levels according to the Equivalent Consumption Minimisation Strategy (ECMS) principle. A modelling approach for a generic electrical power system (EPS), which includes the batteries, the DC/DC converter, the electric loads and the electric machines, was also developed. The governing equations for all the hybrid powertrain architectures were obtained. The strategy was first implemented in the hybrid controller (hycon) and, at a later stage, into CO_2MPAS model. Hycon is a simple tool that was developed to test the performances of the simulation strategy on parallel HEVs; this tool requires that specific input data of the vehicle considered is provided. The results obtained with hycon demonstrated that the simulation strategy is appropriate for obtaining representative values for the instantaneous operation and the overall vehicle energy efficiency. A similar simulation strategy was then implemented into CO_2MPAS to cover all HEVs architectures and electrification levels. The implementation and validation process is not yet completed due to time restrictions, but a working version was already developed and released in October 2019 with CO_2MPAS v4.1.10. It requires a comparable amount of data to that needed for the correlation procedure from the certification of LDVs and almost no detailed input data. Additionally, it is able to self-calibrate the ICE fuel consumption map as for conventional vehicles, although this comes with a lower accuracy with respects to conventional vehicles due to the more challenging calibration process (less calibration points in a restricted area of the ICE map). Currently, CO_2MPAS hybrids is able to cover the most relevant powertrain architectures, although the accuracy needs to be improved; to this aim, the detailed experimental data collected will allow to identify the aspects to be improved with respects to energy consumption for the further development of the model.

The outcomes of this PhD programme are a set of experimental observations, analyses and calculation approaches constituting valuable tools for the evaluation of the CO_2 emissions from road transport.

Acknowledgment

Dedicated to my beloved parents

for their inestimable support.

Contents

List of Tables

List of Figures

xvi

Acronyms

AC	Alternate Current
Ah	Ampere hour
BMEP	Brake Mean Effective Pressure
BMS	Battery Management System
CAN	Controller Area Network
CD	Charge Depleting
CdA	Vehicle drag area
CH	Charging state
CO$_2$MPAS	CO$_2$ Model for PAssenger and commercial vehicles Simulation
CS	Charge Sustaining
CT	Clutch / Torque converter
DAQ	Data Acquisition System
DC	Direct Current
DG	Directorate-General
DQ	Data Quality
EA	Electric Assist state
EC	Energy Consumption
ECBM	Equivalent Circuit Battery Model
ECMS	Equivalent Consumption Minimisation Strategy
EE	Electrical Energy
EM	Electric Machine
EOBD	European On-Board Diagnostics
EP	Electric Propulsion state
EPS	Electric Power System
FC	Fuel Consumption
FCMC	Fuel Consumption Mapping Cycle
FD	Final Drive
FuMEP	Fuel Mean Effective Pressure
GBX	Gearbox
GHG	Greenhouse Gas
HDT	Heavy-Duty Truck
HDV	Heavy-Duty Vehicle
HEV	Hybrid Electric Vehicle
HV	High Voltage
HY	Hybrid state
ICE	Internal Combustion Engine
ISC	In-Service Conformity

JRC	European Commission's Joint Research Centre
JRC-STU	JRC's Sustainable Transport Unit
LCV	Light Commercial Vehicle
LD	Light-Duty
LDV	Light-Duty Vehicle
LH	Long Haul
LHV	Low Heating Value
LV	Low Voltage
MPW	Mileage Payload Weight factor
NEDC	New European Driving Cycle
NOVC	Not Off-Vehicle Charging
OBD	On-Board Diagnostics
OCV	Open Circuit Voltage
OEM	Original Equipment Manufacturer
OVC	Off-Vehicle Charging
PID	Parameter ID
PLA	Planetary Gearset
PLDV	Passenger Light-Duty Vehicle
PS	Planetary Side
RB	Regenerative Braking state
RD	Regional Delivery
RDE	Real Driving Emissions
REEC	Relative Electric Energy Change
REESS	Rechargeable Electric Energy Storage System
REx	Range Extender
RR	Rolling Resistance
RRC	Rolling Resistance Coefficient
SB	Service Battery
SS	Stop & Start
TB	Traction Battery
TR	Transmission
UD	Urban Delivery
UF	Utility Factor
VECTO	Vehicle Energy Consumption calculation TOol
VELA	Vehicle Emissions Laboratories
Wh	Watt hour
WLTC	Worldwide harmonized Light vehicles Test Cycle
WLTP	Worldwide harmonised Light vehicle Test Procedure
ZLEV	Zero- and Low-Emissions Vehicle

Chapter 1

1   Introduction

The PhD programme presented in this work is the result of the collaboration agreement n. 33195 between Politecnico di Torino and the Joint Research Centre (JRC), the European Commission's Science and Knowledge service [3]. The research activities were carried out in the Sustainable Transport Unit of the JRC (JRC-STU), a division of the science centre appointed to perform scientific investigations on sustainable transport: pollutants and greenhouse gas (GHG) emissions, advanced powertrain systems and electric mobility, electromagnetic compatibility, traffic simulations, connected and automated vehicles, safety, alternative fuels and others. More specifically, the activities performed fall under the topic of the determination of road vehicles CO_2 emissions (certified and real-world use). The STU comprises the Vehicle Emissions Laboratories (VELAs), fully equipped facilities to support the previously mentioned activities with the collection of experimental data. Such laboratories allow for the determination of full-vehicle or engine-only GHG and pollutants emissions, and the characterisation of specific aspects of vehicle operation through dedicated measurements. In addition, the STU also makes use of data from third parties and calculation tools to find scientific evidence for the investigated topics. In this thesis, both the test facilities and the calculation tools were exploited to get a better understanding of the road transport CO_2 emissions and support the European Commission in the actions undertaken to quantify and curb them.

1.1 Research objectives

The role of the JRC is to support EU policies with independent scientific evidence throughout the whole policy cycle by making sense of knowledge and develop innovative tools for the policymakers. These activities are commissioned to the JRC by the Directorates-General (DGs), the policy departments of the European Commission, responsible for the implementation and management of EU policies, law, and funding programmes. The research carried out within this PhD programme mainly focused on the development of calculation approaches and tools to support DG for Climate Action (DG Clima) in the regulatory schemes for the reduction of road vehicles CO_2 emissions. The support covered the following sectors:

- CO_2 emissions from Heavy-Duty Vehicles (HDVs)
  - Buses and Coaches
  - Heavy-Duty Trucks (HDTs)
- CO_2 emissions from Light-Duty Vehicles (LDVs)
  - Passenger Light-Duty Vehicles (PLDVs)
  - Light Commercial Vehicles (LCVs)

For both sectors (HDVs and LDVs), the European Commission has worked intensively to put into force regulations defining the best applicable way to determine the tailpipe CO_2 emissions with the aim of setting emissions limits.

The first regulation creating the legislative foundation for the HDVs CO_2 emissions scheme was set into force in 2017 [2]; the entry into force of the CO_2 emissions limits finally happened in 2019 for HDTs exclusively [4]. Throughout this period, the JRC-STU has supported DG Clima in different tasks: the definition of the first HDTs CO_2 emissions baseline, the development of approaches to ensure the representativeness of the certified CO_2 emissions and the assessment of the applicability of the framework to the case of Buses and Coaches.

CO_2 emissions targets for LDVs were already introduced in 2009, 2011 and 2014 [5, 6, 7]; therefore, the activities performed for LDVs are of different nature as other needs had to be satisfied. Specifically, the European Commission wanted to develop a tool for the determination of CO_2 emissions from Light-Duty (LD) Hybrid Electric Vehicles (HEVs). The JRC responded to this need with the development of a simulation strategy for HEVs that was finally implemented into the tool (CO_2MPAS) used for the certification of CO_2 emissions from LDVs.

The need shared by the two different topics (the HDVs and the LDVs) is the development of flexible calculation approaches satisfying the following requirements:

- has a relatively low estimation error on average (±3-7 % bias, depending on the case)
- minimises the variability of the error
- the overall result provides a representative picture of the reference
- uses as few input parameters as possible
- problem modelling is neither over- nor under-detailed
- could potentially be applied to multiple tools or purposes.

Therefore, the work carried out for this PhD programme and presented in this thesis addressed, to the extent possible, the needs outlined in this section.

1.2 Tools used

The activities performed for this PhD required the adoption of a variety of tools and techniques. Most of the data management, analyses, calculation tools development and reporting was carried out through Python programming and language interpreters, a choice justified by the many advantages associated with Python. The Python interpreter is available free of charge for all major platforms, can be freely distributed, is able to interact with most of the other languages and provides an extensive standard library which can significantly reduce the amount of code to be written. Furthermore, is designed in order to have high code readability and its development is driven by a community which continually works on improvements and extensions of its capabilities. For the particular case of the projects related to the European Commission, it ensures that the code can be read and used by anyone, therefore, providing total transparency. The Python libraries mostly used were *pandas*, for data management and analysis, *numpy* and *scipy*, for scientific computing, and others for data visualisation (*matplotlib*, *seaborn*, *plotly*). *Jupyter Notebook*, an interactive Python environment combining code and rich text elements (paragraphs, equations, figures, links, etc.), and *PyCharm*, a Python environment for professional developers, were used for Python scripting and programming, frequently in combination with *Git* (a software version control system) and *GitHub* (hosting platform for collaboration and version control), for keeping track of code changes and facilitate team work. Spreadsheets applications were also extensively used.

Due to the diversity of the activities performed within this PhD programmes, the methodologies adopted are detailed in the dedicated sections of the activities.

1.3 Publications

A list of the works selected for publication is here reported:

- Pavlovic J., Tansini A., Fontaras G., Ciuffo B. et al.
  "The Impact of WLTP on the Official Fuel Consumption and Electric Range of Plug-in Hybrid Electric Vehicles in Europe"
  SAE Technical Paper 2017-24-0133, 2017

- Zacharof N., Fontaras G., Ciuffo B., Tansini A., Grigoratos T. et al.
  "CO_2 emissions of the European Heavy Duty Truck Fleet, a Preliminary Analysis of the Expected Performance"
  22nd int. Transport and Air Pollution conference TAP 2017, Zurich, Switzerland, 2017

- Grigoratos T., Fontaras G., Tansini A., Giechaskiel B., Savvidis D. et al.
  "Assessment of the Measurement Methodology for CO_2 Emissions from Heavy Duty Buses and Coaches", JRC Technical Report, DOI 10.2760/74053, 2018

- Nitzsche G., Edwards S., White E., De Gennaro M., Tansini A. et al.
  "ECOCHAMPS – Project Targets, their Tracking and the Evaluation of the Demonstrator Vehicles", TRA 2018 conference, Vienna, Austria, 2018

- Tansini A., Zacharof N., Prado I. and Fontaras G.
  "Analysis of VECTO data for Heavy-Duty Vehicles (HDV) CO_2 emission targets", JRC Science for policy report, DOI 10.2760/551250, JRC Publications Repository, 2018

- Suarez-Bertoa R., Pavlovic J., Trentadue G., Otura-Garcia M., Tansini A. et al.
  "Effect of Low Ambient Temperature on Emissions and Electric Range of Plug-In Hybrid Electric Vehicles"
  ACS Omega 2019 4 (2), 3159-3168, DOI:10.1021/acsomega.8b02459, 2019

- Tansini A., Fontaras G., Ciuffo B., Millo F. et al.
  "Calculating Heavy-Duty Truck Energy and Fuel Consumption Using
  Correlation Formulas Derived From VECTO Simulations"
  SAE Technical Paper 2019-01-1278, doi:10.4271/2019-01-1278, 2019

- Zacharof N., Tansini A., Prado I., Grigoratos T. et al.
  "A Generalized Component Efficiency and Input-Data Generation Model
  for Creating Fleet-Representative Vehicle Simulation Cases in VECTO"
  SAE Technical Paper 2019-01-1280, doi:10.4271/2019-01-1280, 2019

- Doulgeris S., Tansini A., Dimaratos A., Fontaras G. and Samaras Z.
  "Simulation-based assessment of the CO2 emissions reduction potential
  from the implementation of mild-hybrid architectures on passenger cars to
  support the development of CO2MPAS"
  TAP Conference 2019, Thessaloniki, Greece, 2019

- Di Pierro G., Millo F., Tansini A., Fontaras G. et al.
  "An Integrated Experimental and Numerical Methodology for Plug-In
  Hybrid Electric Vehicle 0D Modelling"
  SAE Technical Paper 2019-24-0072, 2019, doi:10.4271/2019-24-0072, 2019

Based on the activities carried out for this PhD Programme, these are the works
that will be submitted for publication:

- A theoretical and experimental analysis of the coulomb counting method
  and estimation of the electrified-vehicle electricity balance in the WLTP

- A flexible simulation approach for hybrid electric vehicles to support the
  European CO_2 emissions framework

- Emission factors and main observations for Plug-in hybrids from the
  European market

- The evolution of the European light-duty vehicles market as a
  consequence of the CO_2 emissions standards

1.4 Structure

The structure of the document is here presented to provide the reader with a more precise overview of the content of this thesis.

Chapter 2 — Context and background
- Introduction of the European transport characteristics and trends
- Description of relevant events and issues identified
- Presentation of possible solutions to the issues

Chapter 3 — Road vehicles CO_2 emissions certification in Europe
- Regulatory background for LDVs and HDVs
- CO_2 calculation tools already existing and used for certification purposes

Chapter 4 — HDVs CO_2 experimental activities
- Experimental activities on the topic of HDVs CO_2 emissions determination
- Results and important outcomes of the activities

Chapter 5 — HDVs CO_2 calculation methodologies
- Creation of a baseline for supporting the European HDVs CO_2 emissions limit regulation
- Development of verification procedures for ensuring the robustness of the regulatory scheme

Chapter 6 — Hybrid LDVs CO_2 experimental activities
- CO_2 emissions benchmarking
- Data collection for the understanding of HEVs operation
- Identification of aspects to be considered for modelling and simulation

Chapter 7 — Hybrid LDVs CO_2 calculation methodologies
- Proposed simulation strategy for HEVs
- Assessment of the performances
- Application to existing tools

Conclusions

Additional material is reported in the appendixes attached at the end of the document (appendixes A, B, C and D report material about Chapters 4, 5, 6 and 7 respectively).

Chapter 2

2   Context and background

The first emissions regulations for road vehicles in Europe date back to 1988 for HDVs and 1992 for LDVs [8, 9]. For both vehicle categories, regulations are still evolving and are currently subject to major changes affecting the certification procedures. The latest updates for LDVs introduced the Real Driving Emissions (RDE) testing, to measure pollutant emissions outside of the laboratory controlled environment, and the In-Service-Conformity (ISC), to monitor the performances of the emission control system of vehicles after type-approval and within the 5 years or 100'000km windows [10, 11]. For what concerns HDVs, the latest updates regard the entry into force of the CO_2 emissions regulation setting emissions limits for specific categories of trucks for years 2025 and 2030. The following sections provide an overview of the CO_2 emissions trends from road transport in Europe, the difference between the certified and the real-word emissions and the role that calculation tools are going to get with regards to emissions determination and control.

2.1 European road transport and CO_2 emissions trends

In December 2015, during the United Nations Climate Change Conference (COP 21) held in Paris, 195 countries agreed to sign the first global climate deal that sets an action plan to keep global warming under control by limiting the increase in global average temperature at 2°C compared to pre-industrial levels [12]. The agreement renovated and intensified the efforts to reduce the CO_2 emissions from

transport, which have increased between 1990 and 2016, differently from the emissions of other sectors (see Figure 1) [13, 1]. The transport sector is the most significant source of CO_2 emissions contributing to 27% of the total emissions. Of this 27%, road transport accounts for a 72%, with cars (referred to as PLDVs in this thesis) and heavy-duty trucks being the biggest emitters (see Figure 2), building up the 60.7% and the 26.2% of road transport CO_2 emissions respectively. Light-duty trucks take a minor share of 11.9% (also named VANs; referred to as LCVs in this thesis).
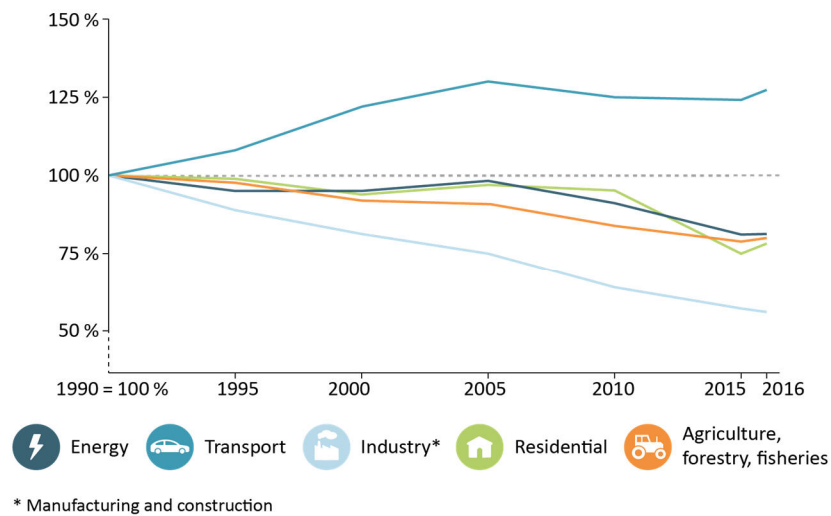
Figure 1. CO₂ emissions trends in the EU by sector (2016, source of the data: EEA)
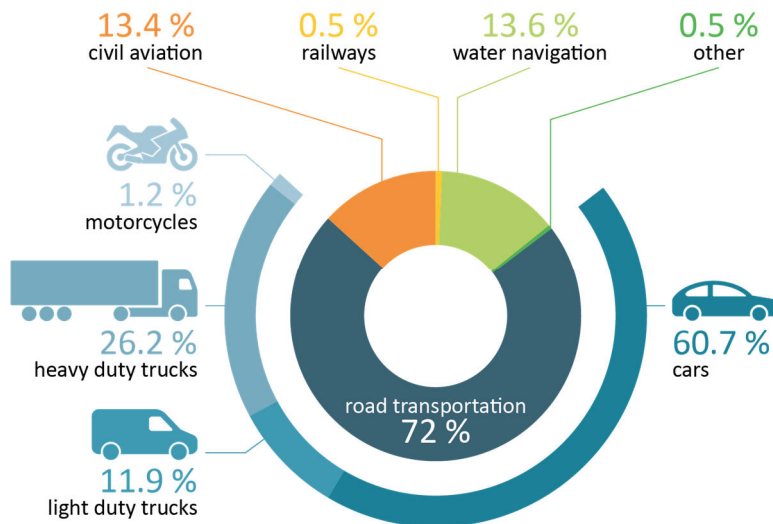
Figure 2. CO₂ emissions breakdown by transport mode (2016, source of the data: EEA)

Anyhow, despite the decreasing trend of the g/km CO_2 emissions of newly certified vehicles with respect to their predecessors, global CO_2 emissions from road transport in Europe are decreasing at a slower rate than what is desirable to meet the ambitious targets set during the COP 21. As it can be seen in Figure 3, after 2030 efforts will have to be further intensified by imposing more abrupt CO_2 reduction rates according to a study from the International Council on Clean Transportation [14]. In 2019 it was also defined the *European Green Deal*, which consists of a growth strategy that outlines the roadmap for achieving "climate neutrality" by 2050 [15]. Given the relevance of the vehicle categories previously mentioned and their impact on overall emissions, it is possible to understand how critical CO_2 regulations are for achieving the goal of limiting GHG emissions and global warming. The European Union has recently been profoundly active under this point of view, putting into force relevant regulatory schemes for the reduction of CO_2 emissions from different sectors including, among the others, transport. Anyhow, the scenario depicted in Figure 3 explains how serious the problem is since the forecasts of CO_2 emissions reduction for 2050 obtained assuming the reference p.a. (per annum) decrease rate (1.5 % for LDVs and 1.7 % for HDVs) and a tighter one (5 % for LDVs) are still far away from what is desired to meet the targets from the COP21. In such a critical situation, it is imperative to have as many and as much practical actions as possible. The European Union has to put into force the appropriate regulatory schemes and control that the desired results are obtained.
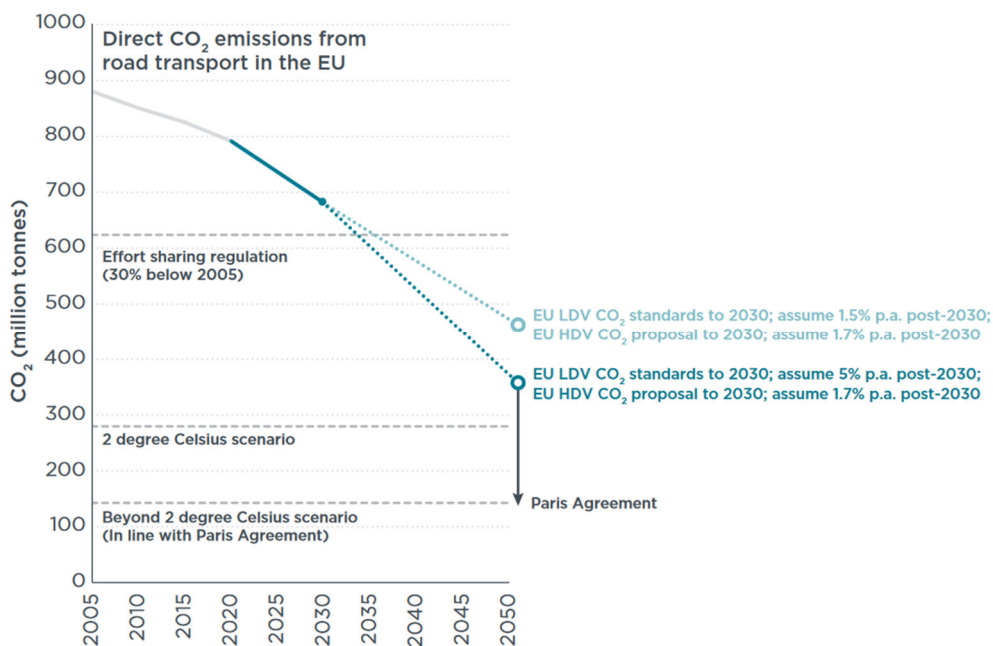
Figure 3. Scenarios of CO₂ emissions decrease rates and Paris Agreement target (source: ICCT)

2.2 Gap between certified and real-word CO$_2$

Technical procedures for vehicles certification define very specific conditions for dynamometer testing: test cell temperature and humidity, vehicle preconditioning, tyres pressure, simulated inertia, mission speed profile, gear shifting pattern (for manual transmission vehicles) and others aspects (e.g. which energy consumers have to be active during the test). All of these measures are needed to ensure the robustness, repeatability and comparability of vehicle emissions measurements, aspects that are always required by certification schemes. Unfortunately, when it comes to real-word vehicles use, such controlled and favourable conditions are never found; therefore, fuel consumption (FC) and emissions performances might deviate significantly from the certified values. The weight carried, components ageing and maintenance, their warm-up or cool-down with extreme temperature conditions, vehicle energy consumers and tyres pressure are all aspects with high impact on the overall performance of the vehicle that are not customarily experimented during the certification cycle. Additionally, the differences between the typical real-world vehicle operation and the mix of urban, interurban and highway driving conditions that are represented in the certification cycle, together with the driving style and the road gradient, largely affect the energy demand and the operating conditions of the vehicle powertrain. The same vehicle can obtain very different efficiency values depending on the characteristics of the duty cycle applied and, for some specific cases, the conditions tested at type-approval might not be appropriate to reflect the ones from real-word use. For example, it is quite unlikely that vehicles designed for urban driving (city cars) are used to drive at high speeds, typical of extra-urban and highway conditions, but still, these conditions contribute to the certification values assigned to the vehicle. Furthermore, flexibilities left by the certification procedures could also bring to more favourable certified values compared to what the vehicle actually gets on real-world use; it is also possible, although less likely, that the actual vehicle outperforms the fuel economy certification values. A Report from JRC published in 2011 [16], which presented one of the very firsts analysis of Portable Emissions Measurement System (PEMS) results, measured and presented the laboratory to road comparison of twelve LDVs (gasoline and diesel); the study says that the road CO$_2$ emissions were in average 21 % higher than NEDC (New European Driving Cycle) type-approved values. Pollutants emissions were also much higher and well beyond the limits of the Euro standards associated with the tested vehicles. When these discrepancies are not limited to few cases, but rather apply to the majority of the fleet vehicles bringing to a significant bias of the estimation, this means that the certification

procedure fails to represent the real-world conditions. This was the case for the NEDC, which was eventually replaced by the more representative Worldwide harmonised Light vehicle Test Procedure (WLTP). The new procedure aims at defining a fuel economy value that is more representative of the real world conditions; this requires that the benefits associated with new vehicle technologies are consistently captured. Consequently, the introduction of the WLTP is expected to affect the gap between certified and real-world CO_2 emissions, which is expected to reduce from 32 % to 13 % [17]. Although this change represents a significant step forward in addressing the problem, this might not be enough and other measures have to be taken to ensure the effectiveness of the regulatory schemes.

2.3 Supporting the regulatory framework with CO_2 emissions calculation tools

In the current scenario of great concern about the effectiveness of the regulatory schemes put into force for achieving a sustainable living, a tighter action of monitoring and control is needed. The certification procedures are being complemented by additional compliance checks to ensure that potential shortcomings are eliminated. This is the main reason behind the introduction of the in-service conformity and the market surveillance checks, which consists of physical testing of the whole vehicles to verify that the emissions comply within certain boundaries with the reference values. Because of their introduction, the robustness of the regulatory schemes is for sure increased, at the cost of an increased burden for the additional physical testing activities to be performed.

In the current situation, the regulatory schemes are associated with quite an intensive effort that is needed to ensure effectiveness and robustness as previously discussed. Potential needs of the authorities to impose additional checks should not be associated with an increased effort for the regulatory scheme. With this aim, physical testing could be partly replaced or complemented by calculation tools. There are many advantages associated with the use of calculation tools:

- it allows to assess the impact of different aspects at vehicle level (new vehicle technologies and control strategies, driving style, etc.)
- the experimental burden is not increased (or not significantly)
- the cost associated with the investigations is low
- there is no variability in the results caused by external factors

- flexibility towards different applications, granted by the possibility to adjust the requirements and target accuracy when needed
- enabling the investigation of aspects that cannot be studied in the real-world
- creation of scenarios and forecasting (e.g. the technology roadmap, the changes in mobility, etc.)

The use of calculation tools is, therefore, a sustainable and flexible solution to address those problems that would otherwise require extensive use of resources, or even making possible something that could be performed in no other ways. Calculation tools are precious support for regulators, authorities or research centres that need to find scientific evidence to support their activities. In the specific case of the European Commission, calculation tools are required for verification of the effectiveness of regulations, or for supporting impact assessment studies creating different scenarios for comparison. In the next chapter, the calculation tools developed by the European Commission for the determination of CO_2 emissions from road vehicles are introduced. In the chapters presenting the activities performed within this PhD programme, the same tools are used in multiple ways to support the activities and the needs of the European Commission.

Chapter 3

3 Road vehicles CO$_2$ emissions certification in Europe

CO$_2$ emissions targets for road vehicles were firstly set in Europe in 2009 (EC Regulation No 443/2009). It imposed a sales-weighted target of 130 g/km for PLDVs for 2015 for the average CO$_2$ emissions obtained in the vehicle fleet of each Original Equipment Manufacturer (OEM). This initiative was followed in 2011 with the CO$_2$ regulation for LCVs (EU Regulation No 510/2011), which similarly set a target of 175 g/km to each OEM sales-weighted fleet-average for 2017 [6]. A second set of regulations was adopted in the EU in 2014 for PLDVs and LCVs, setting targets for 2020 [5, 7]. After 2020, when the transition period for the introduction of the WLTP is over, the compliance check is performed as follows: a first check in 2020 based on NEDC measurements and NEDC-related targets, with CO$_2$ emissions targets of 95 g/km for PLDVs and 147 g/km for LCVs, and a second check in 2021 based on WLTP measurements and WLTP-related targets (to be calculated in 2020 according to regulation 2019/631, using the 2020 WLTP CO$_2$ emissions declared by OEMs). The latest development to this action was the adoption in 2019 of the targets for 2025 and 2030 [18]. Differently from the previous targets, the post-2020 ones are expressed as CO$_2$ reduction percent, to be referred to 2021 WLTP-based reference. The compromise that was finally adopted foresees a reduction of 15% of the g/km CO$_2$ emissions by 2025 for both PLDVs and LCVs. For year 2030, two different targets are set for the two different categories, as PLDVs and LCVs are expected to reduce their emissions by 37.5 % and 31% respectively still referring to 2021 WLTP-based values [18].

HDVs were included for the first time in a CO_2 regulation scheme in 2018 [19], with checks for emissions compliance to be performed in 2025 and 2030 as for PLDVs and LCVs. Differently from LDVs, CO_2 emissions at vehicle-level from HDVs are not obtained through physical measurements but rather by means of a calculation tool. By 2025 the fleet will have to achieve a 15% reduction with respect to the CO_2 emissions of the reference period (1 July 2019 – 30 June 2020), whereas the 2030 target will have to meet a 30% reduction unless decided otherwise pursuant the review process set for the year 2022 [20, 4, 21]. The stringency of LDVs and HDVs CO_2 targets is graphically represented in Figure 4 and Figure 5.
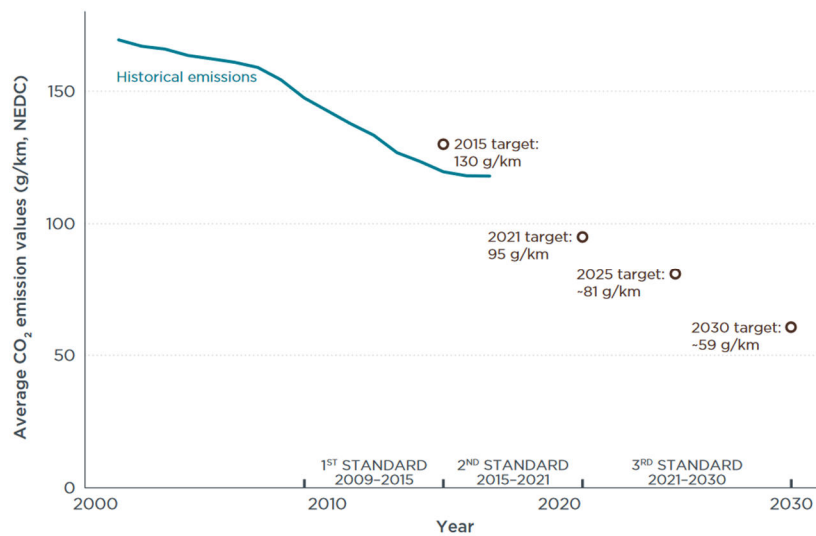
Figure 4. Stringency of PLDVs CO_2 emissions targets as NEDC-equivalent (source: ICCT)
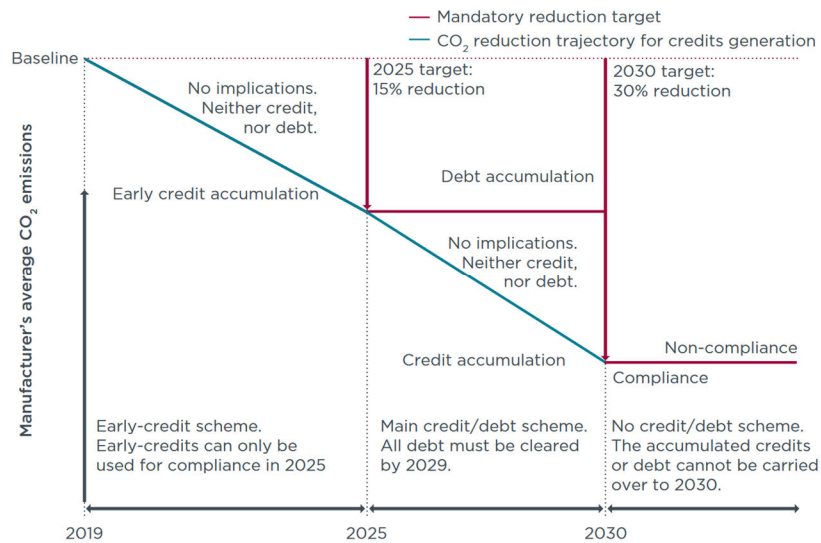
Figure 5. Representation of the stringency of HDVs targets for years 2025 and 2030 (source: ICCT)

The CO_2 determination methodologies for the different vehicle categories are presented in the following sections, along with the criteria to calculate the fleet-wide average value for each OEM for a compliance check.

3.1 Heavy-Duty Vehicles CO_2 certification scheme

HDVs present a unique challenge for pollutants and GHG emissions regulations. They are associated with a great variety of vehicle configurations and purpose of use that makes it difficult for the regulatory scheme to cover all of the different combinations, to put into action measures to promote vehicle sustainability and provide the customers with useful information from the certification process that reflects vehicle performances of real-world usages. The size of these vehicles is an additional issue since dynamometer testing is not always a viable option as for LDVs. Having a dynamometer-based testing procedure to measure pollutants and GHG emission would require the spread of dedicated test facilities of big dimensions associated with very high investments. Furthermore, a poor representativeness of real-world vehicle operation might be obtained when these vehicles are tested on a single-axis dynamometer, unloaded, and with the tyres overheating due to the very high loads applied (for representing on-road vehicle use with payload) with no significant cooling effect. For these reasons, assessing pollutants and GHG emissions at vehicle-level through physical measurements was considered too demanding and possibly inaccurate to comply with the requirements of certification schemes [22, 23]. Pollutants emissions are assessed at engine-level, with the engine fitted on an engine test bench and tested for both stationary and transient operation.

This test also serves for the experimental measurement of engine FC at different operating conditions in terms of speed and torque output. For the assessment of CO_2 emissions, the vehicle-level picture is obtained through a calculation tool named VECTO, the Vehicle Energy Consumption calculation TOol, that was developed to avoid testing the whole vehicle and still satisfy the regulatory needs. VECTO calculates the FC and CO_2 emissions solving the vehicle longitudinal dynamics meanwhile a driver model follows the target speed of the specific regulated cycles. The following sections describe with more detail the way the CO_2 targets are implemented (section 3.1.1) and the approach for vehicle-level CO_2 emissions calculation with VECTO (section 3.1.2).

3.1.1 Overview

There are three key regulations taking part in the process of regulating CO_2 emissions from HDVs (see also Figure 6):

1. Commission Regulation (EU) 2017/2400 of 12 December 2017
   determination of the CO2 emissions and fuel consumption of heavy-duty vehicles and amending Directive 2007/46/EC of the European Parliament and of the Council and Commission Regulation (EU) No 582/2011

2. Regulation (EU) 2018/956 of the European Parliament and of the Council of 28 June 2018
   monitoring and reporting of CO2 emissions from and fuel consumption of new heavy-duty vehicles

3. Regulation (EU) 2019/1242 of the European Parliament and of the Council of 20 June 2019
   setting CO2 emission performance standards for new heavy-duty vehicles and amending Regulations (EC) No 595/2009 and (EU) 2018/956 of the European Parliament and of the Council and Council Directive 96/53/EC.

2017/2400
CO_2 Certification

Defines the procedure for HDVs CO_2 certification (through experimental measurements and VECTO simulation)

2019/1242
CO_2 Emissions Standards

Sets reduction targets to the average CO_2 emissions of the fleet (15 % in 2025, 30 % in 2030)

2018/956
Monitoring and Reporting

Ensure the availability of data for creating the CO_2 emissions baseline (HDVs OEMs have to report fleet performance annually)

Figure 6. Steps taken by the European Commission in the HDV CO_2 action

The entry into force of Regulation 2017/2400 was the first necessary step, according to the mandate expressed in article 1 point 19 of Regulation 595/2009, to define the determination and certification methodology for vehicle-level CO_2 emissions from HDVs [2]. This action officially adopted a methodology based on a combination of physical tests and computer simulation for calculating FC and CO_2 emissions. Physical tests are performed at component-level or vehicle-level to generate input data for the VECTO tool, whose main principles will be introduced in the next section, that finally calculates the metrics of interest for multiple mission profiles and vehicle loading conditions.

In June 2018 the second regulation from the list above, about the monitoring and reporting of CO_2 emissions, was finally adopted [19]; it sets a mandate for HDVs OEMs to certificate the emissions of all the vehicles registered as of 1st of January 2019 (according to the provisions of 2017/2400) and report to the European Commission annually. This measure is meant to increase the transparency of the fuel efficiency figures associated with vehicles in the market, support transport operators in making better-informed purchases and finally support the creation of the 2020 CO_2 emissions baseline as a reference for emissions standards [24].

The calculation mechanism for the CO_2 emissions of an OEM, expressed as grams emitted per kilometre and per tonne of payload g/t-km, to reflect the utility of the HDVs subgroups considered, is shown in Figure 7 [4, 25].
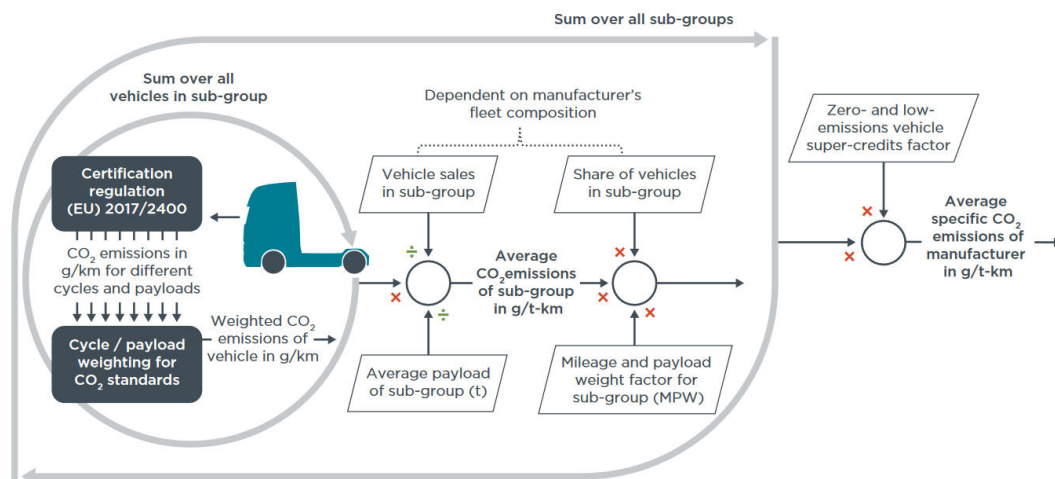
Figure 7. Calculation of the OEM HDV fleet CO2 emissions (source: ICCT)

Each vehicle sold is assigned to a different sub-group depending on the vehicle configuration (rigid or tractor), the traction configuration (4x2, 6x2), the HDV group (4, 5, 9, 10), the cabin type (day or sleeper) and the engine power. The sub-

groups are obtained by combining the HDV groups with the intended typical mission profile, Urban Delivery (UD), Regional Delivery (RD) and Long Haul (LH) respectively. In each sub-group and for each vehicle, the CO_2 emissions in g/km of the different cycle-loading combinations produced at vehicle type-approval are multiplied by weight factors assigned to the specific sub-group; the sum of all the weighted values is then calculated. This value is then divided by the vehicle sales and the average payload in tonnes of the sub-group, therefore obtaining the average vehicle CO_2 emissions of the sub-group in g/t-km. The sub-group value is then multiplied by the share of vehicle sales of that sub-group and the Mileage Payload Weight factor (MPW), to account for the differences in freight activity (i.e., how many tonnes are moved what distance, quantified in t-km) between the vehicle sub-groups [25]. The weight factors for averaging the cycle-loading combinations as well as the MPW values are reported in Table 1.

Table 1. Information for the calculation of the HDVs CO_2 emissions of OEMs (source: ICCT)

Vehicle sub-group	Mission profile weighting	Payload weighting	Average payload (tonnes)	Annual mileage (km)	MPW factor
4-UD	Urban Delivery: 100%	Low: 50% Reference: 50%	2'650	60'000	0.099
4-RD	Regional Delivery: 90% Long Haul: 10%	Low: 50% Reference: 50%	3'180	78'000	0.154
4-LH	Regional Delivery: 10% Long Haul: 90%	Low: 50% Reference: 50%	7'420	98'000	0.453
5-RD	Regional Delivery: 90% Long Haul: 10%	Low: 30% Reference: 70%	10'258	78'000	0.498
5-LH	Regional Delivery: 10% Long Haul: 90%	Low: 30% Reference: 70%	13'842	116'000	1.000
9-RD	Regional Delivery: 90% Long Haul: 10%	Low: 30% Reference: 70%	6'280	73'000	0.286
9-LH	Regional Delivery: 10% Long Haul: 90%	Low: 30% Reference: 70%	13'400	108'000	0.901
10-RD	Regional Delivery: 90% Long Haul: 10%	Low: 30% Reference: 70%	10'258	68'000	0.434
10-LH	Regional Delivery: 10% Long Haul: 90%	Low: 30% Reference: 70%	13'842	107'000	0.922

The possibilities of banking, borrowing and pooling are also considered in the scheme, as well as super-credits for incentivising zero- and low-emissions vehicles (ZLEVs) [20]. Vehicles that are considered vocational are exempted from the regulation. Other exemptions from the CO_2 certification are related to vehicles with advanced technologies or solutions that are not covered by VECTO: hybrid or fully electrified powertrains, waste heat recovery, trailer technologies and others [26, 27]. Efforts are being taken for the development of the CO_2 regulation and VECTO

for the inclusion of such advanced solutions, which will for sure be crucial for meeting the 2020 emissions target.

3.1.2 VECTO – Vehicle Energy Consumption calculation Tool

VECTO is a simulation tool for the calculation of the vehicle Energy Consumption (EC), FC and CO_2 emissions. It uses a backward-looking simulation approach, where the vehicle speed is used as input to characterise the vehicle longitudinal dynamics, in combination with some forward-looking control modules for the modelling of those functionalities that would not be possible with the purely backward-looking approach (e.g. target speed cycles and driver operation) [22]. Its development was commissioned by DG CLIMA to the Graz University of Technology as main contractor, with the JRC as scientific coordinator and with the support of Ricardo. Multiple standardised mission profiles with different loadings are simulated for the certification process, representing the most relevant use cases (e.g. long haul operation, regional delivery or urban delivery). The model calculates the vehicle longitudinal dynamics to obtain the power requested at the wheels, then driveline components losses and auxiliaries consumption are taken into consideration to evaluate the load at the engine. Finally, the FC obtained through interpolation on the engine map (Figure 8). VECTO was validated through test activities performed by the JRC and OEMs confirming the accuracy of the methodology (error within ± 4%) [28, 29, 30].
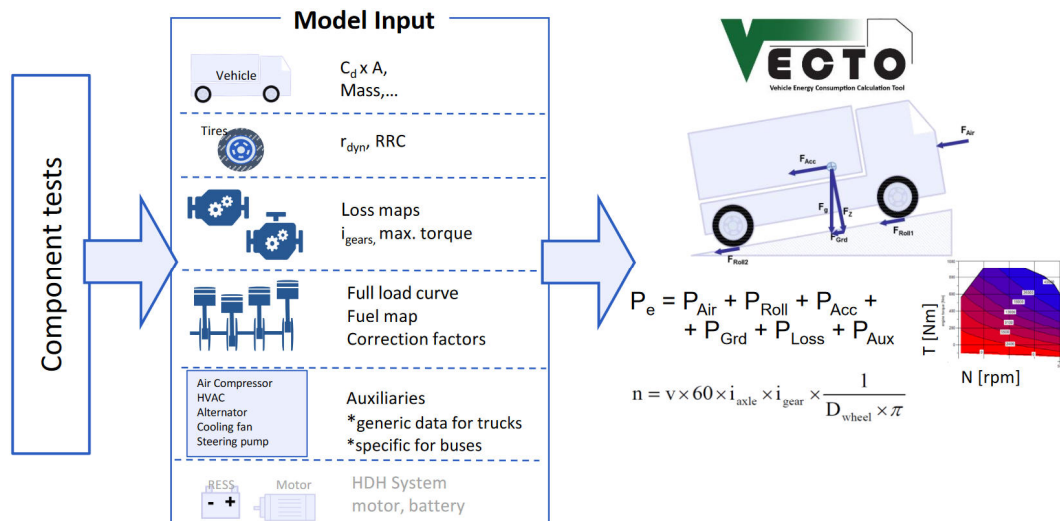
Figure 8. Overview of VECTO inputs and calculation principle (source: European Commission)

VECTO requires a set of inputs, either in scalar or in tabular forms, to perform the calculation of EC and CO_2 emissions. The procedures for the measurements and declaration of VECTO inputs are specified in the technical annexes to Regulation 2017/2400. The main inputs to be inserted to run VECTO simulations are reported in Table 2. The tabular inputs are lookup tables using two dimensions, rotational speed and load of the component, exception made for the retarder that uses only rotational speed, and the gearbox, that additionally uses the engaged gear. The overview of the VECTO data workflow for the certification process is also presented in Figure 9, summarising the steps and data transfer from components/vehicle measurements and until the generation of the record files from the certification. One output of a VECTO run is the summary file, containing the cycle energy use (overall and at different locations in the powertrain), the FC, the CO_2 emissions and other metrics of cycle-average vehicle operation and driving dynamics, which contains as many rows as many cycle-loading combinations simulated. Another output is the modal files, one per cycle-loading combination, containing the time series produced during the simulation.

Table 2. VECTO main inputs

Scalar inputs:	Tabular inputs:
• Vehicle curb mass	• Engine FC map
• Vehicle CdA	• Engine full load curve
• Axles and traction configuration	• Engine motoring curve
• Tyres dimension	• Gearbox loss map (for each gear)
• Tyres rolling resistance coefficient	• Torque converter map
• Engine idling speed	• Final drive loss map
• Engine rated power and rated speed	• Retarder loss map
• Engine max torque	• Angle drive loss map
• Gearbox and final drive ratios	
• Auxiliaries	

VECTO features two additional tools to process the data measured during the experiments: VECTO Air Drag to compute the vehicle drag area (CdA) from the constant speed test data and VECTO Engine to create the engine FC map from the engine test-bench measurements. An additional tool, the VECTO Hashing tool, is used to hash, apply cryptography and validate the relevant data needed for the

certification. VECTO is currently used for the CO_2 emissions monitoring and reporting of HDTs belonging to the HDV groups presented in Figure 10.
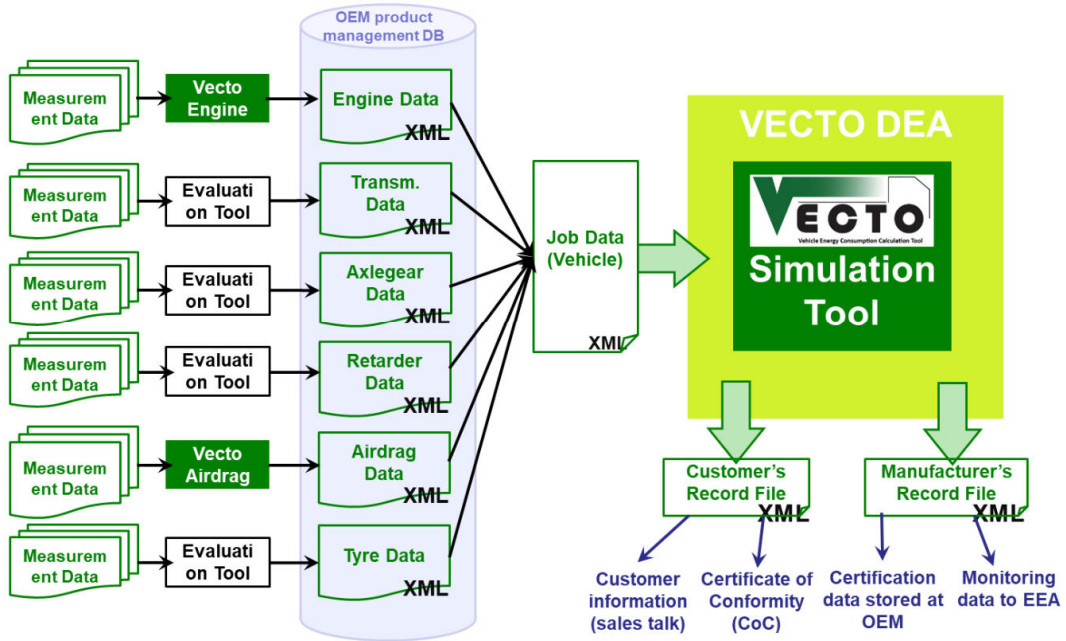
Figure 9. VECTO data workflow for the certification process (source: European Commission)
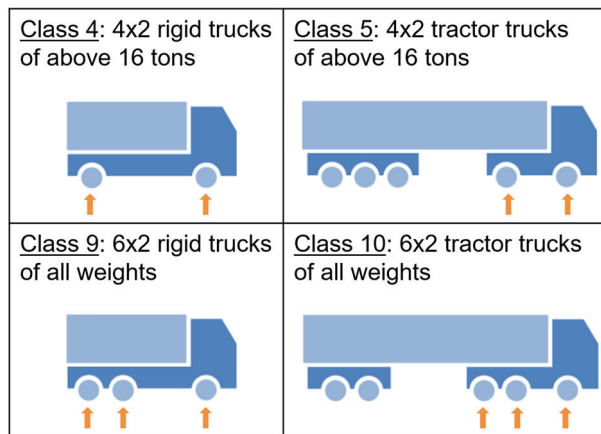
Figure 10. Regulated HDV groups according to Regulation 2017/2400

In the year 2022, the effectiveness of the HDV CO_2 action will be reviewed, and the extension of the certification scheme to Buses and Coaches will be considered [20]. VECTO will also obtain significant updates and changes for the inclusion of advanced fuel-saving technologies. To this aim, the European Commission has

already launched testing activities and studies for the assessment of what technologies are to be introduced and how. For what regards the topic of hybrid electric HDVs, the European Commission launched in 2016 a study with a duration of 18 months in order to assess different solutions for the inclusion of electrified powertrains in the HDVs CO_2 regulation scheme. The results of the study, published in a report from 2018 [31], proposed VECTO (combined with fallback solutions) as the most appropriate solution to handle hybrids.

3.2 Light-Duty Vehicles CO_2 certification scheme

Actions to reduce LDVs CO_2 emissions came in a more straightforward way than HDVs, as there was already a dynamometer-based testing procedure into force for many years that measured pollutants emissions at vehicle-level. Therefore, there was no need to build a measurement methodology from scratch as for the case of HDVs. However, there was another complication to face, since it became evident in the years between 2011 (publication of PEMS results in a JRC Technical Report [16]) and 2015 (year of the Volkswagen scandal) that the type-approval FC and CO_2 emissions figures, as well as pollutants, differed considerably with respect to the real-world ones. Consequently, the community started questioning about the representativeness of the NEDC type-approval procedure and eventually took the decision to replace it in favour of the WLTP. Therefore, the complication behind the CO_2 regulation currently in force for LDVs lays in the fact that the 2020/1 target is based on the NEDC, but currently, the WLTP is being used to measure vehicles CO_2 emissions during the type-approval test. A solution was needed to overcome this problem, and finally, it was agreed to handle the conversion of the WLTP test results into an NEDC equivalent value (the so-called *correlation procedure*) using a simulation tool named CO_2MPAS, developed by the JRC for the purpose [32].

3.2.1 Overview

Since 1st of September 2017, LDVs CO_2 emissions measurement is performed through the type 1 test of the WLTP using the Worldwide harmonized Light vehicles Test Cycle (WLTC) that differs significantly from the NEDC. Due to the transient characteristics, stronger accelerations/decelerations, a smaller share of vehicle standstill and higher speeds (both average and maximum), the increase in CO_2 emissions can be as high as 25% [33]. This difference is partly explained by the driving cycle itself and partly by other differences introduced by the WLTP

procedure (e.g. different road loads). Therefore, it is not possible to use the measured WLTP CO_2 for checking compliance with the pre-existing 2020 targets, as this would turn into a significant tightening of the target stringency. CO_2MPAS processes the data from the WLTP physical test and calculates the NEDC equivalent value, which is then compared with the manufactured declared NEDC CO_2 emissions. If the discrepancy is below a certain threshold (4%), the NEDC OEM declared value can be accepted and used for the official reporting; otherwise the CO_2 emissions are validated through NEDC physical testing (the so-called *double testing*). The conversion of WLTP into NEDC CO_2 emissions is necessary only until 2020 since the WLTP-measured value will be used directly as of 1st January 2021. In the year 2020, the CO_2 emissions from each LDV will be adjusted for vehicle mass according to the following equation:

$$NEDC_{CO_2,2020,target} = NEDC_{CO_2,ref} + a * (M - M_0) \qquad Eq.1$$

where $NEDC_{CO_2,ref}$ is the reference CO_2 value in g/km (95 for PLDVs, 147 for LCVs), M is the mass in running order of the vehicle in kg, M_0 is the reference vehicle mass in kg (1379.88 for PLDVs, 1766.4 for LCVs) and a is the slope for the linear correction (0.0333 for PLDVs, 0.096 for LCVs).
The specific emissions reference target for 2021 is calculated as follows:

$$WLTP_{CO_2,target} = WLTP_{CO_2} * \left(\frac{NEDC_{CO_2,2020,target}}{NEDC_{CO_2}} \right) \qquad Eq.2$$

where $NEDC_{CO_2,2020,target}$ is the one calculated through Eq.1, and $WLTP_{CO_2}$ and $NEDC_{CO_2}$ are the average specific emissions in 2020.
Between 2021 and 2024, each OEM or pool of OEMs, has to comply with a target value calculated using the 2021 measured WLTP emissions according to the following formula:

$$target = WLTP_{CO_2,target} + a * \left[(M_i - M_0) - (M_{i,2020} - M_0) \right] \qquad Eq.3$$

where $WLTP_{CO_2,target}$ is taken from Eq.2, a is the slope (0.0333 for PLDVs, 0.096 for LCVs), M_i is the average of the mass in running order in the target year in kg, M_0 is the reference mass in running order in kg (1379.88 for PLDVs, 1766.4 for LCVs) and $M_{i,2020}$ is the average of the mass in running order in the year 2020 in kg (with $i = 2021, 2022, 2023, 2024$). If the annual target is exceeded, per each

gram exceeding the target and per each vehicle sold a fee of 95€ has to be paid. As for the case of HDVs, the scheme foresees exemptions (e.g. for OEMs registering less than 1'000 vehicles per year) and super credits for ZLEVs. Pooling is also allowed, but not between PLDVs and LCVs OEMs [34, 18].

3.2.2 CO$_2$MPAS – CO$_2$ Model for PAssenger and commercial vehicles Simulation

CO$_2$MPAS (the CO$_2$ Model for PAssenger and commercial vehicles Simulation) is an ad-hoc simulation tool developed to handle the correlation process between WLTP and NEDC CO$_2$ emissions during vehicle certification. It is a crossover between a general-purpose and a fully developed vehicle emissions calculation model, as it requires a limited amount of vehicle input data (and almost no component data in tabular form) but adopting a detailed approach for vehicle modelling to capture the instantaneous behaviour. Overall, CO$_2$MPAS is closer to be a fully developed model rather than a general-purpose one as it has to comply with the accuracy requirements of the regulation [35]. Similarly to VECTO, it solves the longitudinal vehicle dynamics with a backward-looking approach, but without using any forward-looking control module [36]. Major drawbacks of the pure backward-looking approach are associated with the assumption that the vehicle speed profile is always met (drivetrain power limitations are not considered) and that the accelerator and brake pedal signals are typically absent, hindering the development of vehicle control systems [37]. Since the goal of CO$_2$MPAS is to calculate the CO$_2$ emissions of already existing vehicles, using calibration data from experiments and for the prediction of a predefined driving cycle (the NEDC), these drawbacks do not constitute an issue. To deal with the limited level of detail of the input data, CO$_2$MPAS uses a set of techniques/models to automatically obtain the information necessary to perform the fully-detailed vehicle simulation, including:

- data extraction from the official WLTP type 1 test
- components empirical models derived from a pool of real cars
- regressors, classifiers and machine learning algorithms.

Any time CO$_2$MPAS is run with a set of data, the data is used to calibrate the vehicle sub-models, therefore, allowing a detailed vehicle representation. The powertrain operating conditions in terms of components rotational speeds, load and temperatures are accurately captured, along with the energy savings associated with specific technologies or control strategies. The accuracy of the tool is in the order

of 2.0% with respect to physical dynamometer testing. The workflow adopted by CO_2MPAS is presented in the scheme in Figure 11.
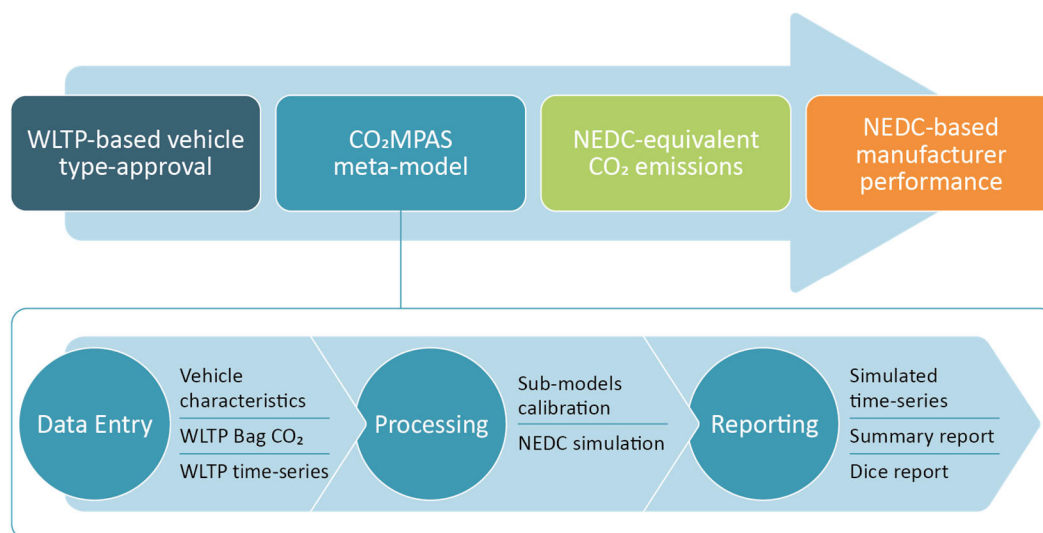
Figure 11. LDVs CO₂ certification and CO₂MPAS workflow scheme (source: European Commission)

CO_2MPAS comprises of the following main sub-models:

- Gear-shifting model for automatic transmissions
- Clutch / Torque Converter model
- Engine speed model (with cold-start characterisation)
- Engine Stop-Start
- Engine coolant temperature model
- Engine FC model
- CO_2 model
- Alternator model

The power at the wheels is calculated based on the road loads coefficients provided in the inputs (for NEDC and WLTP); the engine load is then evaluated considering the driveline losses and the mechanical power consumption (engine torque losses, alternator, etc.). The engine model calculates the FC for each operating condition calculated during the cycle, as a function of power output and rotational speed, using the extended Willans model [38, 39]. The engine FC map that is used is the result of the calibration through experimental data of CO_2 emissions. A semi-physical empirical engine cold-start model is used to adjust engine idling speed and FC when the coolant temperature is low. Specific vehicle/engine technologies are

also included: turbo-charging, exhaust gas recirculation (EGR), variable valve actuation (VVA), cylinder deactivation, lean-burn, periodically regenerating after-treatment systems, gearbox thermal management, braking energy recuperation and others. The most important feature of CO_2MPAS, which also enabled its adoption as an official tool for regulatory purposes, is represented by the self-calibration capabilities of the sub-models; such feature is typically not present in other full vehicle simulation tools. CO_2MPAS was initially developed to handle the correlation of vehicles with conventional powertrains. Due to the spread in the market of vehicles with electrified powertrains, and the growing interest towards the quantification of their energy efficiency, a simulation strategy for HEVs has been introduced in the latest release of October 2019. In its current stage of development, this novel simulation strategy for HEVs does not comply with the requirements of regulatory applications and, therefore, cannot be used for handling the correlation procedure of HEVs and is therefore only used for research purposes.

Chapter 4

4   HDVs CO_2 experimental activities

The JRC-STU is supporting the DGs of the European Commission with different types of activities to support the evolution of the HDVs CO_2 regulatory framework: execution of experimental campaigns, scientific analyses, development of calculation tools, creation of scenarios, reporting and others. Within the PhD programme presented in this work, three main activities were performed that related to the further development and implementation of a new HDV CO_2 certification regulatory framework:

(a) Assessment of the measurement methodology for CO_2 emissions from heavy-duty buses and coaches
(b) Creation of a CO_2 emissions baseline for HDTs
(c) Development of fleet-representative HDTs CO_2 emissions calculation solutions for ensuring the robustness of the CO_2 regulatory scheme

All of these initiatives follow the adoption of the HDV CO_2 Certification Regulation on the determination of the CO_2 emissions and FC from HDVs [2]. They are also related, especially the second and the third (which are directly consequential), to the adoption of the HDV CO_2 emissions standards in Europe. The work carried out within this PhD programme contributed considerably to the outcomes of these activities, which were performed between February 2017 and April 2019. Activity (a), for which the contribution focused mainly on experiments

and data processing, is presented in this chapter. Activities (b) and (c), for which the contribution focused mainly on simulation and other calculation approaches, are presented in the next chapter. Two methodologies highly affecting the HDVs EC calculation are here described: the constant speed test and the engine measurement. The constant speed test is the reference procedure for the determination of the vehicle CdA; additionally, it allows for the estimation of the tyres Rolling Resistance Coefficient (RRC). The accurate determination of such quantities is crucial, as it will be presented in Chapter 5. The engine measurement on the test bench enables to derive the engine steady-state fuel consumption map along with other parameters for the steady-to-transient correction; as it will be presented in section 4.2, this activity contributed to the development of the modelling approach.

4.1 Assessment of the measurement methodology for CO_2 emissions from heavy-duty buses and coaches

Following the adoption of the CO_2 determination methodology for HDTs, the DGs for Climate (DG CLIMA) and Growth (DG GROW) requested to launch a test-campaign to investigate the validity, accuracy, and plausibility of the application of the methodology to buses and coaches. Furthermore, the development of an appropriate verification procedure to be randomly applied to certified and already circulating vehicles was requested. This particular test campaign was decided to be part of a Pre-Pilot Phase (PPP) organised by DG CLIMA, the JRC, the Graz University of Technology and vehicle OEMs (ACEA). Experiments were conducted on two Euro VI vehicles, one interurban bus and one coach (details omitted for confidentiality reasons), both on the chassis dyno and on the road. The full study is presented in a JRC Technical Report [40], of which the primary outcomes are reported in this work. The activity was performed in two phases, the experimental phase and the simulation phase. The experimental phase was further divided into multiple phases: chassis dynamometer testing, on-road testing and proving ground testing. The part of the activity that is relevant for this thesis is exclusively related to the experimental data collection for the calculation of vehicle air drag. Air resistance is for HDVs one of the aspects most affecting the fuel consumption; therefore, its accurate characterisation is of crucial importance. Vehicle air drag is evaluated through the constant speed test, which is described in Regulation 2017/2400 and mandatory to produce VECTO input data. The constant speed test is performed on a proving ground and it requires specific instruments, atmospheric conditions and careful execution. The data collected during the test has to be

processed through VECTO Air Drag, which performs checks on input data quality and completeness, and finally calculates the vehicle drag area corrected for side wind.

4.1.1 Air drag evaluation – Theoretical background

The resulting force $\vec{F}$ acting on a vehicle during motion is

$$\vec{F} = \overrightarrow{F_{trac}} + \overrightarrow{F_{res}} + \overrightarrow{F_{grd}} + \overrightarrow{F_{inertia}} \qquad Eq.4$$

where $\overrightarrow{F_{trac}}$ is the traction force at the wheels, $\overrightarrow{F_{res}}$ is the sum of the resisting forces (rolling resistance and air drag), $\overrightarrow{F_{grd}}$ is the force due to road gradient and $\overrightarrow{F_{inertia}}$ is the inertia of the vehicle during accelerations and decelerations.

The principle laying behind the constant speed test is the fact that, during motion in stationary condition ($\vec{F} = 0$ and $\overrightarrow{F_{inertia}} = 0$) on a flat track ($\overrightarrow{F_{grd}} = 0$), the formula simplifies into:

$$\overrightarrow{F_{trac}} = -\overrightarrow{F_{res}} \qquad Eq.5$$

The equation states that the sum of the resisting forces $\overrightarrow{F_{res}}$ are of equal intensity (but opposite sign) to the traction force $\overrightarrow{F_{trac}}$. The latter is the force pulling the vehicle and acting on the ground, which can be obtained as torque at the wheels divided by the rolling radius of tyres. Therefore, when measuring the traction force acting on the ground at constant speed, the sum of the resisting forces $\overrightarrow{F_{res}}$ is obtained. Figure 12 shows the dependency of the total resisting force with vehicle speed, assuming constant rolling resistance (RR) losses and quadratic air drag losses [41]. As already mentioned, the sum of the resisting forces is:

$$\overrightarrow{F_{res}} = \overrightarrow{F_{RR}} + \overrightarrow{F_{air}} \qquad Eq.6$$

where $\overrightarrow{F_{RR}}$ is the RR of tyres and $\overrightarrow{F_{air}}$ is the resistance due to air drag.
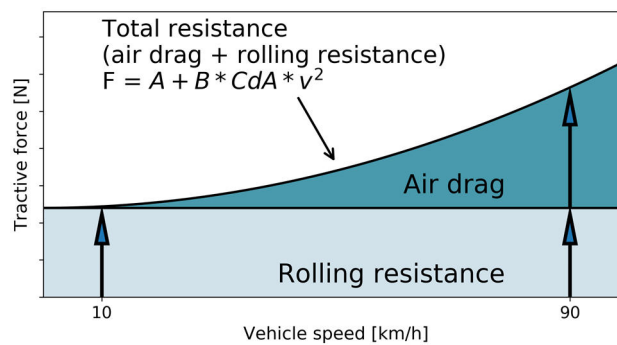
Figure 12. Resisting force acting on a vehicle during a constant speed test on a flat track

The equation that describes the RR force is

$$\overrightarrow{F_{RR}} = RRC * m_{veh} * g \qquad\qquad Eq.7$$

where m_{veh} is the vehicle mass during the test, g is the gravitational acceleration, and RRC is the vehicle speed-independent RR coefficient as defined in VECTO manual. The equation describing the air drag force is

$$\overrightarrow{F_{air}} = C_d(\beta) * A * \frac{\rho_{air}}{2} * v_{air}^2 \qquad\qquad Eq.8$$

where $C_d(\beta)$ is the vehicle air drag coefficient (a function of airflow yaw angle), A is the vehicle cross-sectional area, ρ_{air} is the air density, and v_{air} is the relative speed of air on the vehicle. RR force is assumed to independent from vehicle speed for HDVs applications, while air drag force is zero when the vehicle is standstill and increases with the square of speed [41]. Consequently, it is possible to characterize both forces by driving a vehicle at two different constant speeds: low speed and high speed. When driving at low speed (below 20 km/h approx.), air drag force can be neglected and the total resistance acting is therefore only due to RR of tyres. When driving at high-speed, the air drag contribution is significant and its force is obtained as the total resisting force acting on the vehicle subtracted of the constant contribution given by tyres RR calculated during the low-speed test.

The official methodology adopted in the regulation makes use of correction factors and other formulas to take into account the real conditions that can be encountered during a constant speed test, such as differences in tyres behaviour between the low- and the high-speed test, the influence of wind and atmospheric conditions or test track gradient (this correction is optional). The detailed approach can be found in the "VECTO Air Drag evaluation algorithms" appendix included in VECTO manual.

4.1.2 Air drag evaluation – Experimental setup and requirements

The instruments needed for the constant speed tests are listed in Table 3 and the measured signal requirements are described in Table 4. The anemometer has to be mounted on a dedicated pole on the roof of the vehicle, on the longitudinal plane of symmetry in the 1st to the 3rd fourth of vehicle length. The anemometer pole height has to be one-third of vehicle height, with a tolerance ranging in between 0 and 0.2 metres.

Table 3. Constant speed test instruments

Measured Parameter	Instrument Required
Torque at wheels	Hub torquemeter or Rim torquemeter or Half shaft torquemeter
Vehicle position	GPS system or Differential GPS system
Start and stop of measurement parts	Differential GPS system
Pressure and humidity of ambient air	Stationary weather station
Ambient temperature	Temperature transducer
Airflow velocity and yaw angle (β)	Mobile anemometer
Proving ground temperature	Contactless IR sensor
Vehicle and engine speed	CAN-bus interface – data logger

Table 4. Constant speed test requirements

Signal	Sample rate [Hz]	Remarks
Time	100	
Heading	≥4	
GPS position	≥4	No requirement with respect to the minimum number of digits
DGPS position	100	In case no optoelectronic barriers are used
DGPS velocity	≥20	
Airspeed and Yaw angle	≥4	
Torque	≥20	
Engine speed	≥20	Cardan speed for vehicles with torque converter not locked in a low-speed test
Ambient temperature	≥1	On vehicle measurement
Ground temperature	≥1	
Trigger signal	100	In case opto-electronic barriers are used

The instruments have to fulfil requirements of accuracy, linearity, repeatability, crosstalk, measurement rate and range. The vehicle is tested without payload; tyres have to be of the best class or second-best class for RR and be inflated at the maximum allowable pressure (no active tyre pressure control system should be used). Figure 13 presents the proving ground layouts and the instrumentation.
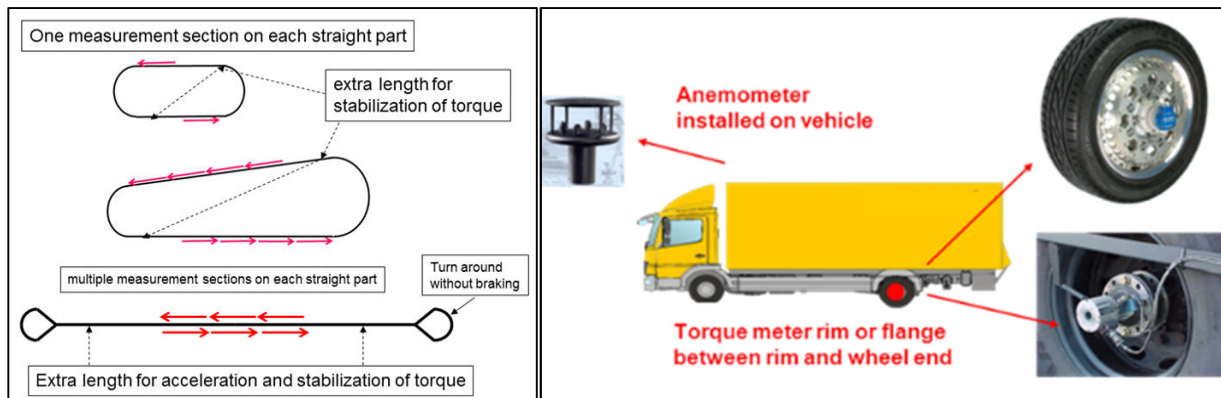
Figure 13. Accepted layouts of proving ground (left) and vehicle instrumentation with anemometer and torquemeters (right) [41]

The proving ground was equipped with weather stations that measured ambient temperature, humidity, average wind speed and gusts speed. During the test, ambient temperature has to be within 0 - 25°C, with dry road surface below 40°C and limited wind strength (average ≤ 5 m/s, gusts ≤ 8 m/s, yaw ≤ 3°). For vehicle position measuring, a DGPS with one stationary receiver and one mobile receiver installed on the vehicle was used. For the torquemeters preparation, vehicle lifts were required to unload the tyres fitted with the sensors and perform the zeroing.

4.1.3 Air drag evaluation – Constant speed test execution

The constant speed test was performed with the following sequence of operations:

1. Preparation of the vehicle and measurement systems
2. Warm-up phase (min 90 minutes)
3. Zeroing of torquemeters (max 10 minutes)
4. Warm-up phase (min 10 minutes)
5. Low-speed test 1 (max 20 minutes)
6. Warm-up phase (min 5 minutes)
7. High-speed test (min 10 valid passings per heading)
8. Low-speed test 2 (max 20 minutes)
9. Drift check of the torquemeters

To identify and correct the possible misalignment of the anemometer, VECTO Air Drag has to process data measured during a vehicle run with high speed, driven in both directions of the test track. Five valid passing inside a straight section of 250m ± 3m should be performed in each driving direction. The data could be collected either during one of the warm-up phases, the high-speed test (if specific requirements are fulfilled) or independently from the constant speed test (as long as the anemometer is not moved or dismounted between the misalignment test and the constant speed test). The data collected during the misalignment calibration test is used to estimate the misalignment error that affects the measurement of airflow yaw angle. The misalignment dataset is the first one to be processed with VECTO Air Drag; at the end of the process, the misalignment error in degrees is shown and automatically kept into consideration when the data of the low-speed and high-speed tests are processed for the calculation of vehicle CdA and RR.

The activities were performed on the proving ground of Balocco (Italy, see Figure 14) on two different days (the first one in February and the second one in March 2017). The atmospheric and track conditions fulfilled the test procedure

requirements. Some technical issues were encountered during the execution of the test:

- Vehicle 1: wrong calibration of the torquemeters
- Vehicle 2: left torquemeter suffering of a failure causing measurement drift

The engineering solutions adopted to address these problems are described in Appendix A as well as in the relevant publication [40].
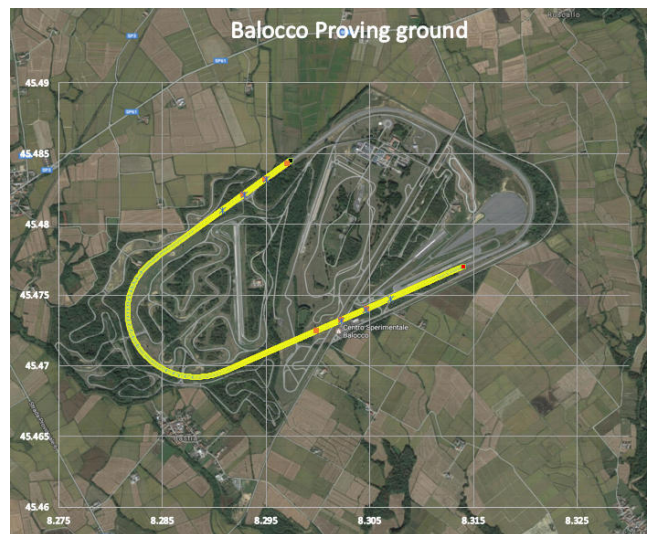
Figure 14. GPS data visualisation of the constant speed test with the identified measurement sections

4.1.4 Air drag evaluation – Calculation with VECTO Air Drag

All the measured data have to be aligned and re-sampled at 100Hz. The following files have to be prepared for running the air drag calculation:

- Vehicle data (csveh)
- Ambient condition data (csamb)
- Misalignment and calibration run data (csdat)
- Low-speed test 1 data (csdat)
- High-speed test data (csdat)
- Low-speed test 2 data (csdat)
- Misalignment run measurement sections coordinates (csms)
- Low-speed and high-speed tests measurement sections coordinates (csms)

Prior to the calculation of air drag, the validity of the data has to be checked. Data rejection might be caused by:

- Invalidating events (disturbance of other vehicles, improper driving, etc.)
- Saturation events of instruments
- Torquemeters drifting over the limits of acceptance

Additional checks on the data are performed by VECTO Air Drag tool itself in the moment the calculation is started by the user. Despite the issues encountered, that required some manipulation of the data and relaxation of the VECTO Air Drag tolerances, high level of agreement was found between JRC results obtained from the constant speed test and OEM suggested values with respect to vehicle CdA and tyres RRC. The comparison is reported in Figure 15 for the interurban bus (vehicle 1) and the coach (vehicle 2). The more significant deviation obtained for vehicle 1 is explained by the more serious technical problems encountered (see Appendix A). In conclusion, the part of the activity relevant for this PhD programme was only the validation of the air drag evaluation through the constant speed test. This methodology was applied in line with the provisions of the related technical annex to regulation 2017/2400, and despite the technical issues that required the relaxation of some of the tolerance checks, the result that was obtained matched the OEM suggested values very closely. Therefore, the study confirmed the accuracy and applicability of the methodology for air drag evaluation. Other outcomes of the study, which are not relevant for this PhD programme, also validated the application of the whole CO_2 certification methodology to buses and coaches with simulation results matching with a good level of agreement the FC experimented from road tests. The applicability of chassis dyno testing versus on-road testing was also compared for the possible adoption as CO_2 determination methodologies, with the latter prevailing in terms of representativeness, lack of restrictions and maturity.
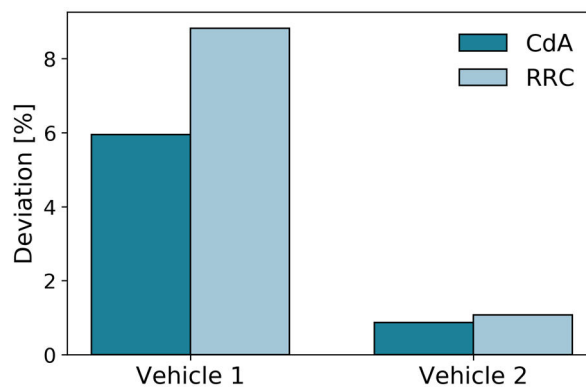
Figure 15. Deviation between JRC results with respect to OEM suggested value

4.1.5 Outcomes of the assessment

The purpose of the activities performed within the assessment were to:

- investigate the applicability of the methodology for the determination of the HDTs CO_2 emissions (Regulation 2017/2400) to buses and coaches
- evaluate the repeatability of the CO_2 verification tests over transient laboratory test-conditions as well as over real-world on-road tests and help in the extension of the ex-post verification method for buses and coaches.

JRC-STU performed an independent comparison between the results of the simulations and those of the measurements (chassis dynamometer tests and on-road tests with PEMS). Chassis dynamometer tests showed excellent repeatability for both the interurban bus and coach cycles (deviations in the order of 5 %); also on-road tests proved to be highly repeatable, regardless of the route chosen. A satisfactory agreement was observed between measured and simulated FC both for the laboratory and the on-road testing, although some drawbacks exist concerning the representativeness and sustainability of the chassis dynamometer testing. Overall, on-road testing seems to be a right solution for the ex-post verification as it overcomes most of the drawbacks related to the laboratory-based testing [40]. The comparison of the two solutions is presented in Table 5.

Table 5. Comparison of the testing procedures evaluated for the HDVs ex-post verification [40]

Option	Chassis Dyno Transient Tests	On-road Tests
Repeatability	Very good	Very good
Representativeness of actual vehicle operation	High with some restrictions in brake applications & acceleration phases over high road gradient	Highest
Applicability to Buses and Coaches	Restrictions for some categories over a certain length	Without restrictions
Cost	High due to specific equipment required and high maintenance costs of the laboratory facilities	High due to specific equipment required
Complexity	Medium provided all equipment available. There is a need for dealing with the auxiliaries	Medium if specific test protocol is established. Still, there is a need for dealing with the auxiliaries
Test Data analysis	Low	Medium due to the need for specific boundary conditions
Maturity	Poor - New protocol is required	Fair - Elements from PEMS protocol and verification tests for trucks can be adopted

4.2 Measurement of Heavy-Duty engines efficiency map

The JRC-STU received in 2017 a Heavy-Duty diesel engine and took the chance to fit the engine on the test bench to perform measurements according to Regulation 2017/2400 and obtain valuable data for supporting the research need. The activity also allowed to validate a simplified engine efficiency model. Specifically, the JRC-STU needed to develop a methodology to calculate the FC of an engine when the relevant detailed engine data is missing. Therefore, the engine was tested according to the provisions reported in annex V ('VERIFYING ENGINE DATA') of the regulation to obtain the engine FC map and start the investigation. In order to obtain the engine data, the Fuel Consumption Mapping Cycle (FCMC) is used. The procedure consists in the definition of setpoints (grid of speed and torque, see Figure 16), at which the engine is kept in steady-state for approximately 95 seconds (55 s for stabilisation, 30 s for measurement, 10 s for post-processing).
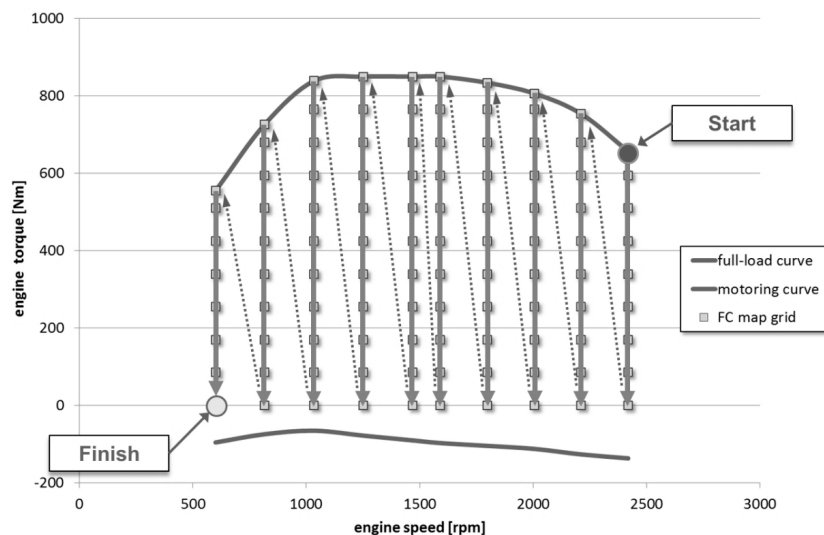
Figure 16. Fuel Consumption Mapping Cycle

For each setpoint, the measured engine FC is averaged and the value is stored in the respective position of the grid. The FCMC produced the FC map reported in Figure 17 a. This result was the starting point for the investigation of a methodology to possibly simplify and generalise the engine fuel map using as few parameters as possible. Different normalisation approaches were tested, which finally led to the solution presented in Figure 17 b. Taking inspiration from what presented in [38], the set of coordinates used to produce the engine map -engine speed, engine torque and FC- were changed to another set of coordinates –BMEP (Brake Mean Effective

Pressure), FuMEP (Fuel Mean Effective Pressure), mean piston speed- of more general validity. Such coordinates are calculated according to the following equations:

$$BMEP\ [bar] = \frac{2\ \cdot\ P_{eng}}{D_{eng} \cdot n_{eng}} \cdot 10^{-5} \qquad\qquad Eq.\,9$$

$$FuMEP\ [bar] = \frac{2\ \cdot\ P_{fuel}}{D_{eng} \cdot n_{eng}} \cdot 10^{-5} \qquad\qquad Eq.\,10$$

$$MPS\ \left[\frac{m}{s}\right] = \ 2 \cdot s \cdot n_{eng} \qquad\qquad Eq.\,11$$

where P_{eng} and P_{fuel} are engine and fuel power in W respectively, D_{eng} is engine displacement in m^3, n_{eng} is engine speed in rps and s is engine stroke in m.

The fuel map expressed through this new set of coordinates highlights the existence of a quasi-linear relationship between $BMEP$ and $FuMEP$, which reflects the quasi-linear relationship between absolute engine and fuel power also presented in literature [38, 42]. The advantage of using the proposed set of coordinates is the possibility to neglect the dependency from the mean piston speed and therefore obtain a 1-D map ($BMEP$- $FuMEP$) defined with two parameters only:

$$FuMEP = \ m \cdot BMEP + q \qquad\qquad Eq.\,12$$

where m is the slope and q is the offset of the linear dependency.
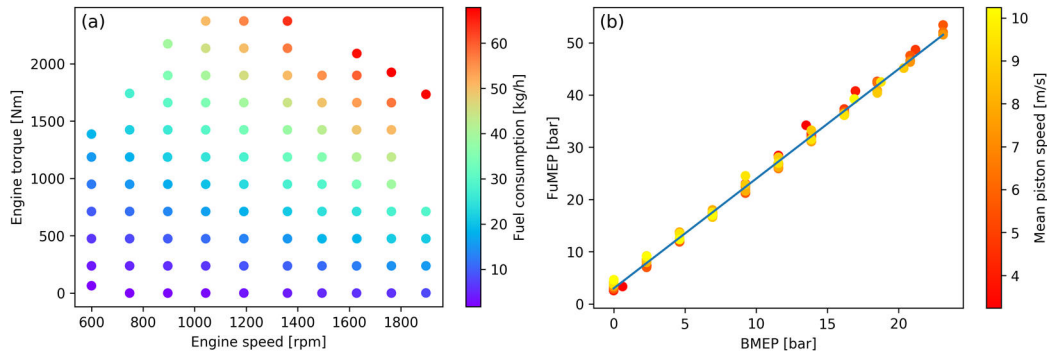
Figure 17. Experimental HDV engine FC map and normalisation approach

In the next sections, the principle presented here is applied to different methodologies as a way to simplify the engine efficiency modelling and calculate the FC having at disposal only the m and q values of the engine considered.

Chapter 5

5 HDVs CO$_2$ calculation methodologies

The action undertaken by the European Commission to regulate HDVs CO$_2$ emissions in Europe grew interest around possible approaches to calculate the average fuel efficiency of HDVs. Besides the official calculation tool, the research community, as well as the European Commission itself, would benefit from the availability of EC calculation tools alternative to VECTO that are able to provide a reasonably accurate result when proprietary inputs (components or vehicle data) are missing. The availability of such solutions would allow independent research groups that are outside of the manufacturing industry to calculate EC, FC and CO$_2$ emissions associated with HDVs, either for research or verification purposes. The methodologies and the results presented in this section wanted to create a sort of manual for components efficiency and vehicle EC ready for consultation and adoption. With VECTO being the official tool for the calculation of CO$_2$ emissions of HDVs, the first necessary step in this sense was the collection of VECTO simulation data for the creation of a fleet fuel efficiency baseline. The collected data was then used to produce alternative methodologies, requiring a smaller amount of input data with a lower level of detail, to support authorities, research institutes and universities in getting a better understanding of the HDVs fleet and obtain answers to their research questions.

5.1 Creation of the fleet-wide CO$_2$ emissions Heavy-Duty Trucks baseline

In the framework of this thesis, a likely baseline of CO$_2$ emissions for the HDTs fleet (groups 4, 5, 9 and 10) for the RD and LH cycles was produced. There are two reasons behind this request: a picture of the HDTs fleet fuel efficiency was still missing and, additionally, the Commission wanted to develop a methodology to assess the quality of the input data and its impact on VECTO simulated FC and CO$_2$ emissions. The activity was crucial to support the drafting of the regulation on HDVs CO$_2$ emissions targets (Regulation 2019/1242). For this purpose, the JRC-STU was provided with VECTO simulation data of vehicles registered in the year 2016. The input data and VECTO results were produced by vehicle manufacturers and consisted mainly of the data included in the summary output of VECTO simulations - except some inputs that were not disclosed for confidentiality reasons - complemented with other vehicle characteristics (e.g. the cabin type that affects air resistance) and information about the inputs (whether the input used to run the simulations were obtained according to the provisions of the technical annexes to Regulation 2017/2400 or other solutions). The exercise produced a database of about 1.7 million rows and 120 columns. The first step taken was data consistency check, secondly a statistical market analysis, thirdly the analysis of the individual EC contributions and lastly the calculation of the fleet CO$_2$ emissions baseline. The activity included four main phases:

1. Database preparation
2. Statistical market analysis
3. Input data quality analysis and components losses characterisation
4. Creation of the HDTs CO$_2$ emissions baseline

A brief overview of each of these activities is given in the following subsections. For the detailed analyses, the relevant publication can be consulted [43].

5.1.1 Database preparation

To process the data in a way that ensured data consistency, a standardised approach for checking, structuring and storing the data had to be developed. A preliminary collection and validation of the data were performed by a third-party company (SIOUX Lime), in agreement with the European Automobile Constructors Association (ACEA), to comply with anti-trust rules and create a basis for comparison with the JRC-STU. An overview of the data handling process is

presented in Figure 18. Most OEMs run one simulation per vehicle sold and have therefore provided a dataset reflecting the number of sales, whereas others ran one simulation per truck model and provided a separate table with the respective number of sales. This resulted in the need to "expand" the data and obtain as many rows in the dataset as vehicles registered for each cycle-payload simulated.
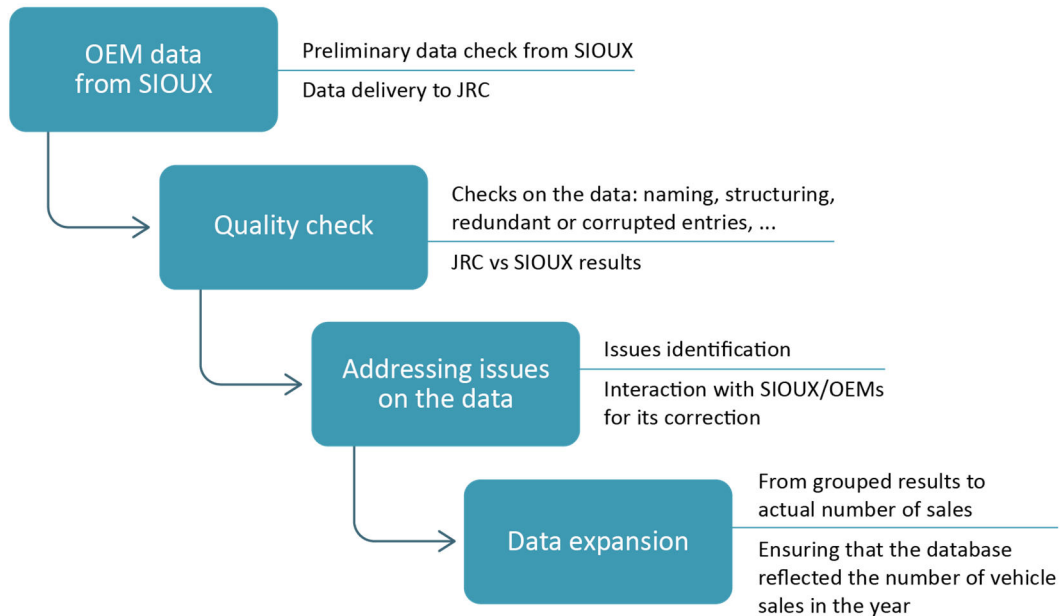
Figure 18. Data management workflow

5.1.2 Statistical market analysis

The fleet data was analysed to obtain valuable information on the configuration of the regulated HDTs and get a picture of the market. The characteristics analysed include technical aspects that could have an impact on the vehicles CO_2 emissions. The list below presents the characteristics that were used for the market analysis:

- Rigid/ Tractor trucks market share
- Curb vehicle mass
- Vehicle drag area
- Engine displacement
- Engine rated power
- Tyres rolling resistance
- Gearbox type

- Retarder type
- Auxiliaries

In the relevant publication [43], pie charts and histograms were used to present how different component types or vehicle characteristics penetrate the market. The JRC-STU also produced a table presenting the data through a clustering approach proposed by DG CLIMA, with the purpose of deriving subgroups statistics and supporting the impact assessment study for the proposal of the HDVs CO_2 emissions regulation SWD/2018/185. Table 6 presents the resulting subgroups per each HDV class clustered according to the engine rated power bins and cabin type, DAY or Long Haul (or Sleeper) cabins. This constituted the main significant contribution to the study, of which the main outcomes are reported in the relevant publication [23].

Table 6. Market overview with the clustering proposed by DG CLIMA [43]

HDV CO_2 vehicle class	Engine rated power [kW]	Cabin type	Vehicle count	Engine displacement median [cm³]	Average estimated CdA [m²]	Average RRC total [kg/t]
4	<164.1	DAY CAB	1469	6700	6.11	6.1
		LH CAB	146	6700	5.75	6
	≥164.1 - 238.5	DAY CAB	10142	7698	6.59	6.23
		LH CAB	3459	7698	5.91	6.23
	≥238.6	DAY CAB	3308	10677	6.25	6.22
		LH CAB	6234	11120	6.37	6.02
5	<238.6	DAY CAB	76	9300	7.06	5.92
		LH CAB	51	7698	7.08	6.01
	≥238.6	DAY CAB	1965	11120	8.04	6.32
		LH CAB	162270	12800	6.3	6.04
9	<238.6	DAY CAB	2794	7698	7.21	6.46
		LH CAB	475	8710	6.42	6.24
	≥238.6 - 372.8	DAY CAB	11156	10837	6.28	6.31
		LH CAB	15146	12740	6.09	6.08
	≥372.9	DAY CAB	157	12809	6.58	6.21
		LH CAB	4391	12800	6	6.23
10	≥238.6 - 372.8	DAY CAB	110	12740	7.99	6.23
		LH CAB	16066	12740	6.59	6.1
	≥372.9	LH CAB	6844	12800	6.36	6.23
Overall			246259	12740	6.33	6.09

For each cluster, the total number of vehicles, median of engine displacement, average estimated CdA and average total RRC (the RRC representative of the whole vehicle as computed by VECTO) are presented. Class 5 vehicles equipped with LH cabin and at least 238.6 kW of rated power is by far the most numerous subgroup. Hence, it is of crucial to capture the real fuel efficiency of these vehicles to reflect the fleet accurately. The JRC-STU also produced estimates of vehicles CdA from OEMs inputs, which did not provide the punctual CdA values but rather a range in which the CdA falls. For many of the engine rated power subgroups, the average estimated CdA is bigger for DAY cabins, which is counter-intuitive (LH cabins generally have bigger cross-sectional area). This anomaly could be explained by the larger use of default values (which are generally higher compared to measured ones) for rigid trucks due to the lack of measured data. The last column of the table presents average total vehicle RRC, which is also taken from VECTO data. The values shown in the table, ranging between 5.9 and 6.5 [kg/t], prove that there is margin for improvements (best efficiency class tyres have much lower RRC, even below 4 kg/t, under specific loading conditions).

5.1.3 Input data quality analysis and components losses characterisation

The official procedures for measuring components efficiency or other vehicle characteristics, here referred to as "efficiency factors", are explained in Regulation 2017/2400, but due to time limitations or other restrictions their adoption was not always possible. OEMs were given with the possibility to create the VECTO inputs with other methodologies, as proprietary measurement procedures, engineering guess or even the use of default values. To account for the quality level of the input data used to run VECTO simulations, the OEMs reported to JRC-STU a rank value (described in Table 7), ranging from 1 (best quality) to 5 (worst quality), reflecting the accuracy of the methodology adopted to obtain data for: engine FC, gearbox losses, axle losses, vehicle air drag and tyres RR. Therefore, it was necessary to understand whether the quality of the inputs affected the efficiency factors and the calculated FC, and possibly normalise the results for better representativeness. To accomplish this task, the efficiency factors were compared with input data quality for each vehicle and cycle-loading combination. The efficiency factors analysed for normalisation are engine average efficiency, gearbox average efficiency, axle average efficiency, vehicle CdA and total vehicle RRC.

Table 7. Input data quality rank description

Data quality rank	Description
1	Measured according to HDV CO_2 annexes and certified
2	Measured in the presence of Technical Services according to HDV CO_2 annexes
3	Measured according to HDV CO_2 annexes but not certified
4	Engineering data (not measured according to HDV CO_2 annexes)
5	Standard values according to HDV CO_2 annexes

The first efficiency factor was calculated as total mechanical energy output divided by total fuel energy input. The second and third efficiency factors had to be calculated by reconstructing the total energy flow in kWh over the cycle in each point of the driveline from the VECTO summary output, and again dividing total energy output by total energy input. The distributions obtained in Figure 19 were then coloured according to the input data quality (DQ) used for the specific component (engine, gearbox, axle) to highlight the dependency. The engine input data used by OEMs ranges between DQ 2 and 4, and no significant difference is found in the average efficiency for the three distributions. Therefore, engine DQ is assumed to have no effect on the average efficiency and no data normalisation is required. The gearbox input data ranges between DQ 2 and 5 (standard values) and a bias in the average gearbox efficiency is found for the different DQs, mainly for DQ 4 and 5, although the difference is in the order of few percentage points. The axle input data ranges between DQ 2 and 5 as for gearboxes, but this case reports a much bigger deviation of average efficiency between DQ 5 results and the rest, in the order of 10-15 percentage points, whereas the deviation of the results for DQ 4 is smaller. A correlation between DQ 4 and 5 and deviations in the VECTO simulation results was also found, meaning that inputs of worse DQ generated a non-negligible increase of the total CO_2 emissions. This finding suggests that VECTO results are sensitive towards the input data creation methodology used. In view of the deviations found, it was decided that gearbox and axle efficiency values of DQ 4 and 5 had to be normalised to reflect the average component efficiency obtained for DQ 2 and 3. Concerning air drag and rolling resistance, the analysis of DQ impact on FC did not return a clear dependency; therefore, no wide efficiency factors normalisations were applied. More specifically, no normalisation at all was applied concerning rolling resistance, and normalisation of a very specific fleet subset was applied for air drag (CdA capped to 7.6 m^2 for group 5 vehicles, with DQ 5 for air drag and equipped with Long Haul Cabins). The process of efficiency factors normalisation is more deeply explained in the relevant publication [43].
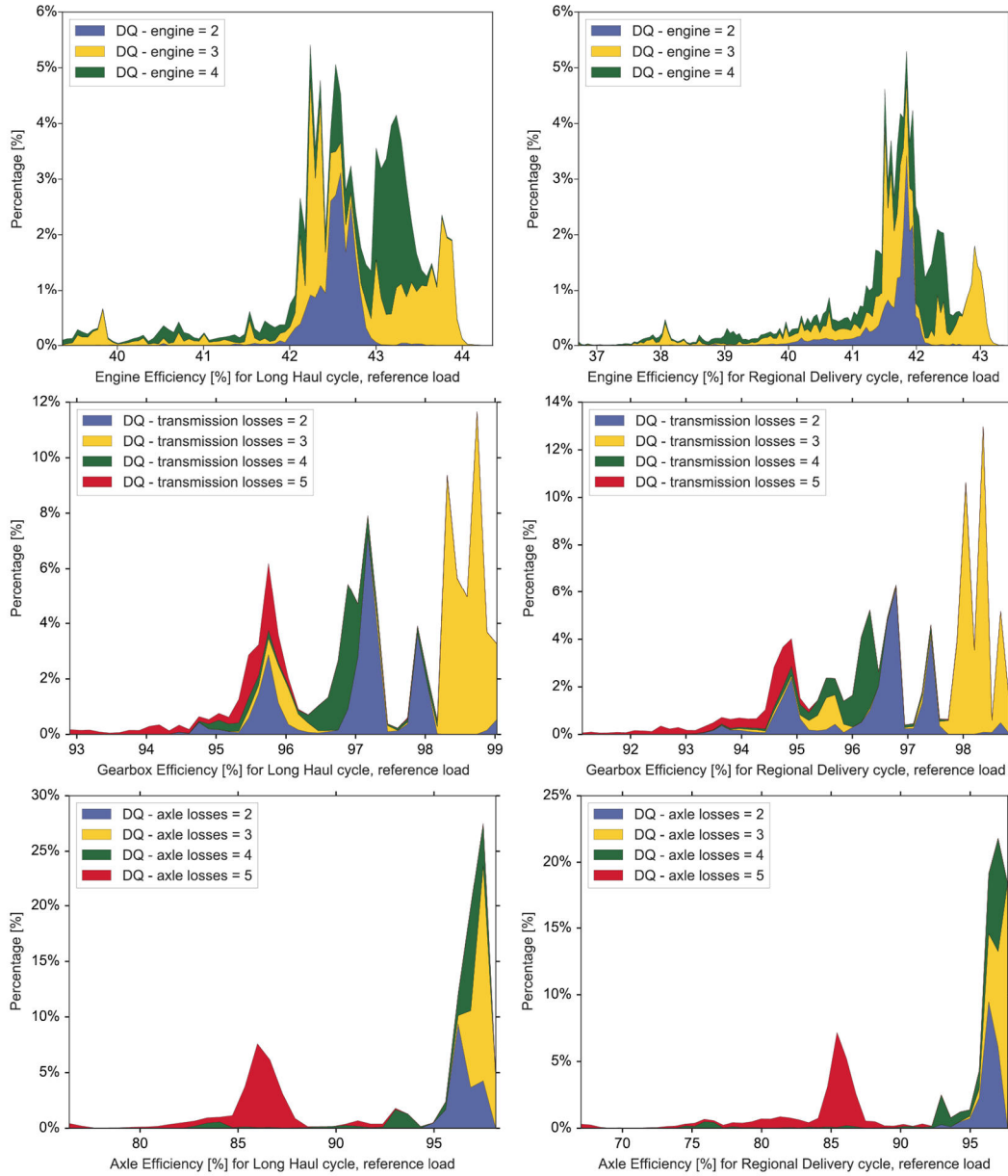
Figure 19. Components efficiency (engine, gearbox, axle) coloured by input data quality

5.1.4 Creation of the HDT CO$_2$ emissions baseline

The normalisation of gearbox, axle and air drag losses resulted in a modified cycle EC for the vehicles affected. When the energy consumed for a specific aspect is modified, the change has to propagate upstream the driveline to account for different conditions for the other components resulting in different component losses. For the vehicles affected, the total positive energy produced at the engine

(*E_fcmap_pos*) has been recalculated, taking as a starting point the energy at wheels (either unchanged or the resulting value using normalised air drag losses) and calculating with a backward-looking approach the updated losses in the driveline (using gearbox and axle unchanged or normalised efficiencies). Other unchanged losses are simply added to the total energy flow in the related position in the driveline (clutch, retarder, angle drive, torque converter, auxiliaries, PTO technologies). This process is described in Figure 20. The red block is the starting point for the normalisation. In case the vehicle considered for the normalisation was subject to CdA normalisation, a new CdA was assigned to the vehicle, and consequently the new energy consumed for air drag losses was calculated.
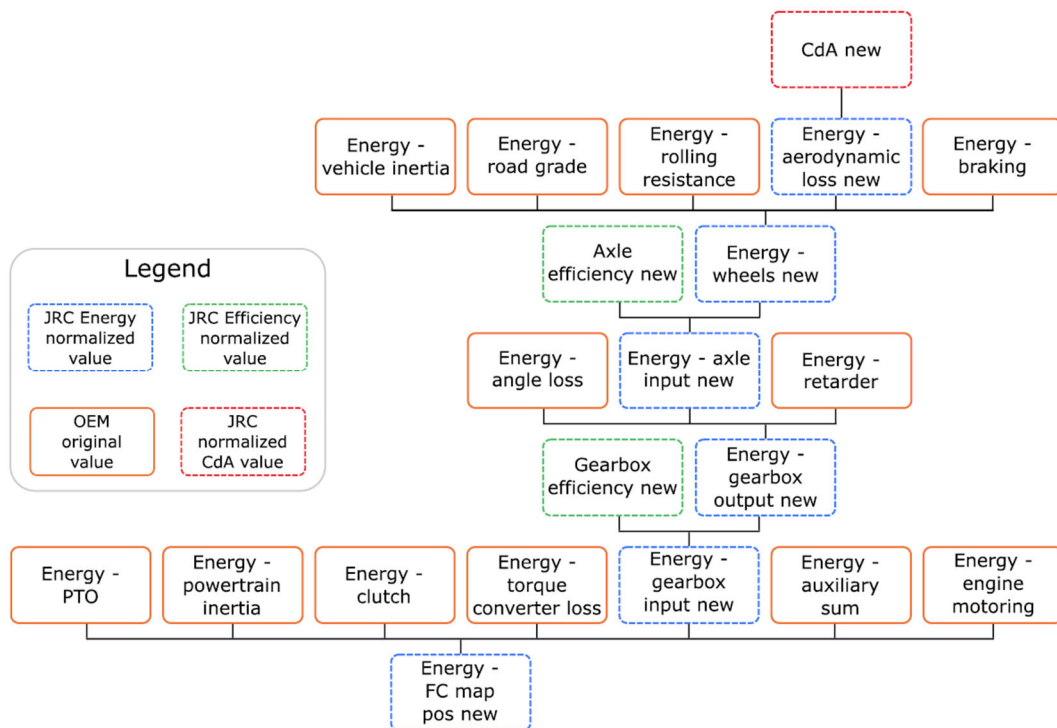
Figure 20. Energy flow normalisation process

The dashed blue blocks are EC contributions that - at the end of the normalisation process - might differ from the initial value contained in the input data from the OEM. The difference could be due to a change in air drag losses, change in axle efficiency, change in gearbox efficiency, or a combination of the previous situations. The dashed green blocks are component efficiency values (gearbox and axle) that could also differ from what derived from the input data. Components associated with data quality 4 and 5 that shows efficiency below a certain threshold

are assigned with a new more realistic efficiency. The orange blocks are energy losses that are not affected by the normalisation process. As a consequence of the modified vehicle EC, the average load of the engine is modified and the average efficiency has to be adjusted. To account for this aspect, a model was developed to coherently assign a new engine efficiency to the different average operating condition. Average Brake Mean Effective Pressure ($\overline{BMEP}$) and Average Fuel Mean Effective Pressure ($\overline{FuMEP}$) are taken as indicators for describing the engine performances. They are representative of the average operating condition and average fuel usage over a cycle, respectively, and are calculated as follows:

$$\overline{BMEP}\ [bar] = \frac{2\ \cdot \overline{Eng.Power\ Output}\ [W]}{Eng.Displacement\ [m^3]\cdot \overline{Eng.speed}\ [rps]}\cdot 10^{-5} \qquad Eq.13$$

$$\overline{FuMEP}\ [bar] = \frac{2\ \cdot \overline{Fuel\ power}\ [W]}{Eng.Displacement\ [m^3]\cdot \overline{Eng.speed}\ [rps]}\cdot 10^{-5} \qquad Eq.14$$

where $\overline{Eng.Power\ Output}$ and $\overline{Eng.speed}$ are average cycle parameters reported in the VECTO summary output (respectively, *P_fcmap_pos* and *n_eng_avg*, to be adjusted for the unit of measure), and additionally

$$\overline{Fuel\ Power}\ [W] = \frac{Fuel\ consumed_{cycle}\ [g]\cdot LHV\ \left[\frac{J}{g}\right]}{Cycle\ Duration\ [s]} \qquad Eq.15$$

where $Fuel\ consumed_{cycle}\ [g]$ and $Cycle\ Duration\ [s]$ are presented in the VECTO summary output, whereas LHV [J/g] (the fuel low heating value) can be found in the *FuelTypes.csv* file contained in the *Declaration* folder of VECTO.

The average engine efficiency is then defined as

$$\overline{\eta_{eng}}\ [\%] = \frac{\overline{BMEP}}{\overline{FuMEP}}\cdot 100 \qquad Eq.16$$

Scatter plots of $\overline{BMEP}$ versus $\overline{FuMEP}$ were plotted for each of the engine models in the fleet, from which it was possible to identify that these two parameters are linearly correlated. The correlation is actually better than the one presented in section 4.2 in Eq.12, since the dependency from the average engine speed is even less evident when the cycle average parameters are used. Therefore, a linear regression was performed on all the points (combinations of $\overline{BMEP}$-$\overline{FuMEP}$ from

all vehicles fitted with the same engine) producing for each engine a linear function using two parameters, m (slope) and q (offset). Consequently, it is also possible to calculate $\overline{\eta_{eng}}$ as function of m and q. An example of the dependency among these three variables is presented in Figure 21. At the end of the normalisation process, the new *E_fcmap_pos* was obtained and the new FC values were calculated using the engine efficiency function described. From *Fuel consumed$_{cycle}$* [g], it is then possible to derive all the FC and CO_2 emissions metrics of interest, by using *fuel density* [g_{fuel}/litre$_{fuel}$] and *CO_2 per Fuel-Weight* [gCO_2/g_{fuel}], both available in the FuelTypes.csv file in the *Declaration* folder of VECTO.
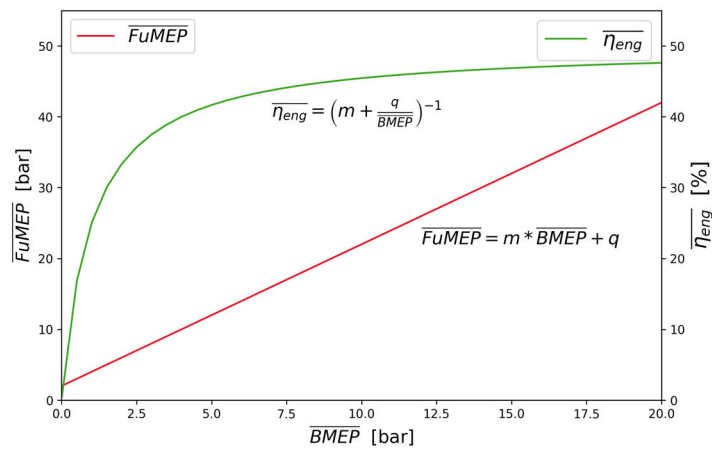
Figure 21. Example of $\overline{BMEP}$-$\overline{FuMEP}$ regression line and engine efficiency curve
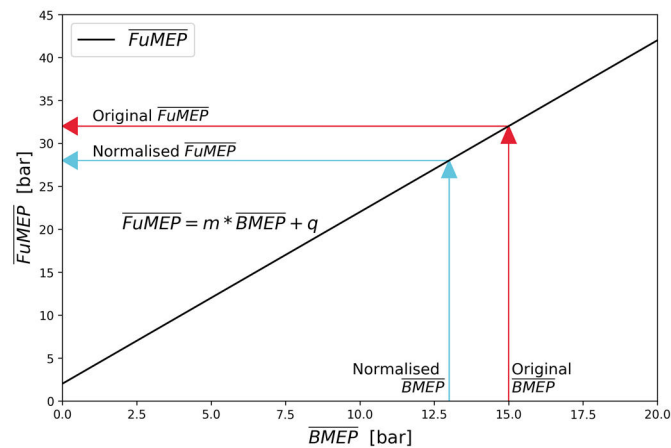
Figure 22. Adjustment of engine operating condition according to $\overline{BMEP}$ normalised

FC and CO_2 emissions values obtained through the normalisation process were then presented in the form of distribution plots and statistics (mean, standard deviation, min, median, max), for the different HDV groups, cycle-loading combinations and

for different metrics of interest. These results are reported partly in the body and partly in the annex of the relevant publication [43]. The CO_2 emissions comparison of the LH reference load is reported in Figure 23 as an example. The results produced with this activity supported the regulators in getting a better understanding of the current HDTs market and a picture of the expected fuel efficiency.
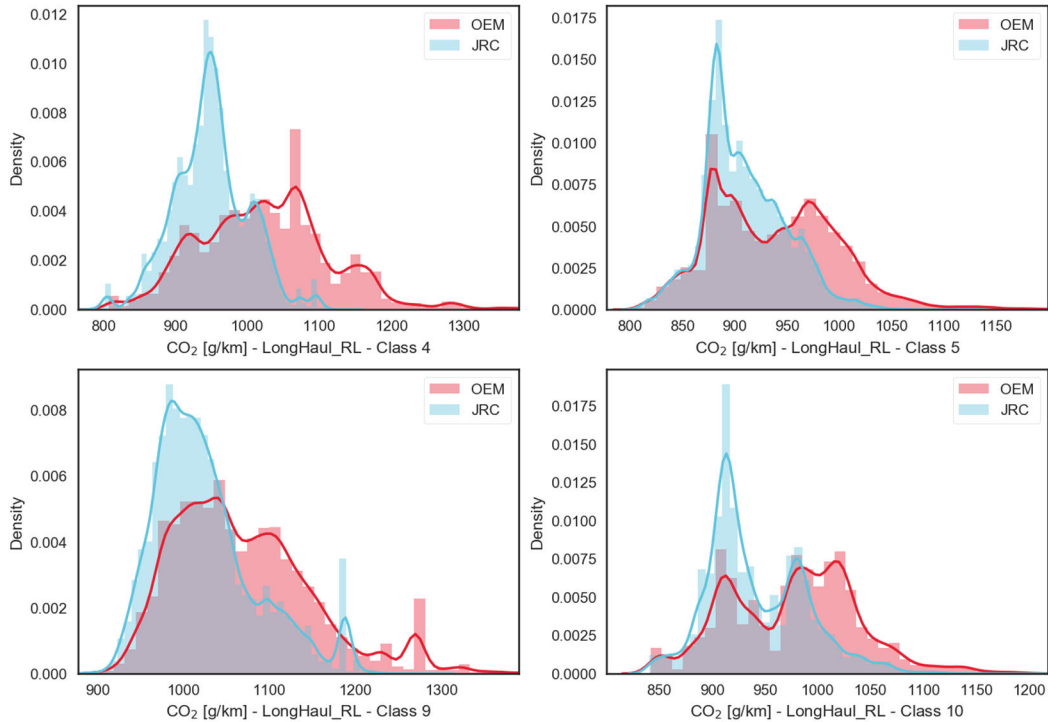
Figure 23. CO₂ emissions [g/km] comparison between OEM values and JRC normalisation (Long Haul, reference load)

The approach developed for obtaining the normalised version of the fleet CO_2 emissions becomes a valuable tool to control the data obtained from OEMs through the monitoring and reporting scheme. For example, a normalisation approach that takes inspiration from the one presented in this chapter is going to be used by JRC-STU to assess and normalise the VECTO results of year 2020; this exercise aims at creating the 2020 baseline needed to define the reference for 2025 and 2030 targets.

5.2 Fleet-representative CO₂ emissions calculation methodologies

To ensure that the official CO_2 emissions from the type-approval procedure are representative of the real efficiency of the vehicle, and that no flexibilities are

exploited by OEMs, the European Commission needs to be in possession of verification tools or procedures; this is necessary both for test-based and simulation-based CO_2 certification. Verification tools are therefore used to provide an indicative range of acceptable results to compare with the official value from the certification. This is normally obtained through an alternative methodology, likely less detailed, but still giving a good indication of a statistically valid result for the vehicle characteristics considered. With the purpose of creating such alternatives, two different activities were carried out which produced two valid solutions for the calculation of fleet-representative fuel efficiency values when some vehicle characteristics are given but the detailed components efficiency maps are missing.

5.2.1 CO₂ emissions calculation through VECTO and fleet-representative input file generation models

As explained in section 3.1.2, VECTO requires input files containing detailed component data and other vehicle characteristics in order to accurately calculate the vehicle fuel efficiency. In this section, a methodology to produce the input data through generalised models is presented. The PhD programme presented in this thesis contributed significantly to the development of this methodology, although the credits go mainly to the author of the relevant publication [44]. The contribution did not take place on specific topics or phases of the activity, but rather consisted in a continuous collaboration with different tasks assigned to each of the contributors; anyhow, the most significant contribution was provided in terms of data analysis, simulation, comparison of results and feedbacks for the models development.

For this activity, several models were developed to produce the required VECTO inputs. The starting point for the development and tuning of the models was the same database created for the obtainment of the HDV CO_2 emissions baseline presented in section 5.1, which was used to find correlations between EC, or FC, and the available technical specifications of the components.

5.2.1.1 Creation of the generalised VECTO input data

The following models were developed to create the necessary input data for engine FC map, engine full load and motoring curve, axle losses, gearbox losses and retarder losses. The models here presented are able to create VECTO simulation cases that are representative of the HDVs fleet. This result was obtained by

combining the observations derived from the HDVs fleet data and other pieces of information provided by the OEMs.

Engine fuel consumption map

The assumption of linear relationship between $BMEP$ and $FuMEP$ introduced in section 4.2 was used for providing a simple approach (using a small number of dimensions and parameters) for the creation of the engine FC map. A Principal Component Analysis (PCA) was then performed to identify families of similar engines referred to as clusters and assigning representative values for slope m and offset q to each of those. The formula for the identification of the engine cluster, according to the PCA, is the following:

$$C = 0.976 \times D + 0.209 \times T_{eng}^{max} \qquad\qquad Eq.17$$

where C is the calculated component value, D is the engine displacement in cubic centimetres and T_{eng}^{max} is the engine max torque in Nm. The value obtained with the formula is to be used in Table 8 to identify the respective engine cluster and get the most appropriate m and q for the engine considered. For the creation of the engine FC map, a grid of engine speeds and torques has to be created; each point of the grid is associated with a specific value of $BMEP$, which is then used in the linear relationship formula to obtain the respective $FuMEP$ and FC values.

Table 8. *BMEP-FuMEP* line parameters for each HDV engine cluster

Cluster	Component range	Slope (m)	Offset (q)
1	[0 - 5977)	2.246	1.411
2	[5977 - 7280)	2.261	2.656
3	[7280 - 8429)	2.222	2.142
4	[8429 - 10005)	2.155	2.691
5	[10005 - 11909)	2.11	2.393
6	[11909 - 14465)	2.146	1.896
7	[14465 -)	2.149	2.283

Engine full load curve

A trapezoidal shape with five points was assumed for the engine full load curve:

(P1)   the idling point

(P2)   the point with the minimum engine speed where the maximum torque is achieved

(P3)   the point with the maximum engine speed where the maximum torque is achieved

(P4)   the point of maximum engine speed where rated power is delivered

(P5)   the point of maximum engine speed where no torque can be delivered
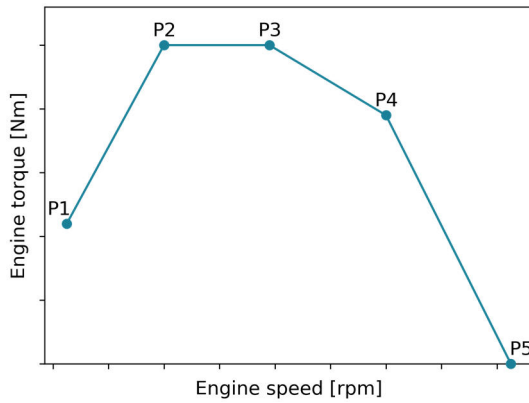
Figure 24. Generic full load curve HDVs engines [39]

Through these five points, it is possible to simplify and generalise with reasonable accuracy the majority of HDVs engines full load curves. This approach was adopted following the analysis of publicly available full load curves of several engine models with very different technical specifications. The resulting trapezoid is presented in Figure 24 and is defined for each of the engine clusters using normalised coordinates as reported in Table 9.

Table 9. Normalised engine speed and max torque by engine cluster

Cluster	Component range	Normalised engine speed					Normalised engine torque				
		P1	P2	P3	P4	P5	P1	P2	P3	P4	P5
1	[0 - 5977)	0	0.38	0.66	1	1.39	0.27	1	1	from torque at rated power	0
2	[5977 - 7280)	0	0.32	0.71	1	1.24	0.23	1	1		0
3	[7280 - 8429)	0	0.37	0.65	1	1.38	0.35	1	1		0
4	[8429 - 10005)	0	0.36	0.61	1	1.34	0.39	1	1		0
5	[10005 - 11909)	0	0.31	0.73	1	1.57	0.49	1	1		0
6	[11909 - 14465)	0	0.31	0.67	1	1.55	0.38	1	1		0
7	[14465 -)	0	0.32	0.66	1	1.58	0.34	1	1		0

To denormalise the coordinates, the following formulas shall be used:

$$T = T_{Px} * T_{max} \qquad\qquad Eq.\,18$$

$$RPM = RPM_{idle} + RPM_{Px} * (RPM_{rated} - RPM_{idle}) \qquad Eq.\,19$$

where T_{Px} and RPM_{Px} are the normalised coordinates from the specific engine cluster, T_{max} is the maximum engine torque in Nm, RPM_{idle} and RPM_{rated} are the engine speed in rpm at idling and rated power respectively.

Axle and gearbox loss maps

The loss maps of axle and each gear of the gearbox can be created through a common model and defined according to a normalised grid of points that indicates the domain to be covered (Figure 25). The torque loss for each denormalised grid point is calculated as:

$$n_{in} = n_{norm} * n_{in}^{max} \qquad \qquad Eq. 20$$
$$T_{in} = T_{norm} * T_{in}^{max} \qquad \qquad Eq. 21$$
$$T_{loss} = (a + b * n_{in} + c * |T_{in}|) * T_{in}^{max} \qquad Eq. 22$$

where n_{in} is the rotational speed of the component, T_{in} is the torque input and T_{in}^{max} the maximum torque input. It was found that gearbox direct gears (gear ratio = 1) have a different set of coefficients than the indirect gears (gear ratio $\neq 1$). For this reason, three sets of model parameters are provided (gearbox indirect, gearbox direct and axle) in Table 10.
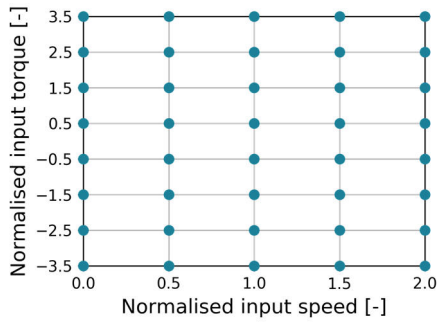
Figure 25. HDVs axle and gearbox grid

Table 10. HDVs axle and gearbox model parameters

Component		a	b	c
Gearbox	indirect	0.001	0.27	0.05
	direct	0.001	0.27	0.01
Axle		0.0005	0.02	0.04

Retarder loss map

The retarder loss model here presented was developed through a normalisation approach and investigation of the existing correlation. It can be applied regardless of the position of the retarder in the driveline [44]. The application of the model requires a normalized series of the input retarder speed with a range of 0 to 1, which is denormalised based on the retarder's maximum input speed. The calculation of losses is finally obtained as:

$$n_{norm} = \frac{n_{ret}}{n_{ret}^{max}} \qquad \qquad Eq. 23$$
$$T_{loss} = (a \cdot n_{norm}^2 + b \cdot n_{norm} + c) * T_{in}^{max} \qquad Eq. 24$$

where n_{ret} and n_{ret}^{max} are retarder speed and maximum retarder speed in rpm, T_{in}^{max} is retarder maximum input torque in Nm, and a-b-c are the regression coefficients (respectively 2.342e-2, 0 and 4.684e-3).

5.2.1.2 Validation and discussion

The methodology was used to create the inputs for running VECTO simulations. The results were then compared with a subset of the data obtained from vehicle OEMs (database presented in section 5.1), not corrected for input data quality, mainly focusing on the overall fleet-wide performance rather than the vehicle-to-vehicle one; this comparison, for each cycle and HDV group, is presented in Figure 26. The error obtained on the individual losses remained in all cases within the ±3 %, exception made for gearbox losses that are associated with discrepancies in the order of -35 % to -40 % but with a minor impact on the overall result (see the relevant publication for the detailed analysis [44]). The relative error distributions do not exceed the ±2 % for most of the cases, but a bias of about -0.6 % and -1 % is found for the LH and the RD respectively, therefore resulting in an underestimation of the CO_2 emissions; an explanation is likely found in the underestimation tendency of the gearbox losses model. The methodology can be applied for the estimation of the fleet-wide average fuel efficiency [44].
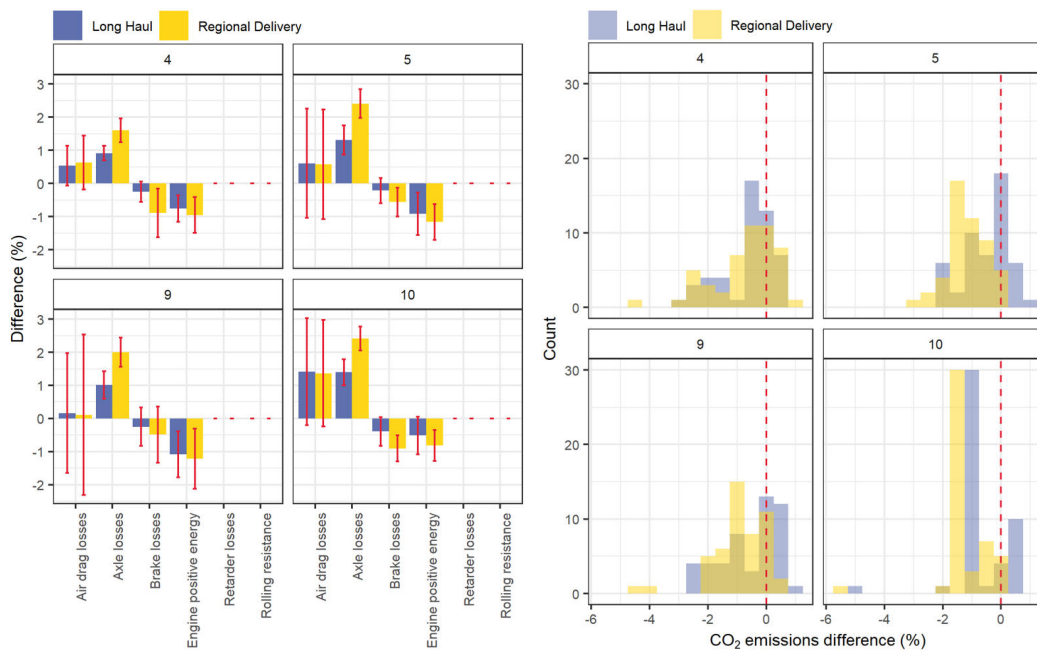
Figure 26. Results of the generalised VECTO input data generation approach [44]

5.2.2 CO$_2$ emissions calculation through VECTO-derived correlation formulas

VECTO uses detailed components efficiency maps to calculate the instantaneous conditions and the associated instantaneous losses at vehicle level. This requires that simulation time is discretised according to the best compromise between accuracy and use of computational resources and that calculations are performed for each time sample. Furthermore, for each vehicle setup, VECTO simulates multiple cycle-loading conditions (from 4 to 10 depending on the vehicle configuration) some of which are associated with a long driven distance (approx. 100km for both Regional Delivery and Long Haul cycles) requiring longer simulation time. The combination of these aspects turns VECTO simulation into a very demanding task for those who want to run multiple simulations for the creation of scenarios. When different scenarios are to be evaluated, and the fleet-level picture has to be obtained, the whole vehicle fleet (or a representative subset) has to be considered and a significant number of cases has to be created and executed through the calculation tool. In such cases, running a fully detailed simulation would require considerable computational resources and amount of time. From JRC internal data, it was identified that the vehicle fleet presented in section 5.1 would require the generation of about 90'000 different VECTO cases; considering an average execution time of 45', its execution would require 47 days approximately. The level of detail associated with fully detailed modelling is undoubtedly necessary for type-approval needs, but for other research purposes (e.g. creation of scenarios) other solutions that require a smaller use of computational resources and time might be considered. This becomes even more legitimate when the detailed components efficiency maps are missing and they can only be replaced by generic models, with an inevitable impact on the accuracy of the instantaneous results and their significance. Therefore, the methodology presented in this section does not make use of VECTO fully detailed simulation approach but rather relies on existing correlations between VECTO input data (e.g. vehicle characteristics) and the output obtained after the VECTO fully detailed simulation.

Furthermore, this activity wanted to analyse the sensitivity of specific inputs with respect to the total calculated EC of a vehicle on a specific mission profile, also presenting the average EC breakdown. The methodology and the information presented in the relevant publication [45] should serve as a guideline to calculate (or guess without any calculation) with acceptable accuracy the energy consumed for the different aspects concurring to the overall vehicle EC, without performing fully detailed simulations.

5.2.2.1   Overview, basic principles and applicability

The data used to support this activity is the same data collected from OEMs for the creation of the HDTs CO_2 emissions baseline (presented in section 5.1) of which only the results of the Regional Delivery and Long Haul cycles were considered. For the presentation of the energy breakdown, the normalised version of the fleet fuel efficiency calculated in [43] was used, whereas for the development of the correlation formulas the original dataset was used as only the sensitivity between inputs and outputs had to be captured. The way energy is consumed in HDTs is presented Figure 27 that includes the Regional Delivery cycle, the Long Haul cycle - in both loading conditions (low and reference) - and all the HDT groups (4, 5, 9 and 10). Pictures of the energy breakdown for the specific cycle-loading combinations and for specific subgroups are reported in the publication [45].

Figure 27. HDTs fleet energy consumption breakdown
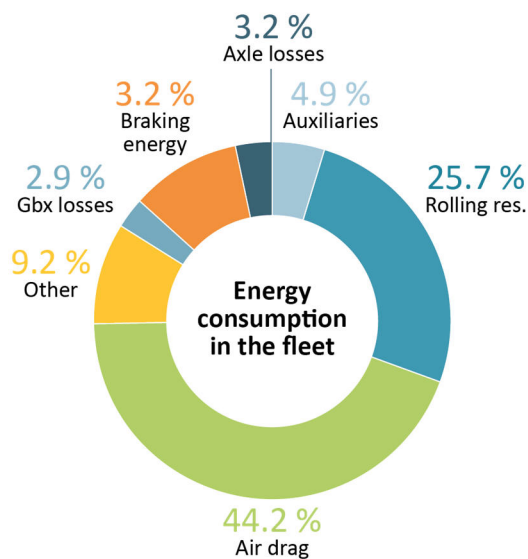
According to the figure, the impact of air drag and rolling resistance on the total EC downstream the engine is approx. 70% (engine efficiency not taken into account). This finding constitutes the main principle on which the methodology presented in this section relies: to obtain an accurate estimate of HDTs EC, the energy spent for air drag and rolling resistance has to be obtained with the best accuracy possible, whereas for the other energy losses it is less important to have an accurate representation. Therefore, the inputs used for air drag and rolling resistance should possibly have the same quality as the ones required by VECTO full simulation for certification purposes. This requirement ensures that an acceptable result is obtained also when generic values

or models are used for the other aspects. The methodology follows a step-wise process that begins with the calculation of the individual energy consumptions that take place downstream the driveline, at wheels level, and reconstructs the total energy flow with a backward-looking approach, finally obtaining the total positive energy produced at the engine and the related FC and CO_2 emissions. All the definitions used here to refer to vehicle specifications and energy balance terms are presented in Table 13 in Appendix B. Some assumptions had to be made with respect to the driveline architecture in order to be consistent with the reconstruction of the energy flow and the subsequent calculation of losses. Figure 28 presents the driveline layout that was taken in consideration and the location where energy losses take place. In particular, the retarder was considered to be of the "secondary retarder" type, as appears in VECTO; this layout is named "transmission output retarder" in Regulation 2017/2400, meaning that its position in the driveline lays between the gearbox and the axle. No angle drive component was considered to be part of the driveline model, because of the marginal share in the truck fleet. Vehicles equipped with fully automatic gearboxes (defined "ATSerial" in VECTO) were excluded from the study since the amount of data available was not sufficient to draft a reliable correlation formula. Hence, losses associated with these two component types were not considered (E_angle for angle drives, E_tc_loss and E_shift for fully automatic gearboxes). For vehicles equipped with manual transmission (MT) or automated manual transmission (AMT), the energy loss due to the operation of the clutch was considered to be negligible and for this reason, excluded from the calculation. Since
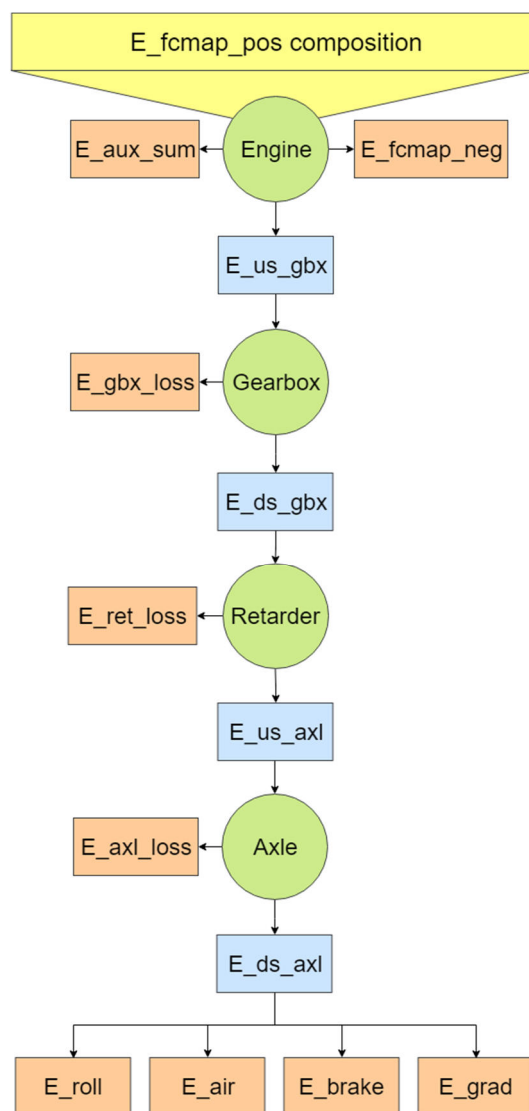

Figure 28. HDVs driveline energy flow scheme

the cycles considered for the analysis are exclusively the Long Haul and the Regional Delivery ones, the energy losses due to Power Take-Off (PTO) devices were also neglected at this stage. Some of the records from the original dataset were rejected in order to keep only the data associated with realistic losses and obtain robust correlations. Python language was used to handle and analyse the data. Plots were created using mainly *pandas*, *numpy* and *matplotlib* libraries. To obtain the correlations, the *curve_fit* tool from *scipy optimize* was used. The applicability limitations of the methodology, which are mainly due to the filtering of the data and the vehicle configurations that were considered, are presented in the relevant publication [45]. Anyhow, the stepwise methodology allows for the replacement with alternative models/calculations of part(s) of the process on the need of the user; consequently, its applicability can be easily widened when a different vehicle configuration has to be covered (e.g. replace the gearbox losses correlation formula with a user-defined one that is tailored for fully automatic gearboxes).

5.2.2.2 Development of the correlation formulas

For every source of energy loss (at component level or vehicle level), the parameters having a direct influence were investigated and the best correlation formula was identified. Where possible, the correlation formula identified reflects the physical phenomena (e.g. energy for rolling resistance, *E_roll*, and road gradient, *E_grad*) and is produced in the most generic way possible (i.e. the same correlation formula applies to multiple HDV groups and cycles); where this was not possible, either for the lack of a clear correlation or the appropriate input parameters, the correlation was produced using a common formula but with different set of fitting parameters for the different HDV groups and cycles. For those energy losses where it was not possible to find a clear and physically valid correlation formula, a generic fitting formula with the following structure was investigated

$$z = a + b*x + c*y + d*x*y \qquad\qquad Eq.25$$

Where z is the energy loss to be calculated, x and y are two variables correlated with z and finally a, b, c and d are the parameters obtained for the fit. Differently from more sophisticated clustering methods, this simple correlation approach allows to extract the main characteristic dependencies between the physical parameters and the observed quantity without losing the underlying physical meaning. The correlation formulas produced are presented and explained in detail in the relevant publication [45]. The dependency among the energy losses and the parameters used for the fits can be seen in the examples presented in Figure 29,

where some of the pictures are reflecting the whole fleet (e.g. energy for rolling resistance in picture *a*) and some other just specific subgroups (e.g. energy for engine friction in picture *f*).
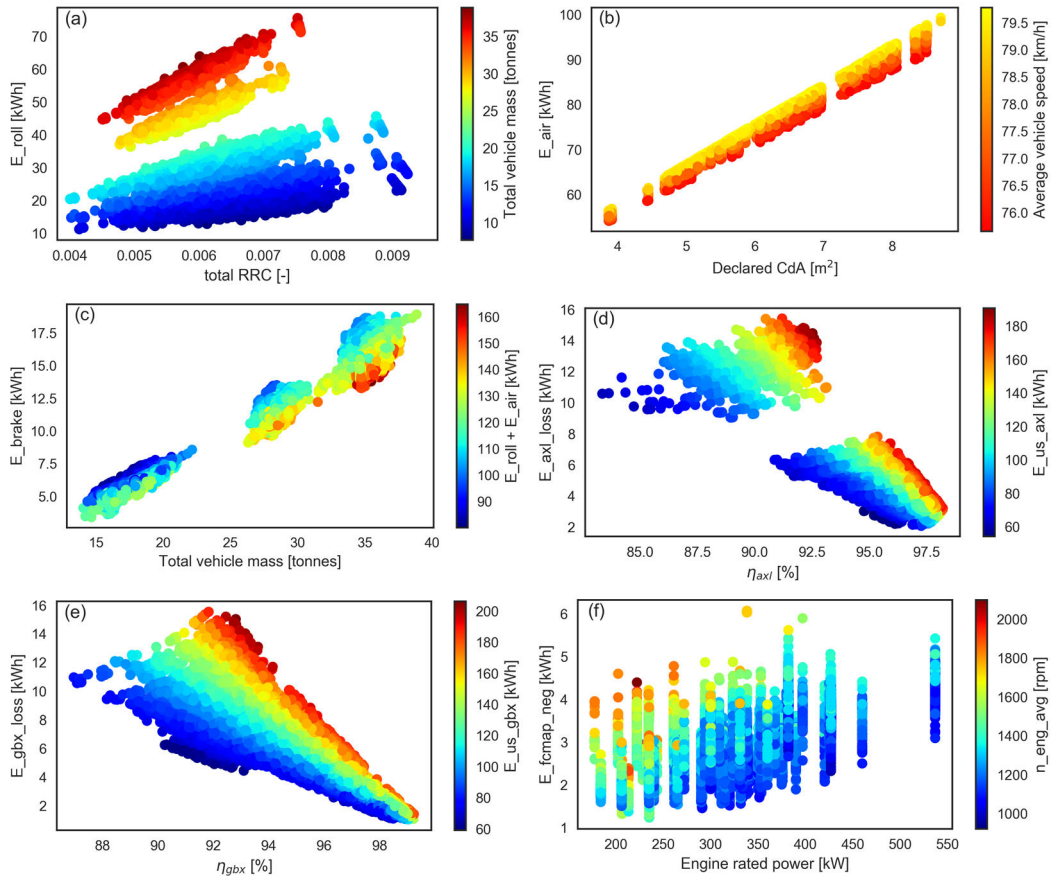
Figure 29. HDVs energy losses correlations

Dependencies of *E_grad*, *E_ret_loss* and *E_aux_sum* are not present in the figure since no correlation is needed but rather a fixed representative value or calculation formula with a physical meaning. The correlation formulas were produced in a way to minimise the error associated with the approximation and have average error close to zero.

5.2.2.3   *Application of the methodology*

As explained in the previous sections, the workflow starts with the calculation of the energy consumed at wheels level and follows with the calculation of the total energy flowed in different locations upstream the driveline through a backward-looking approach. The main steps are here summarised:

(1) *E_ds_axl*: the total energy downstream the axle is calculated as the summation of energy spent for rolling resistance, air drag, braking and road gradient

(2) *E_us_axl*: the total energy upstream the axle is obtained dividing (1) by axle average efficiency through an iterative process

(3) *E_ds_gbx*: the total energy downstream the gearbox is obtained as the sum of (2) with retarder losses (if present)

(4) *E_us_gbx*: the total energy upstream the gearbox is obtained dividing (3) by gearbox average efficiency through an iterative process

(5) *E_fcmap_pos*: the total positive energy produced at the engine is obtained as the sum of (4) with the energy losses for auxiliaries and engine friction (*E_fcmap_neg*)

The steps of the calculation are better detailed in the scheme in Figure 74 (Appendix B), which highlights all the inputs needed and the calculation steps. When the total positive energy produced at the engine in kWh (*E_fcmap_pos*) is obtained, it is possible to calculate the metrics of interest for FC and CO_2 emissions. This step can be performed in multiple ways associated with different accuracy levels depending on the requirements. The easiest way is to derive an indicative average engine efficiency from the distributions presented in [43] (Figure 22 in section 3.3.4.1), which can be used to divide the *E_fcmap_pos*, therefore obtaining the total fuel energy needed for the cycle. Subsequently, the same declaration values used by VECTO with regards to fuel properties (density, CO_2 per FuelWeight, LHV) can be used to derive all the metrics of interest. A more appropriate way to calculate the average engine efficiency is to adopt the approach presented in section 5.2.1.1 and in the relevant publication [44], where the average engine operating condition $\overline{BMEP}$ is used to obtain the indicative $\overline{FuMEP}$ through generalised engine efficiency lines. In Figure 30 are presented the relative error produced with the correlations for each energy loss (left), the overall relative error (top right) and the *E_fcmap_pos* absolute values comparison (bottom right). For all the energy calculation models of which the methodology consists, the correlations proposed have a mean relative error that is close to zero, exception made for *E_aux_sum* and *E_fcmap_neg*, which might need some further tweaking. Anyhow, the impact of such aspects is small and the accuracy of the results is consistent with the purpose of the methodology proposed. The resulting mean relative error of the whole methodology is -0.243 %, meaning that the model is lightly underestimating the EC; this deviation is probably caused by the systematic errors in air drag and auxiliaries EC calculation. From the distribution plot of the methodology relative error, it is possible to conclude that the vast majority of cases falls within the ±3 %. Given that no full simulation was

required to obtain these results, it can be concluded that the methodology is meeting the requirements of accuracy and lightness that are needed to constitute a valid alternative to VECTO simulation for verification purposes.
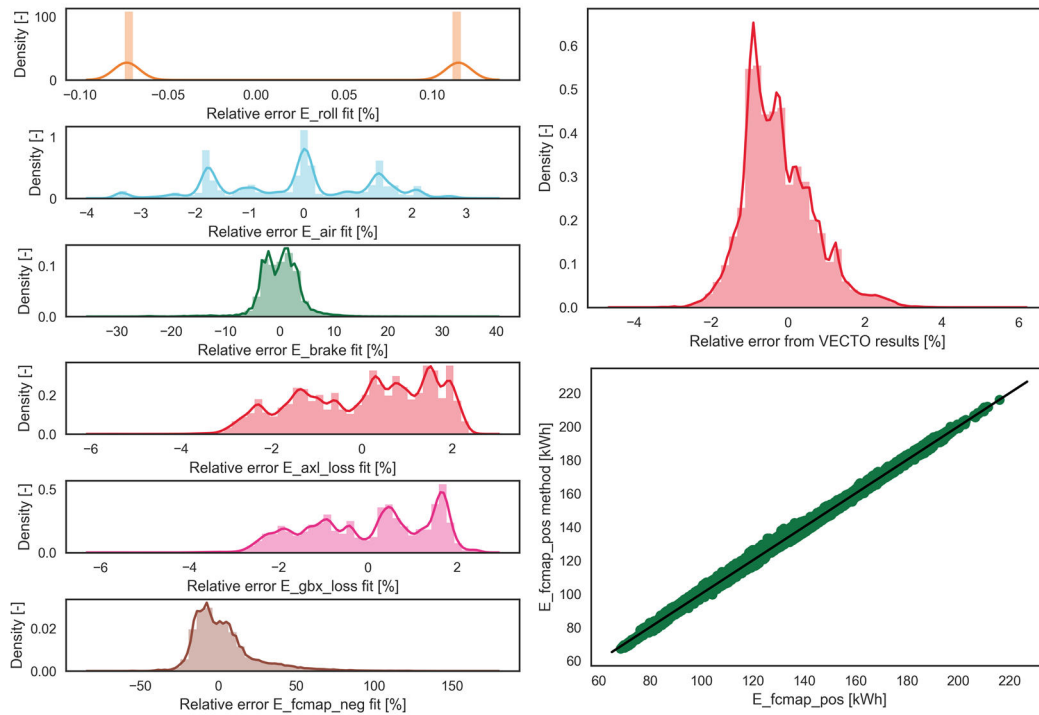
Figure 30. Accuracy of the VECTO correlations methodology

The methodology presented in this section, due to the light calculation workflow, the little amount of input data required and the good accuracy, is suitable to be implemented in calculation tools for the estimation of EC from HDVs with different purposes. For example, it can be used to estimate the expected EC reduction produced by different vehicle specifications (e.g. reduced Air Drag CdA, increased axle or gearbox efficiency, etc.). Furthermore, another possible application of the methodology is to use it as the back end calculation approach for online tools for EC, FC and CO_2 emissions estimation, in a similar way to what is done for LDVs with the Green Driving Tool from the European Commission [46]. The methodology can be supported by a database for generic vehicle specifications to reduce even further the amount of input data required, finally allowing users with all levels of background to obtain the wanted results.

Chapter 6

6   Hybrid LDVs CO$_2$ experimental activities

In the period between 2017 and 2019, several HEVs with different powertrain architectures were tested, with the goal of obtaining the CO$_2$ emissions according to the type-approval procedure and for data collection supporting the development of a simulation strategy. According to Regulation 2017/1151 [47], a vehicle is hybrid electric if, apart from the Internal Combustion Engine (ICE), at least one of the propulsion energy converters is an Electric Machine (EM). The vehicles were tested in the JRC's VELAs, with the minimum instrumentation required to reconstruct the electrical and mechanical energy flow. The experimental setup, the tests carried out and some of the findings are presented in this chapter.

6.1 Test facilities and instruments

The tests were carried out in VELA 8, the Electric and Hybrid Vehicles Testing Facility of the JRC. It consists of a two-axis roller bench of 300 kW each, with maximum speed of 260 km/h and acceleration of ±10 m/s, capable of testing electric and hybrid vehicles and their supply equipment from -30 °C to +50 °C under controlled humidity applying a whole series of analytic scientific instruments. The facility is designed to perform tests on vehicles powered with different fuels (gasoline, diesel fuel, LPG, natural gas, hydrogen etc.). A state-of-the-art measuring system provides a complete analysis of the remaining exhaust gas emissions from hybrids. The possibility to run tests at most different temperatures gives valuable

information about the performance of electric and hybrid vehicles in winter and summer conditions for the evaluation of heating, ventilation and air conditioning influence [48]. VELA 8 emissions measurement system was customised in order to allow reliable hybrid vehicle testing during the phases when the ICE is not active. Tailpipe pressure control avoids sucking intake air through the engine inlet valve when the vehicle shifts from the thermal engine mode to the pure electric mode, so that similarly to real-world operations, the exhaust gas after-treatment system is not artificially cooled down [49]. The standard measurements that are obtained from the laboratory automation software are vehicle speed, force applied by the dyno, ambient conditions (pressure, temperature and humidity), dilution tunnel flows (dilution air flow, exhaust gas flow, constant volume sampler flow), pollutants and GHG concentration and instantaneous emissions, pollutants and GHG bag values and On-Board Diagnostics (OBD) data. In addition to these quantities, depending on the vehicle and the goal of the test campaign carried out, other measurements were added to get a more complete picture of the hybrid powertrain operation. Three main solutions were adopted to increase the amount of information obtained: extended Parameter IDs (PIDs) OBD logging, Controller Area Network (CAN) data logging (typically associated with high sampling rates) and hybrid powertrain electrical measurements through power analysers. In most of the cases, the combination of these three data collection methodologies allowed to collect all the needed instantaneous quantities, characterise the powertrain operation, reconstruct the energy flow and analyse the vehicle energy management strategy choices. The outcome of these testing activities proved to be crucial in supporting the modelling activity presented in the next chapter with respect to its development and validation.

VELA 8 – the Electric and Hybrid Vehicles Testing Facility of the JRC (source: JRC)

6.1.1 CAN logging

The CAN bus is a network used to connect all the control units of the vehicle and enable the communication (see Figure 31). During vehicle operation, all control units send and read messages on the bus. The structure of a CAN message is standardised (see Figure 32), but the way the data is encoded is OEM proprietary. To extract the information contained in the data bytes of the messages, the so-called DBC file is needed; this file describes which bits have to be used and what formula has to be applied to obtain a specific information out of the data bytes, according to the following formula:

$$scaled\ data\ value = offset + scale * raw\ decimal\ data\ value \qquad Eq.26$$

For the vehicles tested, a company collaborating with the JRC provided the DBC files; for each of them, CAN data consistency check was performed. For reading and logging the messages being transmitted, a CAN interface has to be connected to the CAN bus. The access to the CAN bus can be prepared in between the control units, on the two wires of the bus (high and low) after they have been identified. For some vehicles, the CAN bus can be found on the OBD-II plug (explanation in the next section), and no preparation work is needed.
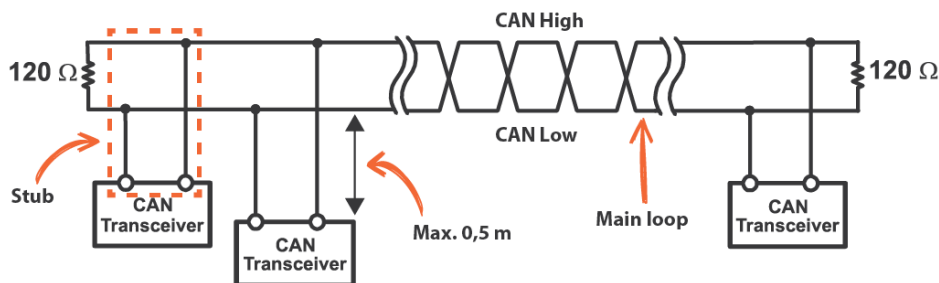
Figure 31. Architecture of the CAN bus (source: www.kmpdrivetrain.com)
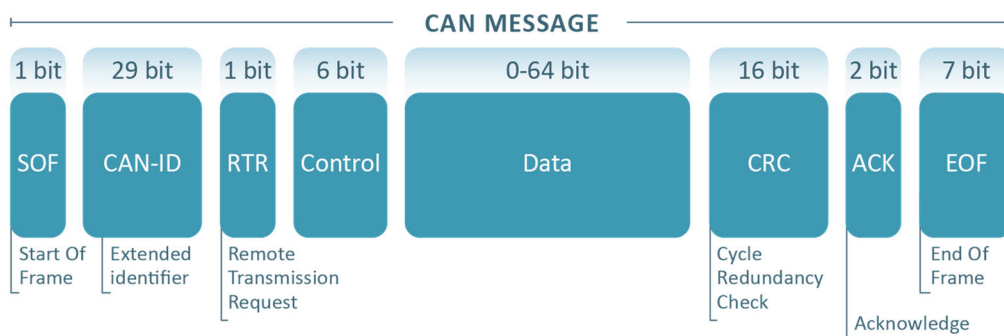
Figure 32. Typical structure of a CAN message (source: www.csselectronics.com)

6.1.2 OBD standard and extended PIDs logging

OBD is the standard that defines the vehicles self-diagnostic and reporting capability. The European OBD (EOBD) standard became mandatory for all gasoline vehicles in 2001 and all diesel vehicles in 2004 [50]. The service is physically supported by the vehicle CAN communication bus; the OBD clients, diagnostic tools or OBD loggers, are interfaced to the CAN bus through the gateway and the standardised OBD-II plug (see Figure 33). The standard allows for the reading of real-time parameter IDs (PIDs) about vehicle and powertrain operation, many of which are standardised according to SAE J1979: vehicle speed, accelerator pedal position, ICE speed, ICE percent load, ICE coolant temperature, mass air flow, equivalence ratio and others. Some of the standardised PIDs are mandatory, hence they will be found in the OBD data; some others are standardised but not mandatory, therefore the OEM can decide whether to provide any of them. Among the standardised not-mandatory PIDs, we can find the high-voltage Traction Battery (TB) State Of Charge (SOC), current and voltage, the ICE torque, the catalyst temperature and many others. Lastly, there are PIDs that are not standardised, so the way to request and decode the information is custom; these extended PIDs, although difficult to obtain, provide very handy real-time data: EMs speed, EMs torque, EMs temperature, TB temperature, TB power limits and others. To obtain the PID value, the same scaling formula presented in $Eq. 25$ for CAN is used.
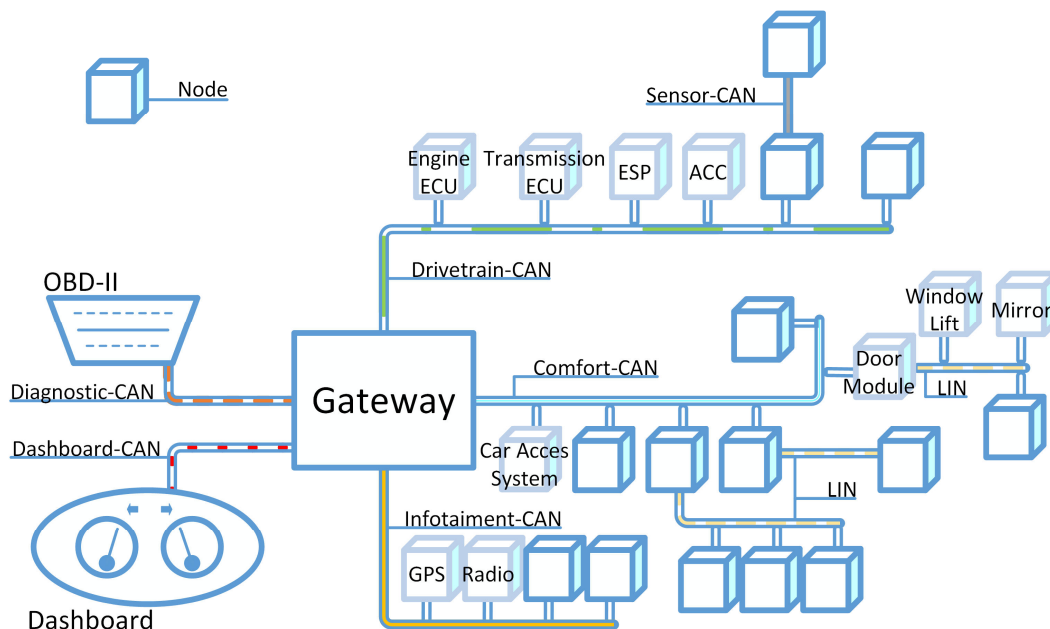
Figure 33. Generic model of a vehicle CAN bus with OBD plug (source: Thomas Huybrechts et al. [51])

OBD data is typically obtained through a request-response process. The request message contains the identifier (address of the receiver, or broadcast address), the length of the request in number of bytes, the mode of the request according to SAE J1979 and the PID. The OBD client formulates a request that passes through the gateway, reaching the control units connected on the CAN bus; one or more receivers reply to the request by sending a response message that circulates on the CAN bus and passes through the gateway reaching the OBD client. In Figure 34, the typical response message received after a standard OBD request is presented; from the picture, it is possible to understand which are the bytes associated with data (A, B, C and D, in hexadecimal system). Some specific OBD requests, differently from the case presented in the picture, trigger a response process that comprises of more than one message (Figure 35); in this case, which is recurrent for the extended PIDs requests, the response obtained is in the form of a matrix and requires to be handled differently. For enabling the extended PIDs logging, the automation software of VELA 8 was improved to grant more flexibility towards the formulation of custom requests and the decodification of the response messages. For some activities, it was not possible to implement the vehicle-specific extended PIDs logging; therefore, other appropriate logging tools were used (when available) and data alignment with the lab measurements was performed. For all the experimental activities carried out, as many PIDs as possible were obtained and recorded from the hybrid powertrain, recurring to both standard and extended PIDs.

OBD2 MESSAGE (response)

11 bit	64 bit							
Identifier	#Bytes	Mode	PID	A	B	C	D	Unused
(e.g. 7E8)	(e.g. 03)	(e.g. 41)	(e.g. 0D)	(e.g. 32)	(e.g. aa)	(e.g. aa)	(e.g. aa)	(e.g. aa)

Figure 34. Typical structure of an OBD response message (source: www.csselectronics.com)

11 bit	64 bit							
Identifier	10	#Bytes	Mode	PID	A	B	C	D
Identifier	21	E	F	G	H	I	J	K
Identifier	22	L	M	N	O	P	Q	R
Identifier	23	S	T	U	V	W	X	Y
Identifier	24	Z	AA	AB	…	…	…	…
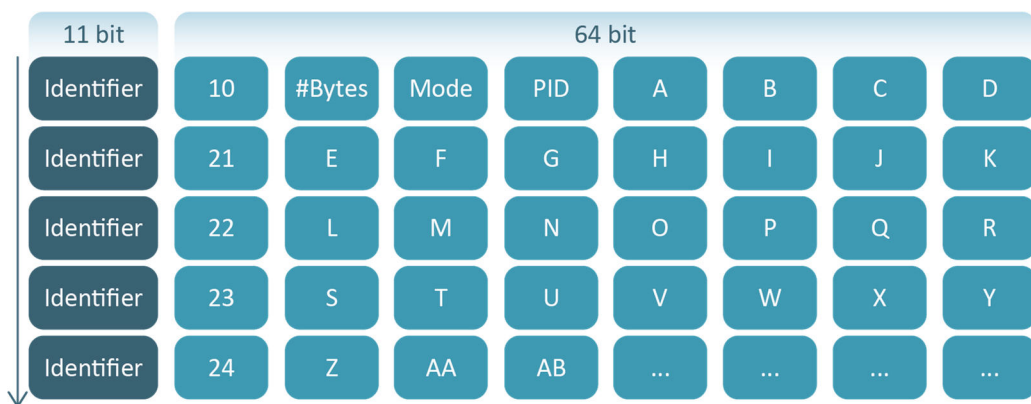
Figure 35. Typical structure of an OBD response with multiple messages

6.1.3 Power Analyser measurements

Measurement of electrical quantities was always performed to obtain the Direct Current (DC) power flowing in or out of the TB, the Service Battery (SB) and the DC/DC converter. To perform power measurements, voltage probes and current clamps were used. Power analysers were employed as a Data Acquisition System (DAQ); these instruments provide multiple channels to perform electrical measurements of voltage and current. The sampled current and voltage values are also processed by the power analysers to calculate the instantaneous power (active, reactive, apparent), integrals (cumulative energy, cumulative charge) and other metrics of interest. The JRC-STU disposes of three power analysers with similar functionalities (see Figure 36): Hioki 3390 (4 channels), Yokogawa WT1800 (6 channels) and Dewesoft Sirius (8 channels).

Figure 36. Power analysers of the JRC-STU (Hioki top left, Yokogawa bottom left, Dewesoft right)

The latter was used to measure the Alternate-Current (AC) power of the EM(s) for those vehicles where OBD and CAN logging did not provide a complete picture of the Electric Energy (EE) use. The measurement can be performed using the delta connection, which required only three wires (one for each EM phase, no neutral line): a current clamp is put on each of the EM phases, and the phase-to-phase voltage differences are measured (1-2, 2-3, 3-1) as presented in Figure 37. The voltage difference 1-2 is to be measured on the same channel with line 1 current, difference 2-3 with line 2 current, and finally difference 3-1 with line 3 current. The

sampling rate for performing the AC power calculation has to be at least 100 kHz; this is necessary for capturing the high frequency switching of the inverter. The source to be used for the identification of the frequency is the current signal, as the voltage signal is not sinusoidal (pulses are modulated in width or amplitude).
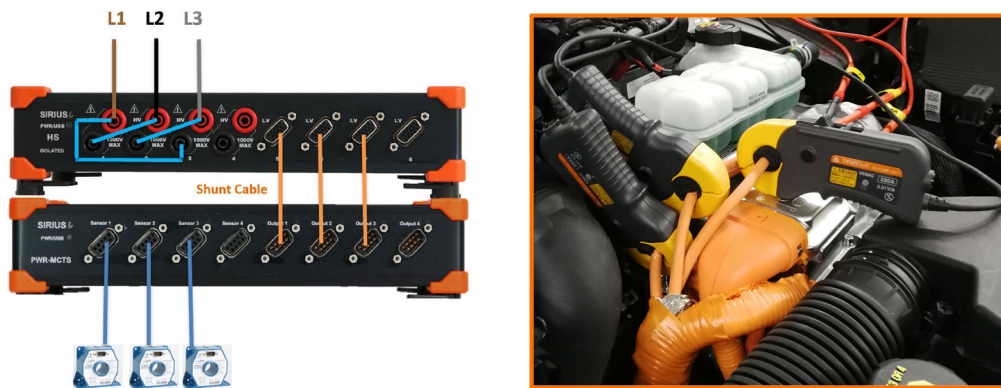
Figure 37. AC motor power measurement with delta connection

6.2 Vehicles tested

The list of vehicles for which the testing campaign provided a detailed picture for the characterisation is reported in Table 11. Because of the type of activities that the JRC-STU is performing, the details for some of the vehicles are confidential; therefore, only the hybridisation level (mild, full, plug-in, range extender), the architecture (serial, parallel, and power-split), the segment and the indicative electric power ratio are reported. The latter is obtained as the sum of the rated power of the EMs used for propulsion divided by the rated power of the ICE; the result is truncated to the first decimal. The vehicle enumeration follows the order in which they were tested.

Table 11. List of hybrid LDVs tested

	Hybridisation level	Architecture	Segment	EMs to ICE power ratio
Vehicle 1	Range Extender	Serial	Hatchback	5.0
Vehicle 2	Full	Parallel	SUV/Crossover	0.4
Vehicle 3	Plug-in	Serial-Parallel	SUV	1.3
Vehicle 4	Plug-in	Parallel	SUV/Crossover	0.6
Vehicle 5	Mild	Parallel	Hatchback	0.1
Vehicle 6	Full	Power-split	Hatchback	0.7

Figure 38 reports the scheme of the generic hybrid vehicle architecture, where FD stands for Final Drive, TR for transmission (gearbox, Continuous Variable Transmission, planetary gearset), CT for Clutch/Torque converter, EPS for Electric Power System, and lastly P* represents the EMs positioning in the driveline according to the following nomenclature:

- **P0** → the EM is connected to the ICE belt
- **P1** → the EM is connected to the ICE crankshaft
- **P2** → the EM is upstream the transmission
- **P2_pla** → the EM is connected to the planetary side (explanation below)
- **P3** → the EM is upstream the final drive (front and rear)
- **P4** → the EM is mounted on the wheel (front and rear, left and right).
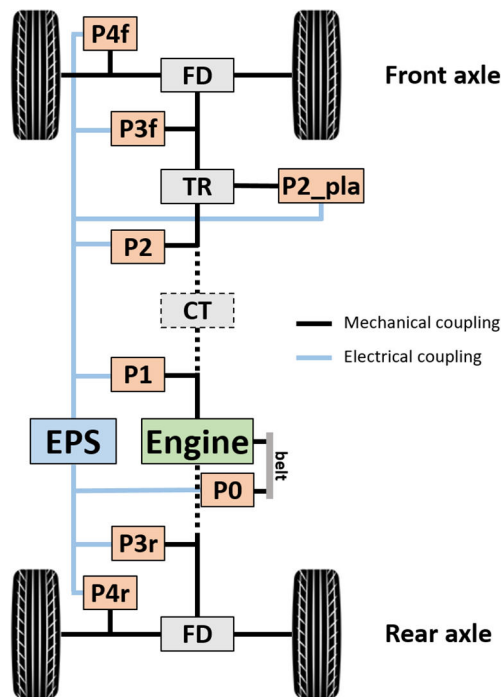
Figure 38. Generic hybrid vehicle architecture

P2_pla only applies to vehicles equipped with a planetary gearset. The presence of this component implies that the hybrid architecture is of the power-split type; the transmission is, therefore, a planetary gearset with three gears (sun, carrier, and ring), that correspond to three different sides: the ICE, the FD and Planetary Side (PS). The latter is where the P2_pla is mounted; this side is typically the one connected to the sun gear of the planetary gearset, and the EM here mounted is typically used as a generator, although for some operating conditions its function switches to motoring. In the picture, some mechanical coupling lines and some components are associated with dashed lines to indicate that these parts might or might not be present depending on the architecture; e.g., serial architectures do not have any mechanical coupling between the ICE and the driveline, therefore they also miss the CT. The ICE is assumed, for simplicity, to be always connected to the front axle. Based on the scheme here presented, the driveline architectures of the tested vehicles are reported in Appendix C (Figure 75 and Figure 76). The generic hybrid vehicle architecture presented in Figure 38 is also essential for modelling purposes as it enables the simulation of different hybrid architectures through a

single modelling approach; this generic hybrid architecture is used for the simulation strategy implemented in CO_2MPAS (explained in the next chapter).

An example of the powertrain characterisation that is possible to carry out by combining electrical measurements with OBD-CAN logging is presented in Figure 39, which shows the data acquired in the test campaign of Vehicle 4; a complete picture of powertrain operation can be obtained. Alternatively, to have a similar overview of powertrain operation, an individual characterisation of the components should be performed, which requires that they are unmounted from the vehicle to perform individual testing and derive efficiency maps. The combination of OBD-CAN logging with electrical measurements allows to get a similar result in a time- and resource-efficient way. With the data obtained from the experimental activities it was possible to reconstruct with reasonable accuracy the energy flow in the driveline, enabling the identification of indicative components efficiency, either in the form of constant values or lookup tables.
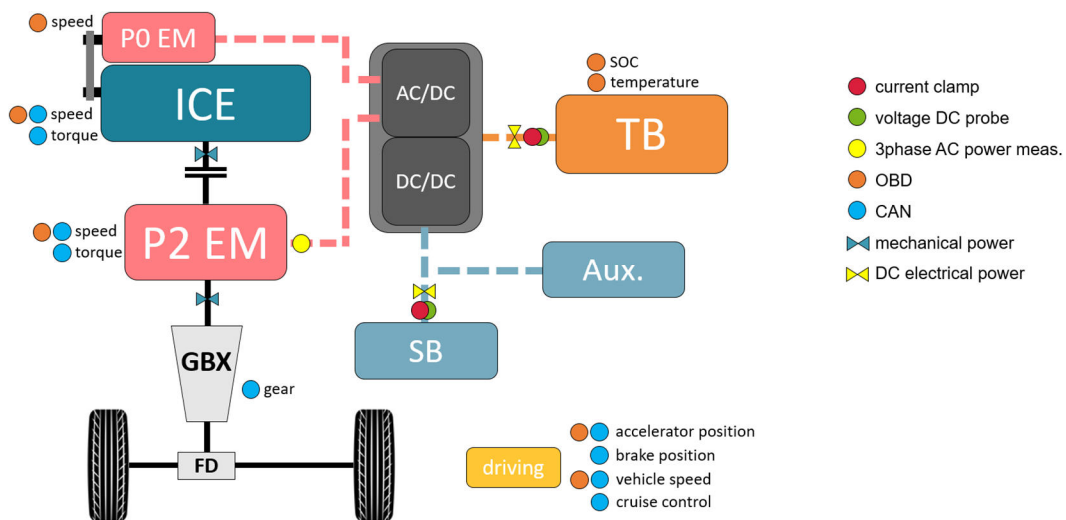
Figure 39. Powertrain characterisation through electrical measurements and OBD-CAN logging

6.3 HEVs Type-approval test

Both NEDC and WLTP procedures require that the electricity balance is measured during the test; this is to correct, when needed, the measured FC and CO_2 emissions to reflect a neutral electricity balance using the formulas later introduced. The NEDC only relies on the difference in the electrical charge stored in the TB; the current flowing in or out of the battery is measured over time and the integral of the current signal is calculated, obtaining a battery balance in Ampere hour (Ah). The

WLTP relies on the difference in electrical energy stored in the whole vehicle. Therefore, all the batteries fitted on the vehicle have to be measured. The current flowing in or out of the batteries is measured over time, and multiplied by the battery instantaneous or nominal voltage; the integral returns the energy balance of the battery in Watt hour (Wh). The total electricity balance is obtained as the sum of the energy balances of the individual batteries. Since the calculation of the electricity balance requires the integration of current over time, even the smallest measurement error might cause a significant deviation of the result. For example, if the current clamp was affected by a constant offset of 1A, this would cause an error in the electricity balance result of 0.33Ah over the NEDC and 0.5 Ah over the WLTC. These quantities correspond to the 6.4 % and the 10 % of a 5 Ah battery (the average battery capacity of a full-hybrid, assuming for example 1.2kWh total energy and 240V nominal voltage), respectively. Therefore, it is crucial to check instruments zeroing at the beginning and at the end of each test to guarantee the correct estimation of vehicle electricity balance. The type-approval procedure requires that the electricity balance is monitored throughout the whole test, which differs between Not Off-Vehicle Charging (NOVC) HEVs, which operate exclusively in Charge-Sustaining (CS) mode, and Off-Vehicle Charging (OVC) HEVs (also called plug-in vehicles), which has the Charge-Depleting (CD) as additional operation mode. The former class refers to vehicles where the TB SOC is always self-balanced; the SOC is allowed to vary within a window to enable the optimisation of the powertrain operating condition, but no intensive and long-lasting use of EE can be achieved. The latter class is associated with larger batteries that are externally chargeable, therefore enabling an intensive use of EE to propel the vehicle in electric mode for long distances. When the TB is fully charged, the energy management system operates the powertrain in CD mode, depleting the battery until the lower SOC threshold is reached and the CS mode is activated. NOVC HEVs are tested exclusively for CS mode, whereas OVC HEVs are tested for both CS and CD mode.

6.3.1 NOVC HEVs

NOVC HEVs (also referred to as charge-sustaining hybrids) can only operate in CS mode, therefore the measurements associated with these vehicles are referred to as CS CO_2 emissions. The initial SOC is stabilised to normal conditions by carrying out the preconditioning; both for NEDC and WLTP procedures, the vehicle is preconditioned by executing one or more driving cycles and left soaking overnight. On the next day, the CS test takes place; the vehicle is tested for the cold-start

driving cycle, while the electricity balance is monitored and the CO_2 and pollutants emissions are measured.

6.3.1.1 NEDC CO2 emissions

Measured CO_2 emissions are not subject to correction if at least one of the following requirements is fulfilled, according to UNECE Regulation No. 101:

- the OEM can prove there is no relation between the electricity balance and the CO_2 emissions
- the test corresponds to battery charging
- the test corresponds to battery discharging and the EE used is within 1% of the fuel energy.

If none of the condition above is fulfilled, the emissions are corrected to reflect a neutral electricity balance according to:

$$M_0 = M - K_{CO2} * Q \qquad\qquad Eq.\,27$$

where M are the uncorrected measured CO_2 emissions in g/km, K_{CO2} is the CO_2 emissions correction factor (determined by the OEM) in g/km/Ah and Q is the electricity balance in Ah measured according to Appendix 2 of the regulation.

6.3.1.2 WLTP CO2 emissions

To determine whether the measured CO_2 emissions are subject to correction for electricity balance, the correction criterion c is calculated as follows

$$c = \frac{\left|\Delta E_{REESS,CS}\right|}{E_{fuel.CS}} \qquad\qquad Eq.\,28$$

where $\Delta E_{REESS,CS}$ is the CS Rechargeable Electric Energy Storage System (REESS) energy change in Wh and $E_{fuel.CS}$ is the energy content of the fuel consumed during the test in Wh, calculated according to paragraph 1.2.1 of Appendix 2 to Sub-Annex 8 in Regulation 1151/2017. Three correction criteria c are calculated for each test, each time considering a different combination of phases: phase low to medium, phase low to high, phase low to extra-high; the thresholds above which the

correction is mandatory are respectively 0.015, 0.01 and 0.005 (correction applies if at least one of the criteria is above the respective threshold).

The balanced CS CO_2 emissions are calculated as follows

$$M_{CO2,CS} = M_{CO2,CS,nb} - K_{CO2} * EC_{DC,CS} \qquad Eq.29$$

where $M_{CO2,CS,nb}$ are the measured non-balanced CO_2 emissions from the test in g/km, K_{CO2} is the CO_2 mass correction coefficient in g/Wh according to paragraph 2.3.2 of Appendix 2 to Sub-Annex 8 of the regulation and $EC_{DC,CS}$ is the EE consumption in Wh/km.

6.3.2 OVC HEVs

OVC HEVs (also referred to as plug-in hybrids) have two operating modes; therefore, the type-approval type 1 testing consists of two tests: the CD and the CS tests. To optimise the number of days needed for the testing, the CD might be executed first. The preconditioning is performed the first day, which involves the vehicle being driven until the TB is depleted; overnight soaking is then applied while the TB is being charged. The next day, with fully charged TB, the CD test can start. The vehicle is driven until the battery is depleted, and the vehicle automatically switches to CS operation. To ensure that the transition happens, criteria are applied to the electricity balance to ensure that it stays within specific boundaries. When this condition is reached, the CD test is over and the TB SOC is already preconditioned for the CS test; the vehicle is left soaking overnight, with no battery charging, and the next day the CS test can start.

6.3.2.1 NEDC CO2 emissions

The CD test, referred to as *Condition A* in UNECE Regulation No. 101, starts with a fully charged battery. The vehicle is driven over one or more NEDCs until the TB is depleted, with a maximum of up to ten minutes stop between two subsequent cycles. Vehicle gaseous emissions and electricity balance are measured for all the cycles driven during this phase. The electricity balance is monitored to understand when the TB reaches the minimum SOC; cycle N is considered to be the end of the CD test when cycle N+1 reflects no more than a 3 % discharge for the TB, calculated as follows

$$\frac{Q_{N+1}}{C_{TB}} * 100 < 3\% \qquad\qquad Eq.\,30$$

where Q is the electricity balance in Ah and C_{TB} is the capacity of the TB in Ah. The data measured during the cycles from 1 to N are relevant to the CD test calculations (CO_2 emissions, EE consumption and electric ranges); cycle N+1 is only needed to define the end of the CD test. If the vehicle is able to drive at least one complete NEDC in pure electric mode, the total CO_2 emissions produced during the CD test can be assumed to be zero. The vehicle CO_2 emissions for the CS test, referred to as the *Condition B* in the regulation, are then obtained performing a cold-start NEDC. The CO_2 emissions from the two tests (CD and CS) are combined to obtain the final value using a weighted average:

$$M = \frac{D_x * M_1 + D_{av} * M_2}{D_x + D_{av}} \qquad\qquad Eq.\,31$$

where M_1 and M_2 are the CO_2 emissions in g/km from the CD and CS tests respectively, D_x is either D_e (the vehicle's electric range in km) or D_{OVC} (the vehicle's OVC range in km) depending on the emissions measurement procedure adopted and D_{av} is a constant distance of 25 km (assumption on the average distance driven in CS mode). With some simplifications, D_e can be described as the distance driven in pure electric mode before the ICE starts, and D_{OVC} as the distance driven until the end of the cycle in which the ICE starts; as can be understood, better CO_2 emissions results can be obtained by using the measurements procedure that implies the use of D_{OVC} as this is slightly larger.

6.3.2.2   WLTP CO2 emissions

The CD test starts with a fully charged battery. The vehicle is tested over a sequence of WLTC cycles until the break-off criterion is satisfied; in all cycles the electricity balance is monitored. The break-off criterion is reached when the Relative Electric Energy Change (REEC) of cycle i satisfies the following criterion

$$REEC_i = \frac{|\Delta E_{REESS,i}|}{E_{cycle}} < 0.04 \qquad\qquad Eq.\,32$$

where $\Delta E_{REESS,i}$ is the EE change of all REESS in cycle i in Wh and E_{cycle} is the cycle energy in Wh calculated for the specific vehicle. The cycle that satisfies the break-off criterion is called confirmation cycle; for this cycle, i is equal to N+1. The cycle before the confirmation cycle (i = N), is called the transition cycle and represents the last cycle of the CD test. Differently from the NEDC procedure, CD test emissions cannot be assumed equal to zero. The emissions associated with every phase of every cycle driven during the CD test are multiplied by the Utility Factors (UFj, where j=1…4xN). UFs are used to assign a weight to the CO_2 emitted; the way they are calculated should reflect the average use of plug-in vehicles, meaning that the sum of all UFs, referred to as the Utility Factor (UF), is equal to the ratio of the distance covered in CD mode to the total distance covered between two subsequent charges [52]. The underlying assumption is: the larger the electric range of the vehicle, the larger the share of distance driven in CD mode and, therefore, the smaller the distance driven in CS. The dependency between UF and electric range is presented in Figure 40. For the calculation of the balanced CS CO_2 emissions, the same correction criteria and formula presented in section 6.3.1.2 apply. The weighted CO_2 emissions, that combine CS and CD, are finally obtained as

$$M_{CO2,weighted} = \sum_{j=1}^{k}(UF_j \times M_{CD,j}) + \left(1 - \sum_{j=1}^{k} UF_j\right) \times M_{CO2,CS} \quad Eq.33$$

where UF_j is the UF of phase j, $M_{CD,j}$ are the CD CO_2 emissions of phase j and $M_{CO2,CS}$ are the balanced CS CO_2 emissions.
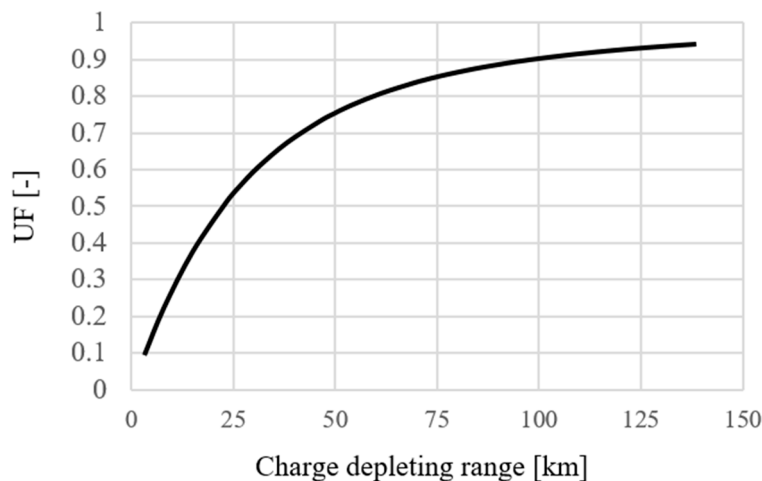

Figure 40. Utility Factor function for plug-in hybrids

6.3.3 NEDC-WLTP comparison of OVC HEVs CO_2 emissions

Based on the instructions reported in the previous sections, two different OVC HEVs were tested and the CO_2 emissions were obtained following the NEDC and the WLTP procedures were compared. The experimental activities and assumptions are detailed in the relevant publication [52]. The purpose of the activity was to understand the impact of the introduction of the WLTP for OVC HEVs and more specifically how the UF affects the weighted CO_2 emissions depending on the vehicle electric range. Therefore, the two vehicles selected for the activity were associated with very different electric ranges to inspect the results obtained for conditions close to the boundaries of the UF function. The All Electric Range obtained for the two vehicles, according to WLTP, are 32 km for Vehicle A and 123.9 km. The weight assigned to each of the cycles performed during the testing according to the UF function is presented in Figure 41. For both vehicles, the last cycle of the CD test, which is generally the one with higher CO_2 emissions due to the activation of the ICE, is the one associated with the smallest weight factor; additionally, the weight associated with the CS test is much smaller than that of the CD test. This implies that the overall CO_2 emissions of an OVC HEV are generally significantly smaller than those of a similar NOVC HEV.
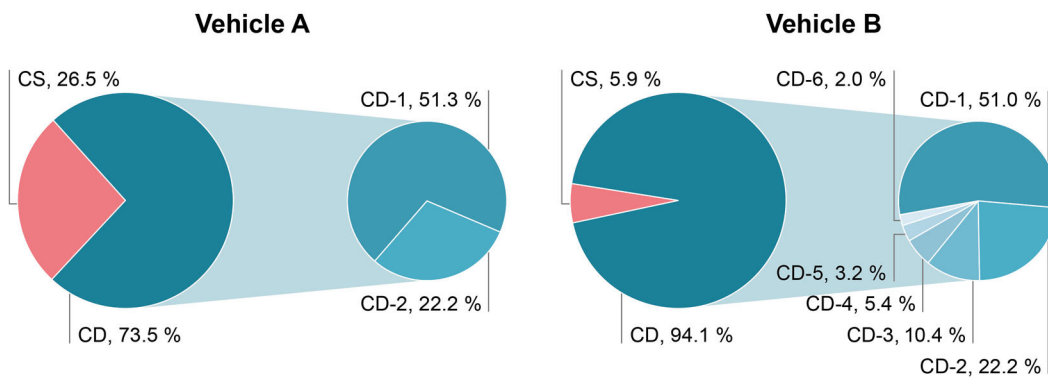
Figure 41. Weight assigned by the utility factors to the test cycles applied for OVC HEVs

To understand whether the WLTP introduction is associated with a decrease or increase of the CO_2 emissions for OVC HEVs, Figure 42 reporting the results of the study is discussed. For the two vehicles, opposite results were obtained; the explanation can be found in the different electric ranges and the resulting UFs.
The conclusions of the study are that WLTP CO_2 emissions can be either lower or higher than the NEDC ones, depending on the vehicle TB size which largely affects the electric range. The calculation of the UF factor has a big impact on the result,

and its influence has to reflect the real usage of plug-in vehicles with respect to the charging behaviour of the users. In 2017, year in which the study was carried out, the number of plug-in vehicles in the market was still very limited. When the penetration of such vehicles is higher, the charging behaviour of the users has to be analysed, with the goal of understanding real vehicle use and evaluate if the UF function presented in section 6.3.2.2 is representative.
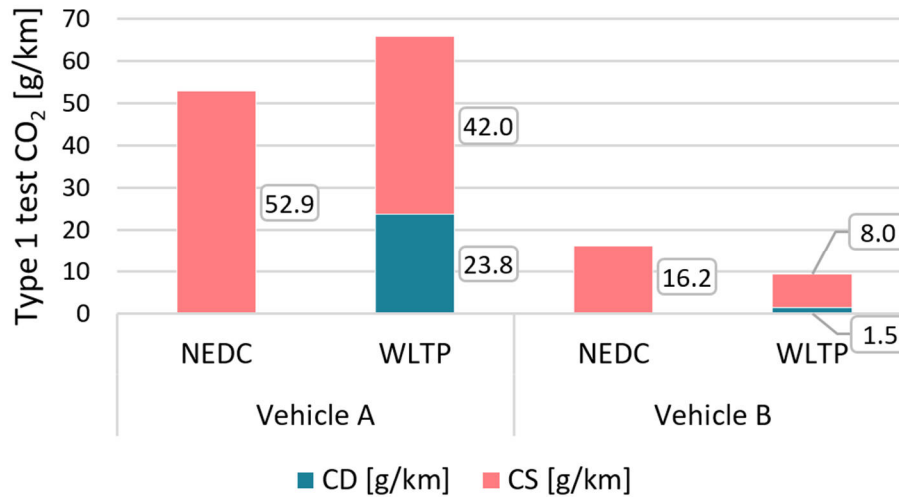
Figure 42. NEDC-WLTP CO$_2$ emissions comparison for OVC HEVs with different battery sizes

Chapter 7

7 Hybrid LDVs CO$_2$ calculation methodologies

With the information found in literature and the data collected during the experimental activities presented in the previous chapter, a calculation methodology for hybrid vehicles CO$_2$ emissions was developed. The goal of the project was to create the foundations for a generic simulation tool that could support the regulatory initiatives related to the WLTP-NEDC correlation exercise and future vehicle in-service performance evaluation. Differently from other models found in literature, which adopt a highly detailed model towards powertrain simulation, some simplifications were made, having the goal of calculating indicative FC and CO$_2$ emissions by keeping the level of detail as limited as possible. The main requirement for the methodology is to obtain representative fuel efficiency results for the most common hybrid architectures and driving conditions; therefore, the accuracy of the calculations of the powertrain instantaneous operating conditions can be partly sacrificed in favour of the wide-adaptability and lightness of the calculation methodology. Another important requirement for the methodology is the ability to use normalised or generic component data, indicative values for efficiencies and EC, and possibly be able to consume experimental data for self-calibrating the sub-models to reflect the behaviour of the specific vehicle that needs to be simulated. These features were addressed to the extent possible; the results are presented in the next sections. Out of the two operation modes of HEVs, the analyses reported in this thesis are limited to the more important CS operation; the investigations on the CD operation of plug-in vehicles are part of an ongoing

research. In general, CD operation is simpler to tackle in terms of control strategy and energy management, pointing instead in the direction of pure electric vehicle operation.

7.1 Generic control strategy for HEVs

A generic control strategy that can be adapted to different powertrain electrification levels (mild, full, plug-in and range extenders hybrids) was developed. Depending on the motive power request and the hybrid powertrain status, the strategy decides, for each loop of the simulation, how to operate the ICE and the EMs. The decision is taken at the end of an evaluation process consisting of three steps, taken at the three different levels of the control strategy (see Figure 43): the Supervisor, the ICE Manager and the Optimiser. The Supervisor has the ability to impose a choice, for example when the TB SOC is outside of the acceptancy boundaries, or when the driving conditions are such that no optimisation should be applied and a predefined solution is selected. The ICE Manager deals with the warm-up and the limitations of the ICE in terms of Stop-Start (SS). When the conditions require that the ICE warm-up is triggered, this choice is passed to the next step of the calculation. Additionally, some other limitations can be implemented: for example maximum rotational speed at which the ICE can be switched off, minimum power output when active, minimum time of operation after an activation event or minimum time before two subsequent activations. Finally, the Optimiser inherits the choices and the limitations from the upper levels and, when multiple solutions are possible, selects the most efficient one according to the optimisation strategy. According to the solution selected, which defines the power output and rotational speeds for ICE and EMs, the TB power is calculated. The battery model is executed to calculate the current value that is needed to deliver the required power; the TB SOC for the next calculation loop is then obtained accordingly. At the beginning and at the end of every calculation loop, the other variables defining the powertrain status are calculated (e.g. temperatures, timers, Boolean variables, etc.).

Figure 43. HEVs generic control strategy

7.1.1 Supervisor

The Supervisor's logic is presented in the domain sketched in Figure 44. The following abbreviations are used: RB (Regenerative Braking), EP (Electric Propulsion), CH (Charging), EA (Electric Assist) and HY (Hybrid). The quantity used in the x-axis, *P*, is the motive power. The following thresholds are reported on the same axis: *0* (to distinguish between propulsion and deceleration), *MAX EP* (the maximum power in electric propulsion), *MAX NO EA* (the maximum power achievable without combining the propulsion of ICE and EMs, electric assist) and *MAX EA* (the maximum power with electric assist). The quantity used in the y-axis is the TB SOC. The following thresholds are reported on the same axis: *SOC_MIN* and *SOC_MAX*, thresholds defining the standard SOC swing window, *SOC_INF* and *SOC_SUP*, the minimum and maximum values for SOC below and above which very aggressive SOC recovery strategies are implemented.
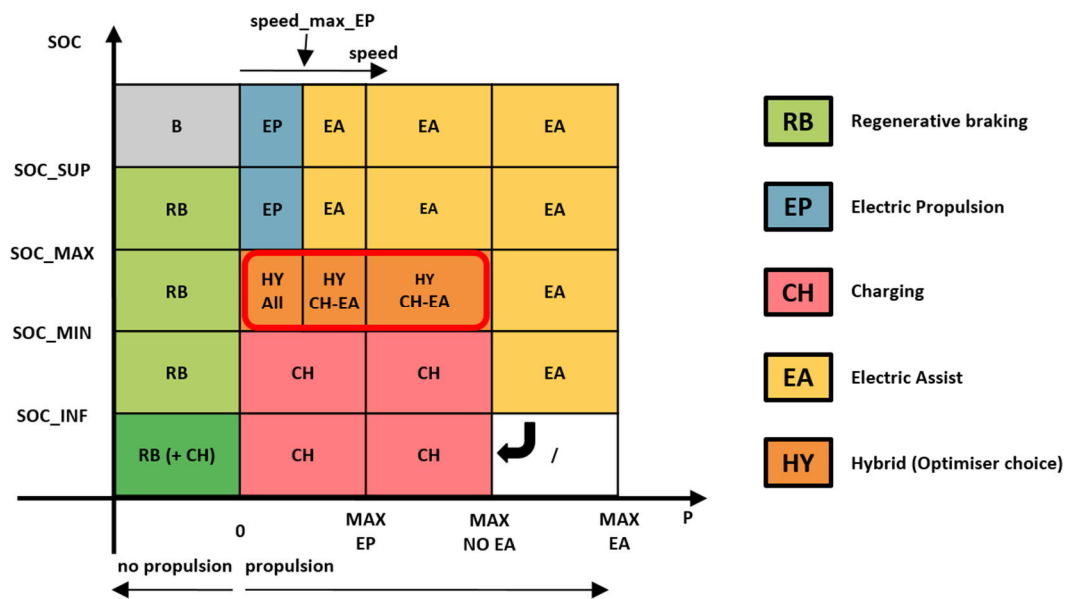
Figure 44. HEVs control strategy - Supervisor

The picture presents which decision is taken by the supervisor, about the operation of the powertrain, in the different parts of the domain; accordingly, a reduced set of possible operating conditions is evaluated in the subsequent steps of the calculation loop. This allows for the identification of a compromise between the optimal solution that the optimiser would pick and the one needed to preserve both the driving dynamics (power dimension) and the self-sustainment of the electricity balance (SOC dimension). The starting point for the explanation of the domain is

the distinction between the *no propulsion* (only RB state) and *propulsion* (EP, CH and EA states) condition. For example, when the motive power is below zero, there is no need for propulsion and there might not be the need of running an optimisation strategy; a separate strategy that identifies the best way to achieve negative power at the wheels, depending on the current TB SOC value, might be used. When the TB SOC is within acceptable boundaries, *SOC_INF* and *SOC_SUP*, RB can be applied; alternatively, when the SOC is extremely high or low, only mechanical braking (B) or RB combined with CH (achieved by keeping the ICE active and increasing the load on the EMs for increasing electricity generation). When motive power is above zero (propulsion), a positive power has to be delivered at the wheels: this can be achieved in different ways since HEVs have at least two machines for propulsion. When the motive power request is limited and the TB SOC is within the optimisation band (*SOC_MIN* < SOC < *SOC_MAX*), the supervisor selects the HY state, which in reality implies that no restriction is applied to the solutions evaluated at the next steps of the calculation loop; the selection of the operation strategy is fully mandated to the ICE Manager and the Optimiser. When the motive power request is above the *P MAX NO EA* threshold, the vehicle performance is prioritised; therefore, the supervisor selects the EA state; this restricts the evaluated solutions to those associated with propulsion for both the ICE and the EMs. When the TB SOC is below *SOC_MIN*, CH is the state selected (positive power from the ICE, negative power from the EMs for regeneration), except for P > *P MAX NO EA* in which case EA is still possible as long as SOC > *SOC_INF*; if this is not the case, EA cannot be selected and the power output of the powertrain is limited to *P MAX NO EA* (see the arrow at the bottom right of the domain in Figure 44). If the TB SOC is above *SOC_MAX*, the supervisor prioritises the states associated with EE consumption: EP (ICE off) and EA (ICE on). A third dimension of the domain should be considered for the choice of the state, the vehicle speed, as some powertrain architectures enable EP only below a certain speed threshold (*speed_max_EP*). The domain presented is applicable to all hybrid types: parallel, power-split and serial. For the latter, which has no mechanical connection between the ICE and the wheels, *P MAX EP (*the maximum power output with ICE off) corresponds to *P MAX NO EA*; therefore, *P MAX EP* threshold disappears from the domain and *P MAX NO EA* becomes the division line between ICE-off and ICE-assisted operation. Similarly, for parallel and power-split hybrids where the maximum propulsive power from the EMs is bigger than that of the ICE, *P MAX EP* disappears from the domain and again is *P MAX NO EA* the only power threshold for the selection of the state; when this threshold is overcome and the SOC is smaller than *SOC_MIN*, the EMs are asked to assist the ICE in propelling

the vehicle. The desired control logic and operating conditions can be achieved for all vehicles by setting proper thresholds. For example, for plug-in HEVs the CD operation can be forced by setting SOC_MAX to the upper SOC value that is representative of CS operation; *speed_max_EP* for a plug-in is surely close to the maximum speed of the regulated cycle, and therefore, according to the supervisor logic, EP state is selected (EMs propel the vehicle and ICE is kept off).

7.1.2 ICE Manager

The ICE Manager is mainly used to start the warm-up and condition the ICE activation and deactivation; therefore, it takes part in the definition of the SS strategy. Depending on the choices made by the Supervisor and the conditions of the powertrain, the ICE Manager assigns a value to the following Boolean variables

- *warming_up*:
  when true, it keeps the ICE active to complete the warm-up strategy
- *keep_ice_active*:
  when true, it prevents the Optimiser to select an ICE-off solution
- *consider_switching_off_ice*:
  when true, the Optimiser decides the ICE state

The steps of the evaluation are presented in Figure 45. The principle that lays behind this approach is that, when needed, the ICE can always be activated, or kept active, to prioritise the driving dynamics and the operational needs (e.g. warm-up). When a warm-up is needed, the ICE Manager starts the warm-up procedure; the ICE is activated and has to stay active, *warming_up* and *keep_ice_active* are set to true. When there is no need for a warm-

Figure 45. HEVs control strategy - ICE Manager

up, but the ICE has to be activated or stay active due to the choice made by the Supervisor, or due to other limitations (e.g. exceeded speed limit for EP, ICE having

to fulfil a minimum activation time, or spinning too fast, etc.), then *keep_ice_active* is set to true. When neither the warm-up nor other conditions require the ICE to be active, then *consider_switching_off_ice* is set to true. This last Boolean variable represents the possibility of switching off the ICE, compatibly with the powertrain status, but the Optimiser finally takes the decision whether to have ICE on or off.

7.1.2.1 ICE warm-up

Commonly, for HEVs with electrification levels above the mild, the activation of the ignition key is not immediately followed by the ICE activation; the ICE only starts when necessary, either for supporting the propulsion or for starting the warm-up according to the logic implemented. Mild-hybrids vehicles, due to their lower electrification degree, are much more similar to conventional vehicles and, for most of the cases, the ICE is activated right after the ignition command; in this case, the warm-up strategy starts at the very beginning of the trip. In the experiments carried out on highly electrified HEVs, it was found that the warm-up strategy generally activates the ICE for conditions of motive power and speed that are lower than those associated with the standard SS strategy. Therefore, besides the standard SS strategy, a warm-up trigger is needed to start the ICE according to a different logic.

Warm-up trigger for highly electrified HEVs

The following Boolean variables might be used to simulate the warm-up behaviour of highly electrified HEVs: *warm_up_needed* and *start_warm_up*. The first defines whether a warm-up is needed, and the second finally triggers the start when certain conditions are met. The need for a warm-up can be evaluated depending on the following conditions: ICE after-treatment temperature, ICE coolant temperature or time elapsed since last ICE deactivation. The former is probably the best criterion since a cold after-treatment would inevitably cause bad emissions performance if the ICE is suddenly activated with high power requests. If an accurate signal or model for after-treatment temperature is missing, then the coolant temperature and/or the time elapsed since last ICE deactivation might be used as a backup solution. Since the tools presented in this thesis are required to work also when specific component data or experimental measurements are missing, it was decided that the warm-up trigger could be defined using ICE coolant temperature, which is normally available from experimental measurements and can also be calculated with fair accuracy during simulation, and eventually also consider the ICE-off time. Therefore, the need for a warm-up can be evaluated as follows

$$warm\_up\_needed = \left(T_{coolant} < T_{coolant}^{min}\right) OR \left(t_{ICE-off} > t_{ICE-off}^{max}\right) \quad Eq.\,34$$

where $T_{coolant}^{min}$ can be derived from experimental data (e.g. coolant temperature at which the warm-up finishes) or reasonably assumed; $t_{ICE-off}^{max}$ is not equally straightforward but, according to experimental evidence, a time period of 1000 s can be used (see the analysis reported in Appendix D). From the experiments, it was also derived that an indicative coolant temperature for the end of the ICE warm-up phase is approximately 40°C when the initial coolant temperature is approximately 25°. The engine coolant delta temperature between the start and the end of the warm-up can be assumed constant for different initial temperatures close to ambient conditions. Therefore, a characteristic $\Delta T_{coolant}$ can be derived for every vehicle from experimental observations and added to the coolant temperature at the start of the warm-up to obtain $T_{coolant}^{min}$. Concerning the second Boolean variable defining the start of the warm-up phase, *start_warm_up*, the following conditions can be monitored: vehicle speed and motive power. When *warm_up_needed* is true, the warm-up might start when the following conditions are met

$$start\_warm\_up = \left(v \geq v_{start}^{warm-up}\right) OR \left(P \geq P_{start}^{warm-up}\right) \qquad Eq.\,35$$

where $v_{start}^{warm-up}$ and $P_{start}^{warm-up}$ are the speed and the motive power, respectively, that trigger the warm-up; foreseeing the two different conditions, allows to better represent the warm-up trigger for different vehicle models.

Warm-up strategy

The warm-up strategy, similarly to the warm-up trigger, differs between the mild and the more electrified hybrids. Due to the lower degree of electrification, mild-hybrids typically start the warm-up right after the ignition activation, which then continues while the ICE is also fulfilling the propulsion needs. Therefore, the warm-up takes place initially under stable conditions until the vehicle is standstill, keeping constant ICE speed and torque, and continues after the vehicle moves, with variable conditions for fulfilling the propulsive needs; for conventional non-hybrid vehicles, the warm-up takes place in a very similar way, therefore no specific warm-up strategy was investigated for mild-hybrids. An option that can be evaluated for future work is to optimise the part of the warm-up after vehicle start by decreasing the ICE load through EA, therefore having a more optimal warm-up at lower loads. For hybrids with higher degrees of electrification, due to the higher EP capabilities, the EMs can fulfil the propulsive needs for longer time and for higher power requests, while the ICE warms up mostly or exclusively in a stable condition; this behaviour was observed on all tested HEVs other than mild-hybrids (see Figure 46).
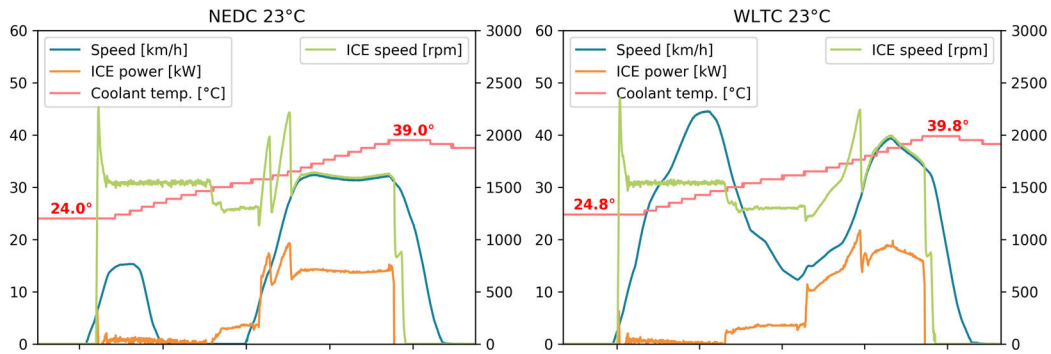
Figure 46. Example of warm-up strategy for highly electrified hybrids

Following the analysis of the experimental data, a warm-up strategy that applies to highly electrified hybrids was developed. To capture the behaviour of different vehicle models, the strategy is associated with two stages, stage 1 and stage 2, that define the type of operation that is actuated. Engine coolant temperature is the quantity being monitored during the warm-up phase for the switch from stage 1 to stage 2 and, later on, for its conclusion. The two stages are highlighted in Figure 47. The behaviour showed in the picture, which was obtained on vehicle 2, was similarly obtained for other full or plug-in hybrids with both serial and parallel propulsion capabilities (vehicle 3, 4, and 6). During stage 1, the powertrain works in serial mode, enabling a high-speed (~1550 rpm) idling warm-up with minimal power output (~0 kW) although the vehicle is following a dynamic driving condition. In the second stage, the ICE speed is reduced (~1300 rpm) and the power output is increased to a constant minimum power output (2.5 – 3.5kW). Initially, the powertrain is still used in serial mode but, as soon as the motive power request increases, the propulsion mode is switched to parallel; this phase was assumed to be still part of the warm-up, rather than being part of the normal operation since the ICE doesn't switch off as soon as the vehicle starts to decelerate and the motive power becomes negative. Therefore, the second stage is seen in the following way: the ICE has to stay active and provide a minimum power output; this is initially accomplished through serial propulsion if the motive power is low, and subsequently switches to parallel propulsion if the motive power exceeds a certain threshold. The warm-up is completed when $T_{coolant}^{min}$ is reached; for the switch from stage 1 to stage 2, a temperature threshold could be derived from experimental observations in a similar way to $T_{coolant}^{min}$ (based on a characteristic $\Delta T_{coolant}$ derived from experiments). The approach proposed enables to apply different target ICE speed and power between stage 1 and stage 2 (Vehicle 2, 3 and 4), or the same speed but different power (Vehicle 6), or lastly, the same power but different

speeds. If one vehicle did not show two different behaviours during vehicle warm-up, like in the cases presented, the thresholds for the two stages could be tweaked in a way to have one stage disappearing. The warm-up strategy proposed in this section also applies to serial hybrids, with the difference that the parallel propulsion is not possible for this architecture; therefore, the strategy only defines the ICE speed and power targets but the propulsion mode is necessarily always serial.
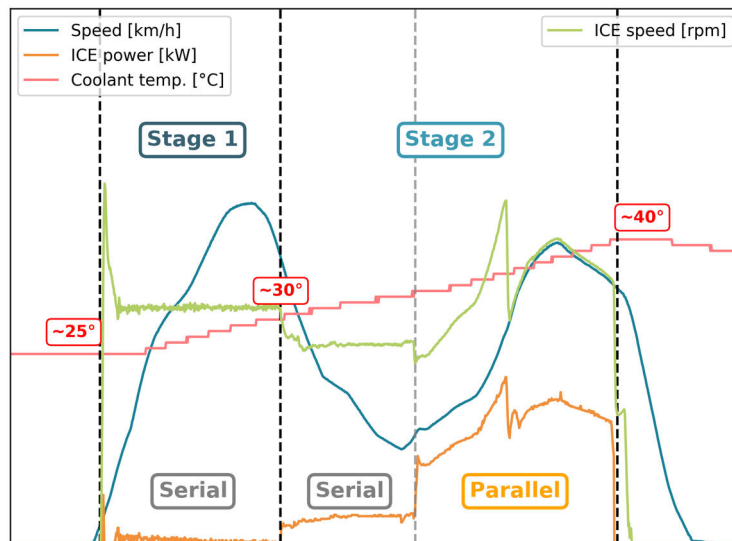
Figure 47. Highly electrified HEVs warm-up procedure

7.1.2.2 ICE limitations

This section presents what parameters can be taken into account to define when the ICE has to stay active. The following variables are defined:

- *vehicle_speed_ice_on*
  when true, the vehicle is running at a speed which requires active ICE
- *min_time_ice_on*
  when true, the minimum activation time of the ICE is not yet fulfilled
- *ice_spinning_fast*
  when true, the rotational speed of the ICE is too high for switching off.

As previously said, the decision whether to keep the ICE active depends on the supervisor decision, the warm-up needs and the ICE limitations. The set of conditions combining the three aspects are reported in Appendix D.

7.1.3 Optimiser

The Optimiser inherits the evaluations made by the upper levels and finds the optimal solution in the domain of viable powertrain conditions (see Figure 48). Additional constraints are added in order to avoid oscillations or inconsistent solutions generated by the numerical solver. The Optimiser is based on the Equivalent Consumption Minimisation Strategy (ECMS), which was firstly introduced by Paganelli et al. [53] and is nowadays widely adopted for all the different hybrid types (parallel, serial and power-split) [54]. It relies on the definition of a virtual cost, in terms of fuel consumed, associated to the use of electrical power. For every calculation loop, the ICE, EMs and TB limitations are considered, and a set of ICE and EMs power combinations to fulfil the powertrain power request is created. The ECMS selects the solution that minimises the equivalent consumption. At the end of the evaluation performed by the ECMS, the TB power selected is used to calculate the current flow and update the TB SOC. Finally, CO_2 emissions are calculated. Among the different strategies for optimising the HEVs FC, the ECMS was selected for the ability to keep a reduced computational burden combined with the possibility of having a cycle-independent optimisation [55, 56, 57, 58].
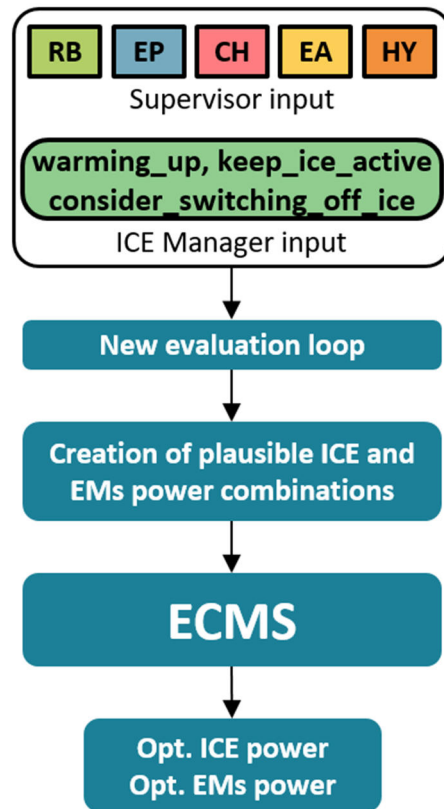
Figure 48. HEVs control strategy - Optimiser

7.1.3.1 Equivalent Consumption Minimisation Strategy

The strategy aims to find the combination of ICE power and TB power that minimises the equivalent FC

$$FC_{eq} = FC_{ICE} + FC_{TB} \qquad Eq. 36$$

where FC_{ICE} and FC_{TB} are the FC of the ICE and the virtual FC associated with the use of electrical power from the TB, which can be expressed as follows

$$FC_{TB} = s * \frac{P_{TB}}{LHV} \qquad\qquad Eq.37$$

where s is the equivalence factor defining the virtual cost of electrical power, P_{TB} is the TB power and LHV is the Low Heating Value of the fuel. Depending on the sign of P_{TB}, the virtual TB FC can be either positive or negative; therefore, the equivalent fuel consumption can be either higher or lower than the actual ICE FC. For any given driving condition, there is an optimal equivalence factor s_{opt} that enables the charge-sustaining operation. Using $s > s_{opt}$ means that the cost of EE is overestimated; consequently, the storage of EE is promoted and the SOC increases returning a positive electricity balance. Using $s < s_{opt}$ means that the cost of EE is underestimated. As a result, the use of EE is promoted and the SOC decreases returning a negative electricity balance. Therefore, it is of crucial importance that the choice made for s is as close as possible to the optimal value. To contain the side effects, instead of using a constant value the EE cost can be dynamically evaluated depending on the current TB SOC. To have a very little adjustment when the SOC is close to the reference, and a larger one when the SOC deviation is big, the following cubic s-SOC dependency can be implemented

$$s\,(SOC) = \; s_{const} * \left(1 + k * \left(\frac{SOC - SOC_{ref}}{\Delta SOC_{window}}\right)^3\right) \qquad\qquad Eq.38$$

where SOC_{ref} and ΔSOC_{window} are tunable parameters representing the centre value and the size factor of the SOC swing window, that can be derived from experiments, and k is an additional tunable parameter for adjusting the weight of the cubic SOC dependency when needed (k=1 no adjustment, k<1 reduced SOC dependency, k>1 increased SOC dependency). The s function obtained accordingly is presented in Figure 49. This approach is similar to the one proposed by Onori et al. [57]. Anyhow, this solution does not reduce the importance of finding s_opt but rather only limits the side effects when the driving dynamics are not well represented by the selected s, preventing the SOC to go either very high or very low. SOC_{ref} can be obtained as the average of the SOC values observed. ΔSOC_{window} can be obtained as the difference between the minimum and maximum SOC values observed.
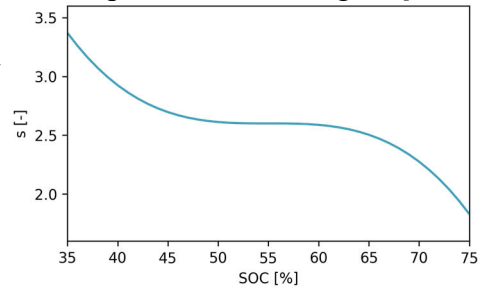

Figure 49. Equivalent cost of electric energy as a function of SOC

7.1.3.2   Definition of the power combinations

The ECMS needs a set of solutions to evaluate. This set of solutions has to be produced beforehand and needs to fulfil the power required from the powertrain while complying with its physical limitations. The number of possible power combinations that can be obtained in the generic driveline model presented in Figure 38 is high, which makes it difficult to formulate the problem in a way that considers all the possible logics and flow-paths for ICE and EMs power optimisation. In the attempt of trying to capture as many different logics as possible, a distinction was made between the part of ICE power that is used for propulsion of the wheels and the part that is used to charge the TB. The part that contributes to wheels propulsion is used in the following equation, which is obtained balancing the power at wheels

$$P_w = P_{ICE}^{prop} * \eta_{ICE}^{prop} + \sum_{PX} P_{PX}^{prop} * \eta_{PX}^{prop} * j_{PX}^{prop} \qquad Eq.\,39$$

where P_{ICE}^{prop} and η_{ICE}^{prop} are the ICE power and the respective driveline efficiency factor that is used for propulsion at the wheels, P_{PX}^{prop} and η_{PX}^{prop} are the mechanical power and the respective driveline efficiency factor for EM PX, also in this case used for propulsion at the wheels, finally j_{PX}^{prop} is a vector consisting of zeros and ones indicating which EMs are able to contribute to the propulsive needs in the current situation (depends on the clutch status). Eq.39 also applies when the wheel power is negative and the power flow is reversed (the driveline efficiency factor has to be adjusted accordingly). The part of ICE power that is used to charge the TB is used in the following equation, which is obtained balancing the power at the ICE, excluding the part used for propulsion

$$0 = P_{ICE}^{ch} + \sum_{PX} P_{PX}^{ch} * \eta_{PX}^{ch} * j_{PX}^{ch} \qquad Eq.\,40$$

where P_{ICE}^{ch} is the part of ICE power that is absorbed by the EMs acting as generators, P_{PX}^{ch} and η_{PX}^{ch} are the mechanical power from the EMs that are acting as generators and the respective efficiency seen by the power flowing from the ICE, finally j_{PX}^{ch} is a vector consisting of zeros and ones indicating which EMs are able to contribute to TB charging through the ICE (depends on the clutch status).
The total power from the ICE is finally calculated as follows

$$P_{ICE} = P_{ICE}^{prop} + P_{ICE}^{ch} \qquad\qquad Eq.\,41$$

The problem formulated in this way is able to cover those HEVs that can have one EM acting as a generator and another one as a motor (serial and power-split hybrids). To create all the possible power combinations, an array with ICE power outputs ranging from zero to the maximum power can be created, using the desired resolution (it can be defined depending on the expected accuracy). The ICE zero power output is the solution associated with EP mode, therefore only the EMs fulfil the propulsive needs by balancing Eq.40. When ICE power is bigger than zero, the hybrid architecture has to be taken into consideration to coherently distribute the power to the EMs. For serial hybrids P_{ICE}^{prop} is always zero; additionally, the lack of a mechanical coupling between the ICE and the wheels implies that the EMs used for propulsion are only P2, P3 and P4 (front and rear), whereas for charging only the P0 and P1 are used. For power-split hybrids, P_{ICE}^{ch} is obtained using the fundamental equations of the planetary gearset [59, 60]; in this powertrain layout, the EM P2_PLA torque is linearly dependent from the torque entering the ICE side of the gearset and the power output will depend on the rotational speed of the component. The EM P2_PLA torque is calculated as follows

$$T_{P2\,PLA} = \left(\frac{T_{ICE\,side}}{1+\tau}\right) * r_{gear} \qquad\qquad Eq.\,42$$

where $T_{ICE\,side}$ is the torque at the ICE side of the planetary gearset, τ is the fundamental ratio of the planetary gearset and r_{gear} is the torque reduction or multiplication factor of a possible reduction gear between the EM and the planetary gearset (if absent, $r_{gear} = 1$). The rotational speed of the P2_PLA is

$$\omega_{P2\,PLA} = \omega_{ICE\,side} * (1+\tau) - \omega_{FD\,side} * \tau \qquad\qquad Eq.\,43$$

where $\omega_{ICE\,side}$ and $\omega_{FD\,side}$ are the rotational speed of the ICE and FC sides of the planetary gearset. Finally, the P2_PLA power is obtained from torque and speed.
For parallel architectures, the rotational speed of the components is fixed; therefore, the ECMS simply selects the optimal ICE load that returns the optimal FC. For serial and power-split hybrids, the power combinations generated will have to be associated to both different loads and rotational speeds for the ICE. Additionally, for those vehicles that can run both in serial and parallel mode, one set of power combinations should be produced for each propulsion mode and evaluated by the ECMS; the solution associated to the propulsion with smaller FC shall be selected.

7.2 Electric Power System

Besides the control strategy, the other main difference between the simulation of conventional and hybrid vehicles is the Electric Power System (EPS). HEVs are equipped with the following additional components, which are part of the EPS: one or more EMs, the TB, the DC/DC converter and the SB (see Figure 50).
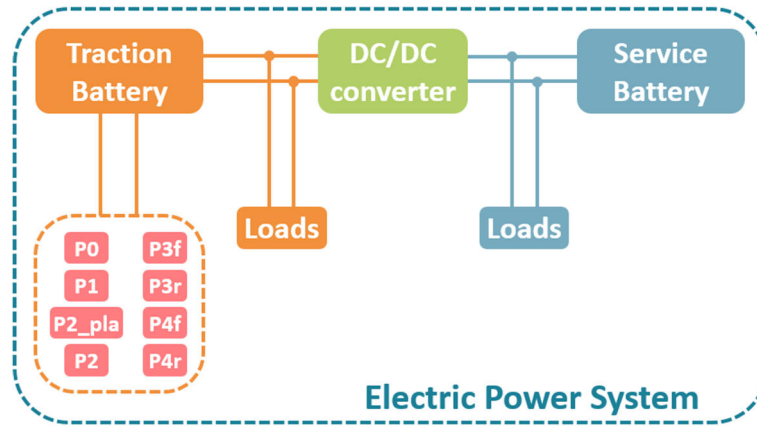

Figure 50. HEVs generic Electric Power System

7.2.1 Electric Machine model

An EM is an energy converter that transforms electrical energy into mechanical energy, and vice versa. Although there are several EMs types (synchronous vs asynchronous, AC vs DC), the performance of an EM machine can be modelled by means of a 0D approach using efficiency maps. A very common approach is to use lookup tables, where EM rotational speed and torque are used to obtain the efficiency value [61]. The relationship between electrical and mechanical power is

$$P_{EM}^{el} = P_{EM}^{mech} * \eta_{EM}(\omega, T)^{-sign(P_{EM}^{mech})} \qquad Eq. 44$$

where P_{EM}^{el} and P_{EM}^{mech} are the EM electrical and mechanical power (both positive when the EM is propelling), η_{EM} is the overall EM efficiency which includes the losses of the conversion from DC to AC (for AC EMs), and lastly ω and T are the rotational speed and torque of the EM. To take into consideration that the power flows in opposite directions when the EM switches its function from motor to generator, η_{EM} is powered to the sign of the mechanical power. To generate a generic EM efficiency map, a scaling approach could be used as proposed in [62].

An existing EM efficiency map can be normalised dividing the speed and torque setpoint by the respective speed of rated power and maximum torque. For every new EM, the rated speed and torque are used to rescale the normalised map. For the generation of the full load curve, it can be assumed that the EM is characterised by two different regions for the operation, the constant torque and the constant power region, as showed in Figure 51 [63]. A further assumption that can be made is that the upper limit of the constant torque region is the EM max torque, and the upper limit of the constant power region is the EM max power. Therefore, when two quantities among EM rated speed, EM rated power and EM maximum torque are known, the entire domain for the efficiency map can be found. Lastly, the maximum efficiency can also be scaled from the normalised map, considering that the maximum efficiency varies with the rated power [63] as showed in Figure 52.
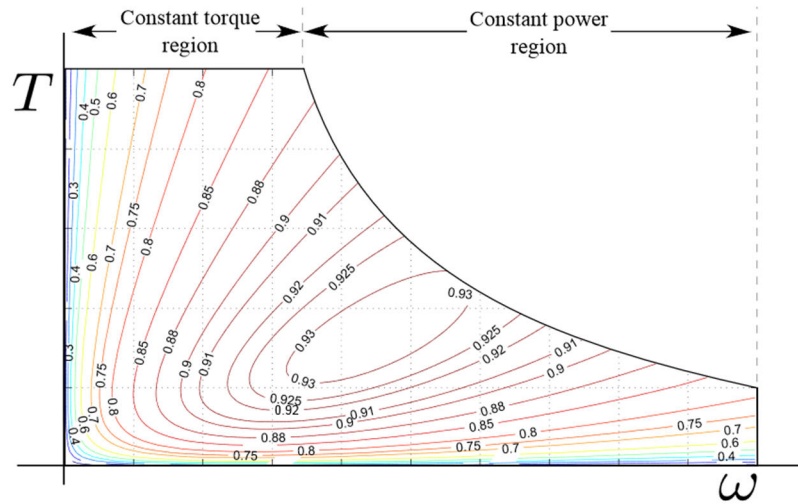

Figure 51. Generic full load curve and efficiency map of an electric motor [63]
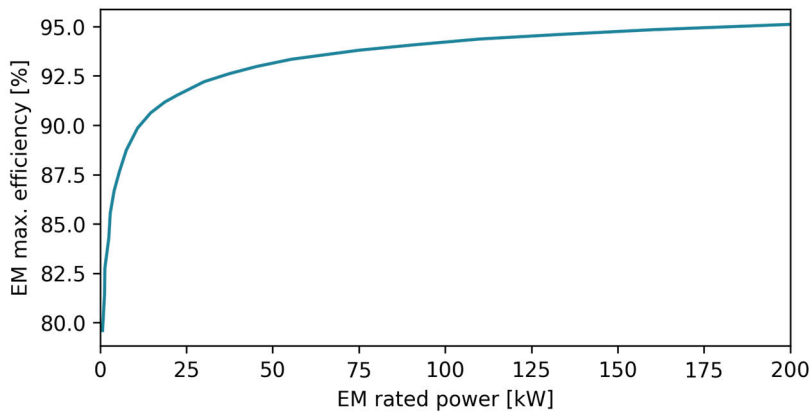
Figure 52. Dependency between EM rated power and maximum efficiency [63]

93

7.2.2 Traction Battery model

The TB model consists of two sub-models. The first one deals with the calculation of the voltage and current needed to deliver a certain power output; the resulting voltage-current combination is function of the battery efficiency. The second one calculates the SOC evolution, using the result of the first sub-model.

7.2.2.1 Efficiency and dynamics modelling

To simulate the TB efficiency and dynamics, the Equivalent Circuit Battery Model (ECBM) was chosen, which models the battery as an electrical circuit consisting of a voltage source, the Open Circuit Voltage (OCV), plus resistors and capacitors [64]. The OCV is normally assumed to be function of SOC only, whereas for resistors and capacitors the influence of temperature and current are also taken into account. The model can be applied either at battery-level or at cell-level; the latter solution has the advantage that literature data can be used for defining the parameters of the electrical circuit if the battery technology is known. The circuit presented in Figure 53 is defined zero-order ECBM due to the presence of only one resistor and the lack of resistor-capacitor circuits.

From the battery to the cell level, and vice versa, the following equations are used

$$n_c = n_c^s * n_c^p \qquad\qquad Eq.45$$
$$P_{bat} = P_c * n_c \qquad\qquad Eq.46$$
$$V_{bat} = V_c * n_c^s \qquad\qquad Eq.47$$
$$I_{bat} = I_c * n_c^p \qquad\qquad Eq.48$$

where $P_{bat}, P_c, V_{bat}, V_c, I_{bat}$ and I_c are the power, the voltage and the current of the battery and cell respectively, n_c is the total number of battery cells, n_c^s and n_c^p are the number of cells in series and parallel. Using the equation that defines the cell power, Kirchoff's voltage law and Ohm's law, and combining them, the following equations are obtained

$$P_c = I_c * V_c \qquad\qquad Eq.49$$
$$V_c = OCV - V_0 \qquad\qquad Eq.50$$
$$V_0 = R_0 * I_c \qquad\qquad Eq.51$$
$$V_c = \frac{OCV + \sqrt{OCV^2 - 4R_0P_c}}{2} \qquad\qquad Eq.52$$

which are used to calculate the values of V_c and I_c needed to deliver P_c.

V_c = cell voltage [V] R_0 = cell internal resistance [Ω]
I_c = cell current [A]   OCV = Open Circuit Voltage [V]
P_c = cell power [W] V_0 = voltage drop on the resistance [V]
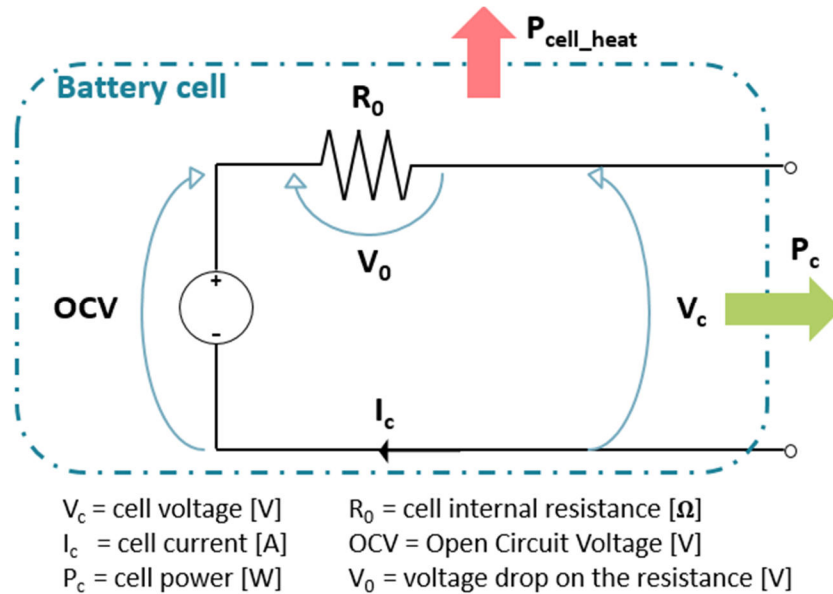
Figure 53. HEVs generic Traction Battery model

The modelling of a battery dynamics is a complex task since all the main parameters are correlated to each other in a highly non-linear way. The maps that express the dependency of OCV and R0 from the operating conditions (SOC, temperature, current) are normally obtained experimentally, through a constant current discharging characterisation [61]. To develop a generic model for battery simulation and avoid the need to obtain detailed battery data, some simplifications were made. For the easier case, the OCV and R0 can be considered constants and derived from voltage and current measurements during vehicle operation; to improve the accuracy of the model, different R0 values could be obtained for battery charging and discharging, by means of a parameters fitting procedure on the Thevenin's equation (Eq.50 combined with Eq.51) using the experimental V_c and I_c (calculated from V_{bat} and I_{bat}). This approach is applicable with reasonable accuracy to NOVC HEVs, since the SOC window in which their batteries are operated is typically limited to the region where the behaviour is almost linear (see left picture in Figure 54). For OVC HEVs, since their batteries are associated with a larger depth of discharge (CD test starts with fully charged battery and ends when the SOC is 10-30 %), a more detailed approach that considers the non-linearity is needed. To this aim, depending on the battery technology, literature data like the one presented in Figure 54 can be used, and the R0 curves can be scaled to match the average resistance measured experimentally.

Source: Lecture notes and recordings for ECE4710/5710 [65]   Source: JRC internal data
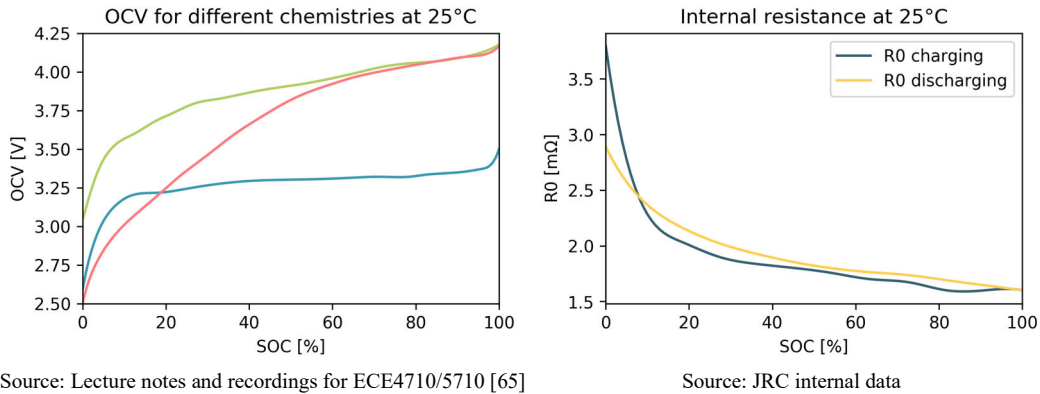
Figure 54. Dependency of battery parameters from SOC and technology type

7.2.2.2   Calculation of SOC

The instantaneous SOC is calculated through the Coulomb Counting method

$$SOC(t) = SOC_0 + \frac{\eta_c * \int_0^t I_{bat} dt}{Q_{batt} * 3600} * 100 \qquad Eq.53$$

where SOC_0 is the initial SOC (it has to be known beforehand), η_c is the charging or coulombic efficiency and Q_{bat} is the battery capacity in Ah [60]. The efficiency η_c is typically assumed unitary, although experimental findings showed that, sometimes, the SOC logged from the Battery Management System (BMS) was not properly replicated by using the equation above with $\eta_c = 1$. For such cases, one way to obtain a better matching is to use a charging efficiency, or better *charge correction factor*, accounting for the intensity of current and possibly temperature of the battery (more details are reported in Appendix D).

7.2.3 DC/DC converter model

The DC/DC converter allows the energy transfer between the High Voltage (HV) and Low Voltage (LV) circuits. The energy can potentially flow in both directions, although it is less common to have transfer from the LV to the HV circuit. The relationship between the electrical powers on the two sides of the DC/DC converter is written as

$$P_{DC/DC}^{HV} = P_{DC/DC}^{LV} * \eta_{DC/DC}^{sign(P_{DC/DC}^{HV})} \qquad Eq.54$$

where $P_{DC/DC}^{LV}$ and $P_{DC/DC}^{HV}$ are the electrical powers on the LV and HV sides of the DC/DC respectively, and $\eta_{DC/DC}$ is the efficiency of the DC/DC converter. Similarly to the case of the EMs, the efficiency is powered to the sign of the power flow to account for the direction and coherently adjust the calculation. Although the efficiency is function of the operating conditions, it can be assumed that using a constant efficiency does not introduce a significant error; a representative value derived from measurements is in the order of 93-95 %, which finds confirmation in [66]. Typically, a DC/DC converter transfers energy from the HV to the LV side, to charge the SB and supply the electrical loads (lights, cockpit, etc.). In the experiments, it was found that DC/DC converters could be used in two ways, with constant or intermittent energy flow from the HV to LV side. In the first case, the DC/DC always supplies the electrical loads and charges the SB until the desired SB SOC is reached (typically, the current signal measured for SB reflects a transitory that asymptotically reaches 0 A current charge). In the second case, the DC/DC is temporarily activated to charge the SB, while supplying the electrical loads, until the upper SB SOC is reached; when this happens, the DC/DC is deactivated, and the SB takes care of supplying the electrical loads. When the SB SOC reaches the lower SOC threshold, the DC/DC is reactivated and the cycle repeats. For energy modelling purposes, it was assumed that the two strategies have similar efficiency, and therefore the more straightforward constant energy flow strategy was selected for simulation, which was also found to be more common among the vehicles tested. The average DC/DC power flow from the HV side, $P_{DC/DC}^{TB}$, was found to be in the order of 300-600 W in the vehicles tested.

7.2.4 Equations for power balance

Considered the layout presented in Figure 50, the equations for the power balance on the HV and LV side of the EPS can be written as follows

$$P_{TB} + \sum_{PX} P_{PX}^{el} + P_{loads}^{HV} + P_{DC/DC}^{HV} = 0 \qquad\qquad Eq.55$$

$$P_{SB} + P_{loads}^{LV} - P_{DC/DC}^{LV} = 0 \qquad\qquad Eq.56$$

where P_{TB} and P_{SB} are the power outputs of the TB and SB (positive means charging), P_{PX}^{el} is the electric power of EM PX (P0, P1, P2 etc., positive means propulsion), $P_{DC/DC}^{HV}$ and $P_{DC/DC}^{LV}$ are the powers flows from the HV side and into the

LV side (positive when the power flow is from the HV to the LV side), and finally P_{loads}^{HV} and P_{loads}^{LV} are the electric loads in the respective circuits.

7.3 Implementation of the approach

The methodology presented in this chapter was implemented in two different calculation tools. It was firstly implemented in the Hybrid controller (Hycon), a tool developed specifically for testing and validating the performances of the strategy. After the methodology proved to be valid in hycon, the implementation into CO_2MPAS started, with the support of the CO_2MPAS team. Due to time restrictions caused by the new software release for regulatory purposes (v4.1.10), the implementation of the hybrid simulation strategy was temporarily interrupted at the end of September 2019; further development, bug-fixes and validation are starting again in 2020. The results obtained with the tools are presented in this section.

7.3.1 Hycon

Hycon is a tool written in Python language for the simulation of the FC and CO_2 emissions from HEVs. It was developed to test the performances of the strategy presented in this chapter. A 0D kinetic approach was adopted in order to obtain in little time feedback on the validity of the optimisation methodology. The adoption of the quasi-static approach, that should grant better a better representation of powertrain operating conditions [61], will be taken into consideration if the tool will prove to be inaccurate in estimating the FC. In the current version, the tool is able to simulate hybrids with parallel architectures, and has been tested on vehicle 2. For this purpose, the actual FC map of the vehicle was obtained and used. Only the HV side of the EPS was considered, the DC/DC converter and the LV side were taken into account by considering a constant electric power consumption of 500 W. The ICE activation, which is performed by the P0 machine of the vehicle considered, is associated to an electric power consumption of 8000 W (derived from the experimental data). Since the purpose of the tool is to be included into some other simulation environment, other sub-models that are not strictly related to the selection of the ICE and EMs load, e.g. gear-shifting or ICE temperature, were not modelled. All the signals needed by the tool are taken from the experimental data; consequently, a full simulation of driving conditions different from the input data is not possible. To represent the efficiency of the power transmission in the driveline and the EMs, representative constant values were selected.

7.3.1.1 Comparison of the warm-up behaviour

The warm-up strategy presented in section 7.1.2.1 was implemented for vehicle 2 with the two stages approach with manually tuned parameters (results in Figure 55).
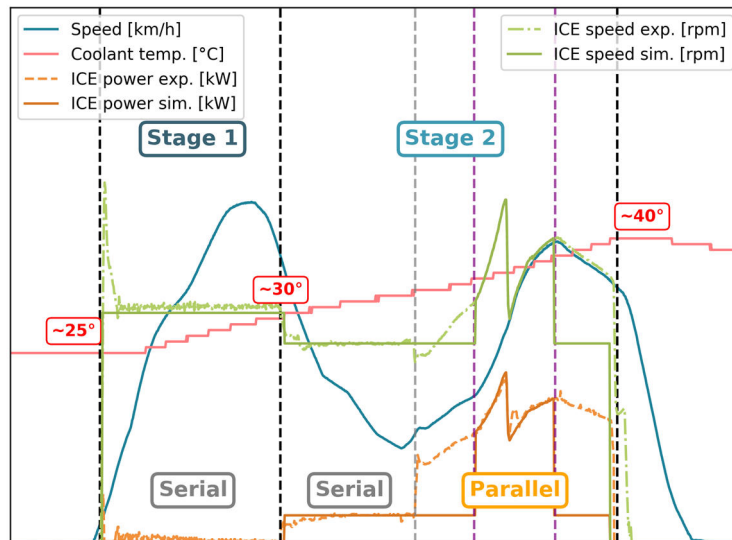

Figure 55. Warm-up simulation with hycon for a parallel full-hybrid

The warm-up phase starts as soon as the vehicle starts moving. In stage 1, the powertrain is operated in serial mode: ICE speed and power are constant and the experimental reference is matched. When the target coolant temperature is met (30°), stage 2 begins and the vehicle is allowed to switch to parallel propulsion. Since the transition takes place during a deceleration event, the powertrain does not immediately switch to parallel propulsion as an effect of the negative power request, and the serial propulsion mode is kept; therefore, the ICE speed is decreased and the power increased to match the target values associated with stage 2 and serial propulsion. When the power request is sufficient for switching to parallel propulsion, the ICE adapts its speed to that of the driveline and the power is then defined by the ECMS. When both the target temperature and the conditions for switching off the ICE are met, the warm-up ends and the ICE finally deactivates.

7.3.1.2 Comparison of ICE and EM operation

This section presents the performances of the tool in matching the choice for the operation of the vehicle powertrain. Figure 56 presents the operating conditions in the ICE FC map for a cold-start WLTC, where the black dots represent the experimental results, and the red and orange points are the simulated ones,

associated to CH and EA mode respectively; the simulation control strategy is able to push all the operating points within the region associated with higher efficiency. The instantaneous ICE and EM power comparison is presented in Figure 57 for the last 400 seconds of the WLTC (where the results can be better examined).
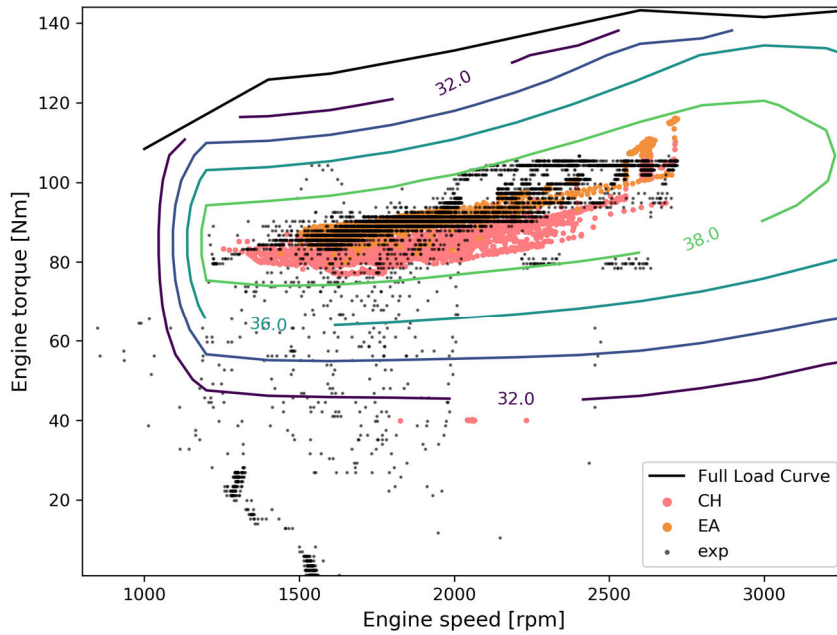

Figure 56. ICE operation for a parallel full-hybrid, experimental vs hycon simulation (exp = experimental operating points, CH = charging and EA = electric assist simulated operating points)
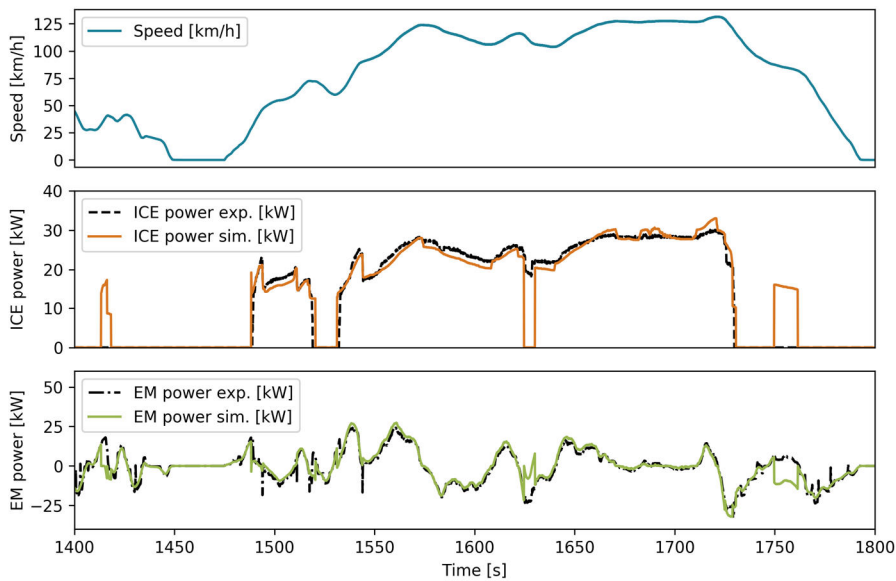

Figure 57. ICE and EM power for a parallel full-hybrid, experimental vs hycon simulation

7.3.1.3 Comparison of ICE Stop-Start

This section presents the overall results of the cold-start WLTC simulation. Figure 58 presents the instantaneous CO_2 emissions comparison; in the same figure, it is possible to examine the performances of the SS operation. Figure 59 additionally presents the comparison of the ICE total activation time, the ICE average power, the difference in the TB SOC and the average CO_2 emissions (normalised and expressed in percent points for confidentiality reasons). Despite the simplifications introduced, a good agreement was found between the experiments and the simulations.
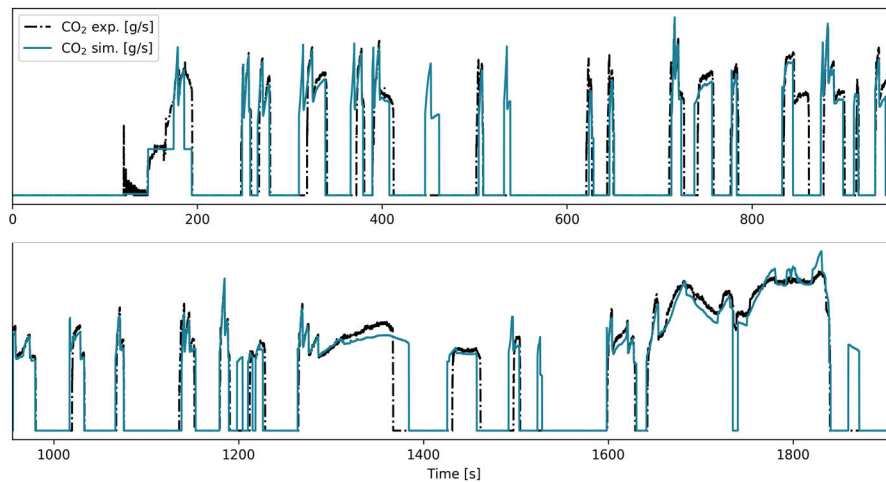

**Figure 58. CO₂ emissions for a parallel full-hybrid, experimental vs hycon simulation**
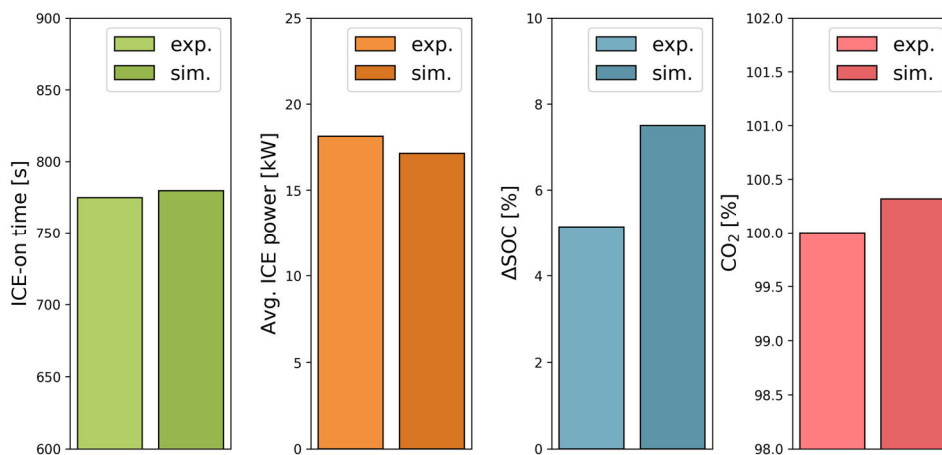
Figure 59. Results of the parallel full-hybrid hycon simulation

7.3.2 CO$_2$MPAS hybrids

Differently from hycon, the implementation of the generic powertrain architecture for CO$_2$MPAS covers all the hybrid types (serial, parallel and power-split) and all the possible EMs combinations. On the other hand, the implementation of the control strategy is more challenging due to the complex integration with the code already existing; for this aspect, a considerable amount of work still has to be done.

7.3.2.1 Overview

The starting point for the implementation was the refactoring of the electrical system, in which additional components had to be modelled (TB, DCDC converter, EMs). Afterwards, the equations governing the driveline power flow had to be modified due to the introduction of the new power sources (the EMs). Finally, the control strategy implemented to the extent possible. The dependency of the equivalent factor s on the current SOC presented in Eq.38 could not be included due to time restrictions and the way CO$_2$MPAS is currently structured.

As presented in section 3.2.2, CO$_2$MPAS uses experimental data to self-calibrate the sub-models and generate a simulation environment that replicates the vehicle behaviour also under different driving conditions. The workflow of CO$_2$MPAS consists of three main phases: identification, calibration and prediction. The first phase uses the input data to calculate additional time series and efficiency values, therefore expanding the set of data based on the vehicle model. For example, using for conventional vehicles the vehicle speed, the size of the wheels, the final drive and gearbox ratios it is possible to identify the rotational speed of the components and the gear engaged. For HEVs, the rotational speeds of the EMs are additionally calculated given the reduction gear ratios that connects them to the driveline. After important parameters have been identified, the calibration phase uses the expanded set of inputs for calibrating the sub-models: e.g., the gear shifting strategy, the ICE coolant temperature model and most importantly the ICE FC model. The latter constitutes one of the main strengths of CO$_2$MPAS, since the generation of an ICE FC map is something required from any simulation environment; this aspect is automatically taken care of by CO$_2$MPAS, using the calculated ICE load and FC, calculated from the experiments using the power at wheels and the instantaneous CO$_2$ emissions complemented with some other information (fuel, gearbox type, presence of a torque converter, etc.). When all the sub-models are calibrated, the vehicle model is complete and CO$_2$MPAS can predict the vehicle FC for the desired driving conditions. Concerning hybrids, the performances of CO$_2$MPAS concerning identification, calibration and prediction are here discussed.

7.3.2.2   Potential of CO$_2$MPAS hybrids

This section presents the potential of the implementation of the HEVs simulation strategies into CO$_2$MPAS. As mentioned already, CO$_2$MPAS is able to adjust the calculation workflow depending on the number and the type of the inputs provided. The information passed in the inputs enters the CO$_2$MPAS model, which can be seen as a graph constituted with nodes and paths. From the nodes, the information goes through the graph, being processed by functions that create additional information traveling towards other nodes. Multiple ways can be followed to travel from one node to the other, and the concept of path distance is used to select the way that returns the best accuracy of the calculation for the given set of inputs. Therefore, CO$_2$MPAS offers multiple ways of use. For vehicle type-approval, the set of input data is defined and limited in size, therefore many default values and standard paths are used to expand the information and obtain the result (the NEDC CO$_2$ emissions). Another way to use CO$_2$MPAS is to feed it with a rich set of data. In such a way, it is possible to use it as a complex calculator that does not need reprogramming if the input data set is changed. For example, for complex hybrid powertrains that are fitted with many EMs in different positions of the driveline(s), CO$_2$MPAS can be used to reconstruct the energy flow and obtain the efficiency of the components and energy converters. The results of the identification and calibration can be extracted and stored for later use. Since hybrid powertrains are associated with a great variability of their architectures, CO$_2$MPAS represents an efficient solution for performing calculations and simulations, since its approach is flexible towards the provided input data and the specifications of the vehicles.

Identification

Two examples of CO$_2$MPAS use for performing calculations for very different powertrain architectures are here presented. Figure 60 shows the comparison between the experimental and identified EMs rotational speed for a power-split hybrid. To obtain this result, CO$_2$MPAS requires two time series, vehicle and ICE speed, and the following scalar values: wheels size, FD ratio, fundamental ratio of the planetary gearset and EMs reduction gear ratio. Figure 61 shows the identification of the propulsion modes for Vehicle 3, which has a serial/parallel architecture. Using vehicle speed, the wheels size, the FD and GBX ratio, CO$_2$MPAS calculates the driveline speed and compares it with the ICE speed. A correlation coefficient is calculated, and where a good correlation is found the parallel propulsion mode is identified, the other cases are assumed as serial mode.
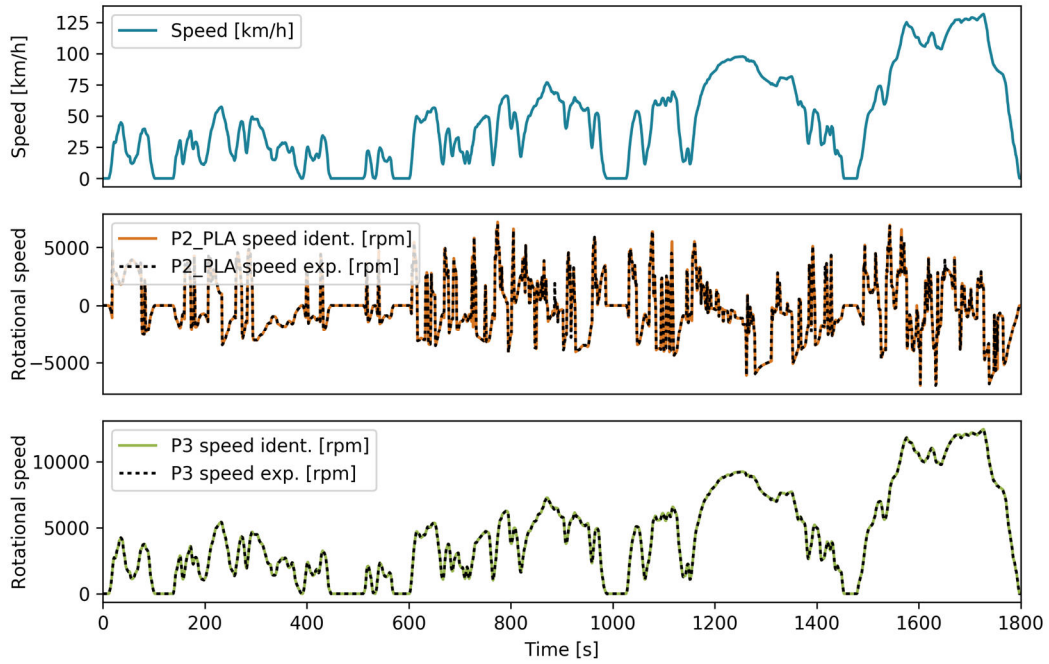
**Figure 60. Identification of the electric motors rotational speed for the power-split hybrid (Vehicle 5)**
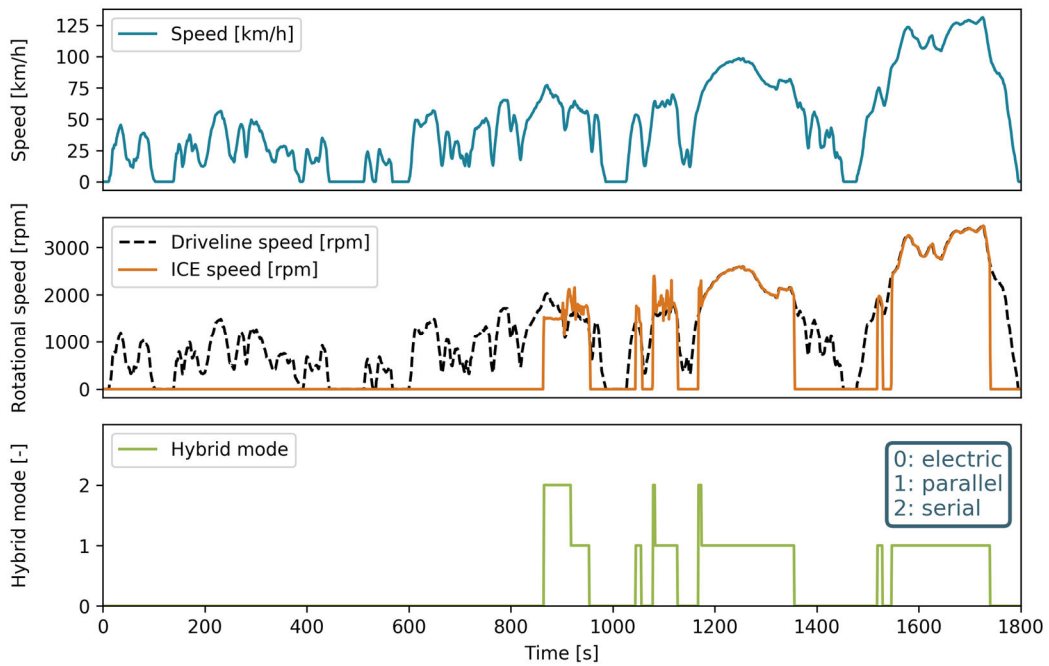
Figure 61. Identification of the serial and parallel propulsion modes (Vehicle 3)

Calibration

The automation of components and energy converters efficiency calibration is a powerful technique that allows the simulation of many different vehicle models without requiring the demanding activity of parameters tuning. For HEVs, besides what is done for conventional vehicles, CO_2MPAS additionally calibrates the TB model, returning the R0 and OCV for the specific battery considered. On the other hand, the calibration of the ICE FC map requires a different approach for HEVs. CO_2MPAS FC map is based on the Willans model; the experimental CO_2 and the identified ICE power and speed are used to fit the Willans parameters. For HEVs, most of the ICE operating points fall within the area of maximum efficiency; therefore, the fitting strategy finds the optimal parameters to capture the ICE efficiency of this region. Consequently, other less frequent ICE operating conditions have a much smaller weight in the fitting process. The calibrated FC map might deviate significantly from the real one for low and high ICE loads, as shown in Figure 62, where the green surface is the real FC map of the ICE considered and the yellow one is obtained from CO_2MPAS. The surfaces are close to each other in the area where the ICE is most frequently operated (1500-2500 rpm and 15-25 kW), but the yellow one tends to have a flatter shape, therefore the efficiency is high on a wider range of power outputs. This problem introduces inaccuracies in the simulation, both for the selection of the operating point and for the FC calculation. Currently, this is the bigger problem for the full applicability of the CO_2MPAS self-calibrating approach to hybrids. Future investigations will focus on the possibility to constrain the shape of the calibrated FC map, or alternatively assume some efficiency values in the boundaries of the domain, with a sufficient weight, to condition the fitting and obtain a more realistic result.

Figure 62. Real (green) vs CO_2MPAS (yellow) FC map

The further implementation of the approach into the CO2MPAS model largely depends on the decisions to be made at policy level regarding its future use. However, the first test case examined here revealed, as presented onwards, that such an implementation would be possible provided the issues mentioned above are addressed.

7.3.2.3   Results

This section presents the results obtained with CO_2MPAS for all the vehicles tested. Since the strategy presented in section 7.1 was only partly implemented into CO_2MPAS, logics ensuring that instantaneous operation is matched and unphysical behaviours are avoided are still missing; therefore, the instantaneous results are not presented. Only the overall results obtained on the test cycle (WLTC cold-start) are presented. To obtain the results, only the inputs relevant to the correlation procedure were used; based on the work presented in this chapter, the correlation regulations 2019/1152 (LCVs) and 2019/1153 (PLDVs) were amended with regulations 2019/1839 and 2019/1840 of the 31st of October 2019 to include the inputs needed for HEVs in the list of the mandatory ones for vehicle type-approval. The additional time series required are the TB current and voltage, the DC/DC current. Some additional scalar values are also required to identify the hybrid architecture, to obtain the most important specifications of the powertrain and some other data for the calculations: TB capacity, EMs maximum power and torque, EMs reduction gear ratio (when applicable) and TB initial SOC in the applicable cycles. No data is required with respect to ICE or EMs power output time series, which are identified reconstructing the power flow in the driveline using the TB and the motive power. The performances obtained with the current version of the software (CO_2MPAS v4.1.10) are presented in Figures 63 to 68. For each vehicle, the ICE activation time, the average ICE power when the ICE is active, the ΔSOC and the CO_2 emissions (normalised for confidentiality reasons) are presented. For better comparability, a correction is applied to CO_2MPAS results in order to obtain the same vehicle EE balance as the experiments. The correction impact is reported with the black error bars in the ΔSOC and CO_2 subplots, which are associated with the values in the text boxes at the bottom (EE gap and CO_2 gap). The ICE activation time is, in most of the cases, close to that of experiments, except for Vehicle 1 (the serial REx). The CO_2MPAS optimisation strategy selects a more aggressive operating condition with respect to the real vehicle, since the ICE is operated at a higher average load; consequently, after every ICE activation the TB is more quickly charged and the ICE can run for a smaller time. The cause is found in the ICE FC map calibration problem explained in the previous section, leading to the identification of the optimal operating point at higher loads because of the flatter shape of the map. Anyhow, despite the different operation, the results are consistent and the ΔSOC is similar to the experimental one. For the other vehicles, the ICE activation time is similar to the experiments. The average ICE power comparison presents a significant deviation also for vehicle 5, where the more intensive use of EE, associated with a TB ΔSOC of 38 %, allows the ICE to run at a lower average power output.
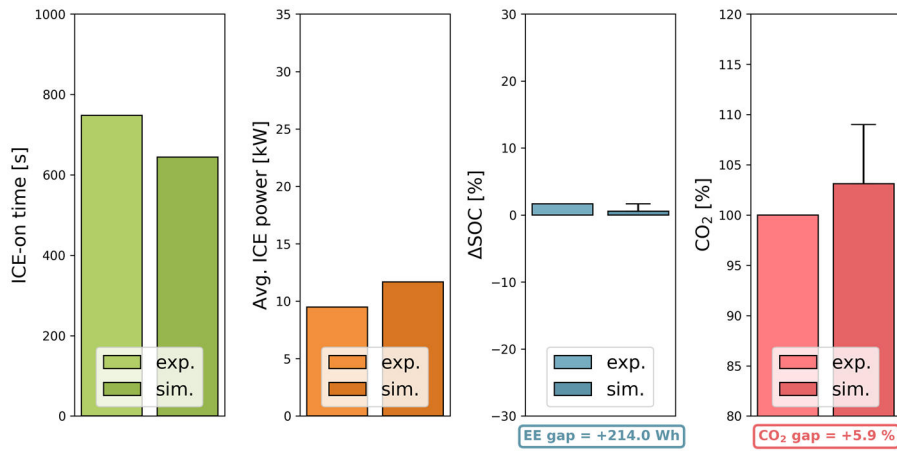
Figure 63. CO2MPAS results - vehicle 1 (serial range extender), SOC$_0$=12.7%
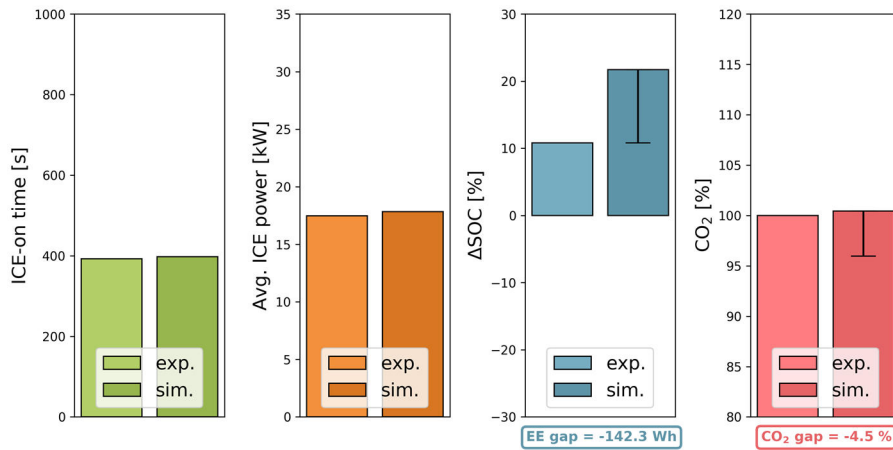
Figure 64. CO2MPAS results - vehicle 2 (parallel full hybrid), SOC$_0$=52.5%
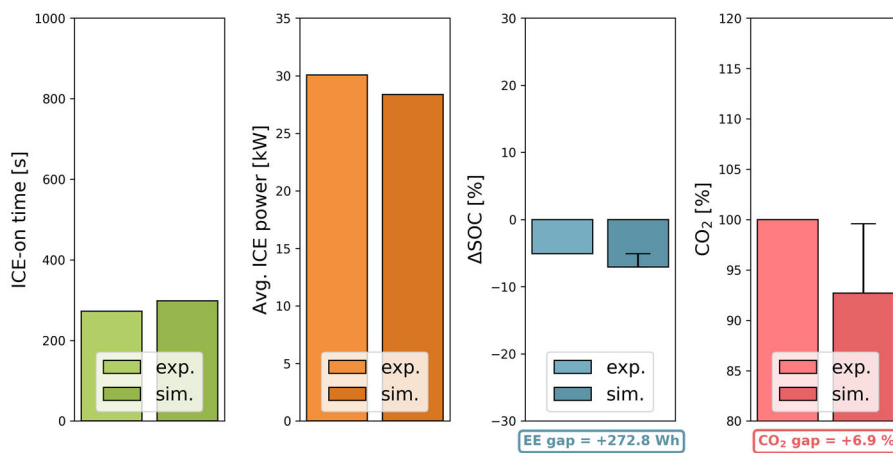
**Figure 65. CO2MPAS results - vehicle 3 (serial/parallel plug-in hybrid), SOC$_0$=33.8%**
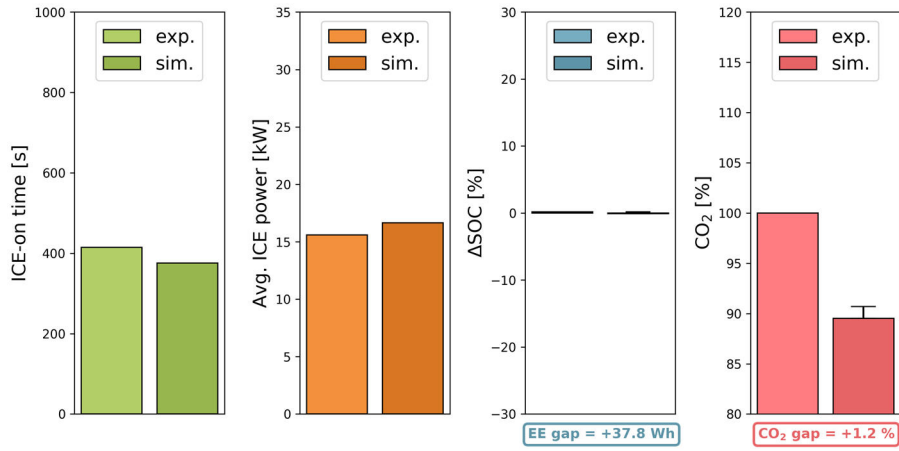
**Figure 66. CO2MPAS results - vehicle 4 (parallel plug-in hybrid), SOC_0=13.0%**
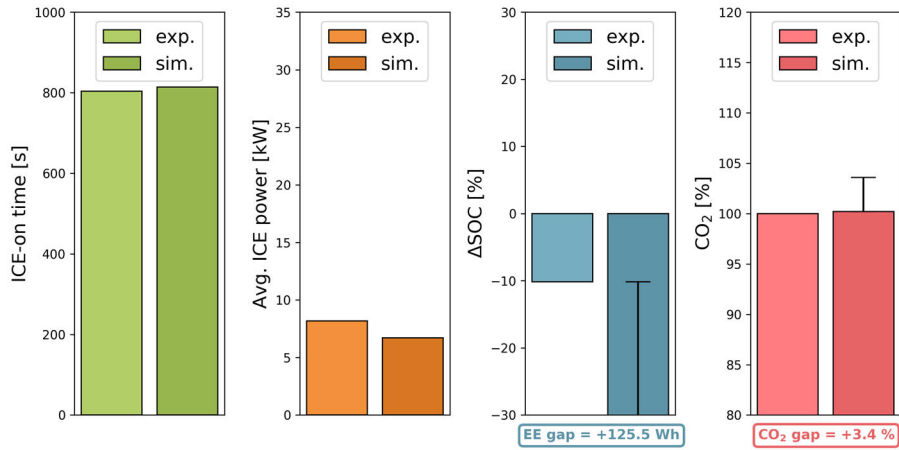
**Figure 67. CO2MPAS results - vehicle 5 (parallel mild hybrid), SOC_0=60.4%**
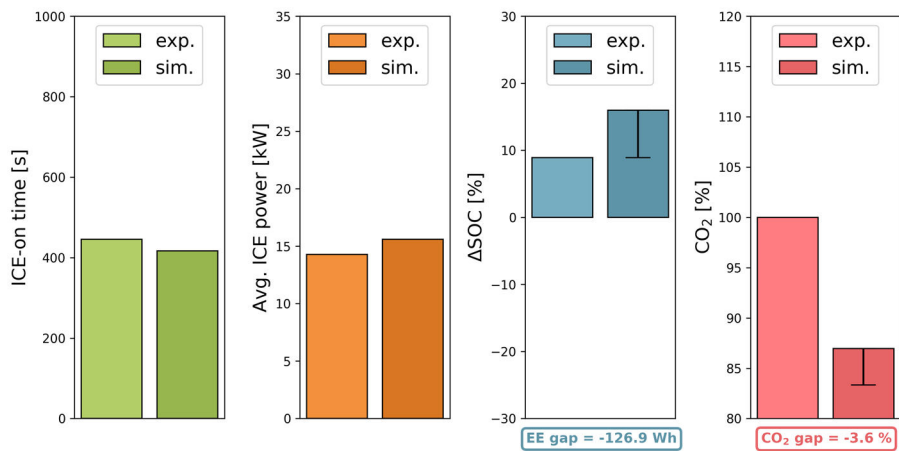
Figure 68. CO2MPAS results - vehicle 6 (power-split full hybrid), SOC_0=51.0%

One aspect that is not properly represented with the current version of CO_2MPAS, which might explain the TB deep discharge obtained in the simulation of vehicle 5, is the asymmetry in the use of the EM; the real vehicle uses the P0 machine mostly as a generator and rarely as a motor. Furthermore, the maximum power reached in generator and motor mode is asymmetric, since during regenerative braking the rated EM power is reached (~6 kW) whereas during charging the power delivered is limited (~1 kW). Additionally, the strategy presented in Eq.38 and Figure 49 of section 7.1.3 would allow for a better TB SOC control, preventing the TB to reach such high discharge depths; its implementation is programmed for the next version of the software. Exception made for vehicle 5, which has been discussed in the lines above, and vehicle 6, the ΔSOC comparison finds a good matching. For the latter, the problem is likely caused by inconsistencies in the implementation of the power-split architectures; further investigations will have to be carried out to explain the opposite trends of the ΔSOC and CO_2 emissions deviations. For vehicles 1 to 5, the CO_2 emissions estimation error is always within ±10 %, with an average error of +0.22 %. For vehicle 6, because of the said inconsistencies, the estimation error is -16.6 %. Analysing the results of the simulation, it was possible to realise that the ICE speed selected by the optimiser differed significantly from the experimental reference. Therefore, an additional simulation was performed for vehicle 6 imposing the experimental reference as the simulated ICE speed; the simulation returned the results presented in Figure 69, associated with an estimation error of -7.1 %. Fixing the said inconsistencies will allow the optimiser to perform a correct selection of the ICE speed and load, finally returning accurate CO_2 emissions estimations. If the last result for vehicle 6 is considered, the average CO_2MPAS estimation error for all vehicles becomes -1.4 %, which is considered a promising result with margin for improvements.
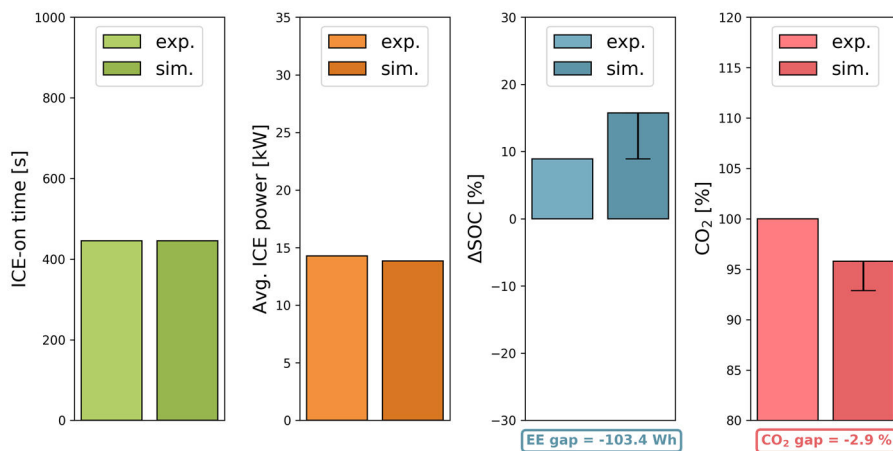

Figure 69. CO₂MPAS results - vehicle 6 (power-split full hybrid) with imposed ICE speed

7.4 Future work and use of the tools

The tools presented in this chapter will be further developed, with the idea of tailoring them for different purposes depending on the application. Hycon, due to its less complicated structure, can be used to easily test some new ideas or control strategies before the implementation into CO_2MPAS. For each vehicle, the model can be tuned for specific applications in order to have an accurate and robust response from the assessment. The limitations implemented inside the ICE Manager and Optimiser allow for a realistic representation of powertrain operation, since the unwanted non-physical solutions that might be returned by the numerical optimiser are rejected. Therefore, the results obtained with this tool can also be taken as a reference for the instantaneous operating conditions when the specific application requires it. This allows that the core of the model is extracted to be used in another simulation environment where a powertrain model is needed, taking as input the requests from the driver and the road load and providing as output the acceleration achieved and the EC, FC and CO_2 emissions (see Figure 70). A topic that could see the application of Hycon to fulfil this task is the simulation of traffic flow, which needs a reliable representation of the actual acceleration that can be achieved by the powertrain for any given moment, which for hybrids it can be function of the SOC and the temperature of the components.
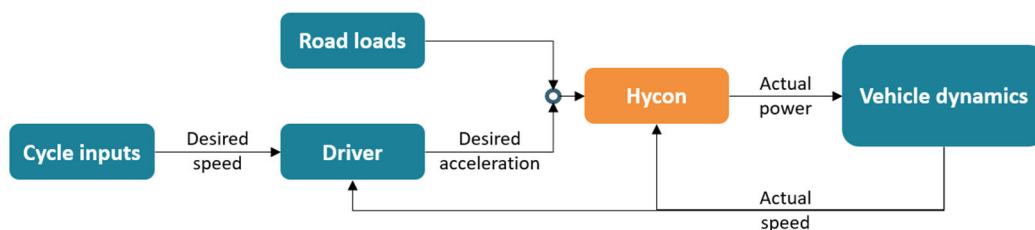

Figure 70. Use of Hycon as powertrain model for hybrid vehicles in other simulation environments

Concerning CO_2MPAS, the flexibility of its graph-based structure and the self-calibrating potential are for sure the more interesting aspects. When experimental activities are performed, many different signals are normally recorded and analysed. It is possible to exploit the identification capability of CO_2MPAS to easily enrich the experimental dataset and perform the analysis with all the additional time series of interest ready for consultation and comparison. Additionally, it will allow the JRC-STU to run FC simulations with either absent or very little model tuning effort.

Conclusions

The activities presented in this thesis fall under the topic of the CO_2 emissions evaluation for road vehicles and the use of calculation approaches. The focus of the investigations was the development of calculation approaches able to estimate, with good accuracy, the CO_2 emissions of the most common vehicle types of the HDVs and hybrid LDVs fleet. Additionally, the approaches were required to be flexible towards different applications, which include regulatory needs, development of publicly accessible services for dissemination (e.g. the Green Driving Tool [46]) or pure research purposes. The work carried out in this framework also wanted to address the issue faced by many research centres and institutes, which are required to perform road vehicles CO_2 emissions assessments with insufficient data and, sometimes, with limited knowledge and technical background. With this aim, the number and the level of detail of the inputs required by the calculation approaches was kept as small as possible to ensure higher usability.

VECTO and CO_2MPAS calculation tools constituted the starting point of the research activities, on top of which further assessments, validations and developments were carried out.

The activities carried out under the topic of HDVs CO_2 emissions determination had the following outcomes:

(a) the applicability of the VECTO methodology to buses and coaches was proved

(b) a CO_2 emissions baseline of the HDTs fleet was produced, with the aim of supporting the development of the emissions targets regulation

(c) two calculation approaches were developed, the first consisting of a generic input-data generation model for VECTO simulation and the second relying on VECTO-derived correlation formulas for the direct calculation of the energy consumption at vehicle level, which both constitute valid methodologies for verification purposes.

Outcomes (a) and (b) represented essential support for the further development of the HDVs CO_2 regulatory framework. Outcome (c) provides two viable options for the development of calculation tools for different applications, e.g. the development of an online service similar to the Green Driving Tool for LDVs that allows

calculating the CO_2 emissions of a vehicle given few input parameters. The approach used for the reconstruction of the energy flow in the driveline, presented in sections 5.1.4 and 5.2.2, can also be adopted for developing a simple CO_2 emissions calculation approach for hybrid HDVs which doesn't rely on a time-based simulation. This might be accomplished by considering the amount of energy that can be recuperated from the braking phases, the higher average engine efficiency that can be achieved because of the optimisation performed by the hybrid controller and the ICE-off time achievable with the architecture considered.

The activities carried out under the topic of hybrid LDVs CO_2 emissions determination had the following outcomes:

(a) the refinement of the measurement methodology and the unified test matrix for vehicle testing

(b) the creation of a database of experimental measurements from HEVs, which includes different hybrid powertrain architectures and electrification levels, for the characterisation of the instantaneous operation and the overall performance

(c) the development of a generic HEVs simulation strategy that covers the most relevant architectures

(d) the implementation of the generic HEVs simulation strategy into two different tools, hycon and CO_2MPAS

The results obtained with hycon demonstrated that the simulation strategy is appropriate for obtaining representative values of the instantaneous operation and the overall vehicle energy efficiency. Motivated by the good performances achieved with the first tool, it was decided to include the strategy also in CO_2MPAS and proceed with the implementation of all HEVs architectures and electrification levels. Based on the simulation model presented in Chapter 7, the correlation regulations (2017/1152 and 2017/1153) were amended to include the input data relevant to hybrids. At vehicle type-approval, the CO_2MPAS input file will now be filled out also for HEVs (previously excluded by the correlation procedure with CO_2MPAS). The vehicle specifications and experimental measurements data relevant to the hybrid powertrain have to be declared and certified; this allows the European Commission and the JRC to receive valuable data for the further development of CO_2MPAS and for supporting other assessments related to the effectiveness of the CO_2 actions.

The generic HEVs simulation strategy also represents a viable option for the inclusion of HEVs into other simulation environments, e.g. traffic simulation models.

The work carried out within this PhD programme addressed the research goals defined at its beginning and presented in the introductive chapters. The developed calculation approaches are capable of obtaining CO_2 emission values close to those defined by the certification procedures, by using a generic modelling approach and a limited amount of input data. The prediction performances of the on-road CO_2 emissions should be assessed, for defining whether these approaches could be adopted to study the gap between certified and real-world values.

A considerable amount of data was collected, along with other findings, constituting a fertile and solid basis for the further development of the tools and the publication of scientific articles related to transport sustainability.

References

[1] European Parliament, "CO2 emissions from cars: facts and figures," April 2019. [Online].
Available:
http://www.europarl.europa.eu/news/en/headlines/society/20190313STO31218/co2 -emissions-from-cars-facts-and-figures-infographics.

[2] European Parliament, "Commission Regulation (EU) 2017/2400 of 12 December 2017 implementing Regulation (EC) No 595/2009 of the European Parliament and of the Council as regards the determination of the CO2 emissions and fuel consumption of heavy-duty vehicles," 2017. [Online].

[3] European Commission, "EU Science Hub | The European Commission's Science and Knowledge Service," [Online]. Available: https://ec.europa.eu/jrc/en.

[4] European Parliament, "Regulation (EU) 2019/1242 of the European Parliament and of the Council of 20 June 2019 setting CO2 emission performance standards for new heavy-duty vehicles and amending Regulations (EC) No 595/2009 and (EU) 2018/956," 2018.

[5] European Parliament, "Regulation (EC) No 443/2009 of the European Parliament and of the Council of 23 April 2009 setting emission performance standards for new passenger cars as part of the Community's integrated approach to reduce CO 2 emissions from light-duty vehicles," 2009.

[6] European Parliament, "Regulation (EU) No 510/2011 of the European Parliament and of the Council of 11 May 2011 setting emission performance standards for new light commercial vehicles as part of the Union's integrated approach to reduce CO 2 emissions from light-duty vehicles," 2011.

[7] The International Council on Clean Transportation, "EU CO2 EMISSION STANDARDS FOR PASSENGER CARS AND LIGHT-COMMERCIAL VEHICLES," 2014.

[8] TransportPolicy.net, " EU: Heavy-duty: Emissions," [Online]. Available: https://www.transportpolicy.net/standard/eu-heavy-duty-emissions/.

[9] TransportPolicy.net, "EU: Light-duty: Emissions," [Online]. Available: https://www.transportpolicy.net/standard/eu-light-duty-emissions/.

References

[10] European Commission Press Release Database, "Testing of emissions from cars," European Commission, May 2018. [Online]. Available: http://europa.eu/rapid/press-release_MEMO-18-3646_en.htm. [Accessed July 2019].

[11] Z. Kregar, V. Franco and P. Dilara, "Real-driving emissions regulation," in *ERMES plenary meeting*, Zurich, 2017.

[12] European Commission, "Paris Agreement," [Online]. Available: https://ec.europa.eu/clima/policies/international/negotiations/paris_en. [Accessed September 2019].

[13] European Environment Agency, "Greenhouse gas emissions from transport," July 2019. [Online]. Available: https://www.eea.europa.eu/data-and-maps/indicators/transport-emissions-of-greenhouse-gases/transport-emissions-of-greenhouse-gases-11.

[14] The International Council on Clean Transportation, "CO2 EMISSION STANDARDS FOR PASSENGER CARS AND LIGHT-COMMERCIAL VEHICLES IN THE EUROPEAN UNION," 2019.

[15] European Commission, *COM(2019) 640 fina - The European Green Deal,* 2019.

[16] M. Weiss, P. Bonnel, R. Hummel, U. Manfredi, R. Colombo, G. Lanappe, P. Le Lijour and M. Sculati, "Analyzing on-road emissions of light-duty vehicles with Portable Emission Measurement Systems (PEMS)," Publications Office of the European Union, 2011.

[17] G. Fontaras, B. Ciuffo, N. G. Zacharof, S. Tsiakmakis, A. Marotta, J. Pavlovic and K. Anagnostopoulos, "The difference between reported and real-world CO2 emissions: How much improvement can be expected by WLTP introduction?," *Elsevier,* vol. 25, no. Transportation Research Procedia, pp. 3933-3943, 2017.

[18] European Parliament, "Regulation (EU) 2019/631 of the European Parliament and of the Council of 17 April 2019 setting CO2 emission performance standards for new passenger cars and for new light commercial vehicles, and repealing Regulations (EC) No 443/2009 and (EU) No510/2011," 2019.

[19] European Parliament, "Regulation (EU) 2018/956 of the European Parliament and of the Council of 28 June 2018 on the monitoring and reporting of CO2 emissions from and fuel consumption of new heavy-duty vehicles," 2018.

[20] European Commission, "Reducing CO2 emissions from heavy-duty vehicles," [Online]. Available: https://ec.europa.eu/clima/policies/transport/vehicles/heavy_en. [Accessed September 2019].

[21] The International Council on Clean Transportation, "CO2 STANDARDS FOR HEAVY-DUTY VEHICLES IN THE EUROPEAN UNION," 2019.

[22] G. Fontaras, M. Rexeis, P. Dilara, S. Hausberger and K. Anagnostopoulos, "The Development of a Simulation Tool for Monitoring Heavy-Duty Vehicle CO2 Emissions and Fuel Consumption in Europe," *SAE International,* 2013.

[23] European Commission, "IMPACT ASSESSMENT Accompanying the document Proposal for a Regulation of the European Parliament and of the Council setting CO2 emission performance standards for new heavy duty vehicles".

[24] European Commission, "EU Regulation on monitoring and reporting of HDV CO2 emissions adopted," 2018. [Online]. Available: https://ec.europa.eu/clima/news/eu-regulation-monitoring-and-reporting-hdv-co2-emissions-adopted_en. [Accessed September 2019].

[25] The International Council on Clean Transportation, "THE EUROPEAN COMMISSION'S PROPOSED CO2 STANDARDS FOR HEAVY-DUTY VEHICLES," 2018.

[26] The International Council on Clean Transportation, "THE FUTURE OF VECTO: CO2 CERTIFICATION OF ADVANCED HEAVY-DUTY VEHICLES IN THE EUROPEAN UNION," 2019.

[27] N. G. Zacharof and G. Fontaras, "Report on VECTO Technology Simulation Capabilities and Future Outlook," 2016.

[28] G. Fontaras, R. Luz, K. Anagnostopoulos, D. Savvidis, S. Hausberger and M. Rexeis, "Monitoring CO2 emissions from HDV in Europe – An Experimental Proof of Concept of the Proposed Methodological Approach," in *20th International and Transport Air Pollution Conference 2014*, Graz, Austria, 2014.

[29] G. Fontaras, T. Grigoratos, D. Savvidis, K. Anagnostopoulos, R. Luz, M. Rexeis and S. Hausberger, "An experimental evaluation of the methodology proposed for the monitoring and certification of CO2 emissions from heavy-duty vehicles in Europe," *Energy,* vol. 102, pp. 354-364, 2016.

[30] T. Grigoratos, G. Fontaras, B. Giechaskiel and B. Ciuffo, "Assessment of the monitoring methodology for CO_2 emissions from heavy duty vehicles," Publications Office of the European Union, 2017.

[31] G. Silberholz and S. Hausberger, "Feasibility assessment regarding the development of VECTO for hybrid heavy-duty vehicles," Publications Office of the European Union, 2018.

[32] B. Ciuffo, "CO2MPAS," 2016. [Online].
Available: https://e3p.jrc.ec.europa.eu/articles/co2mpas.

[33] J. Pavlovic, B. Ciuffo, G. Fontaras, V. Valverde, A. Marotta, "How much difference in type-approval CO2 emissions from passenger cars in Europe can be expected from

References

changing to the new test procedure (NEDC vs. WLTP)?," *Elsevier,* vol. 111, no. Transportation Research Part A: Policy and Practice, pp. 136-147, May 2018.

[34] European Commission, "Reducing CO2 emissions from passenger cars," [Online]. Available: https://ec.europa.eu/clima/policies/transport/vehicles/cars_en. [Accessed September 2019].

[35] B. Ciuffo and G. Fontaras, "Models and scientific tools for regulatory purposes: The case of CO2emissions from light duty vehicles in Europe," *Elsevier,* vol. 109, no. Energy Policy, pp. 76-81, 2017.

[36] European Commission Joint Research Centre, "CO2MPAS: Vehicle simulator predicting NEDC CO2 emissions from WLTP," [Online]. Available: https://co2mpas.readthedocs.io/en/stable/intro.html.

[37] K.B. Wipke, M.R. Cuddy, and S.D. Burch, "ADVISOR 2.1: a user-friendly advanced powertrain simulation using a combined backward/forward approach," *IEEE Transactions on Vehicular Technology,* vol. 48, no. 6, pp. 1751-1761, 1999.

[38] L. Guzzella and C. H. Onder, Introduction to Modelling and Control of Internal Combustion Engine Systems, Springer, 2010.

[39] S. Tsiakmakis, G. Fontaras, K. Anagnostopoulos, B. Ciuffo, J. Pavlovic and A. Marotta, "A simulation based approach for quantifying CO2 emissions of light duty vehicle fleets. A case study on WLTP introduction," *Transportation Research Procedia,* vol. 25, pp. 3898-3908, 2017.

[40] T. Grigoratos, G. Fontaras and A. Tansini, "Assessment of the measurement methodology for CO2 emissions from heavy-duty buses and coaches," Publications Office of the European Union, 2017.

[41] Fontaras, G., Dilara, P., Berner, M., Volkers, T. et al., "An Experimental Methodology for Measuring of Aerodynamic Resistances of Heavy Duty Vehicles in the Framework of European CO2 Emissions Monitoring Scheme," in *SAE 2014 World Congress & Exhibition*, Detroit, 2014.

[42] J. B. Heywood, Internal Combustion Engine Fundamentals, Mc Graw Hill.

[43] A. Tansini, N. Zacharof, I. Prado Rujas and G. Fontaras, "Analysis of VECTO data for Heavy-Duty Vehicles (HDV) CO2 emission targets," Publications Office of the European Union, 2018.

[44] N. Zacharof, A. Tansini, G. Fontaras, I. Prado Rujas and T. Grigoratos, "A generalized component efficiency and input-data generation model for creating fleet-representative vehicle simulation cases in VECTO," in *SAE WCX 2019*, Detroit, 2019.

[45] A. Tansini, G. Fontaras, B. Ciuffo, F. Millo, I. Prado Rujas and N. Zacharof, "Calculating heavy-duty truck energy and fuel consumption using correlation formulas derived from VECTO simulations," in *SAE WCX 2019*, Detroit, 2019.

[46] European Commission, "Green Driving," [Online]. Available: https://green-driving.jrc.ec.europa.eu/.

[47] European Commission, "COMMISSION REGULATION (EU) 2017/1151 of 1 June 2017," 2017.

[48] European Commission, "The European Interoperability Centre for Electric Vehicles and Smart Grids".

[49] M. C. Galassi, K. Stutenberg, M. Otura Garcia, G. Trentadue, H. Scholz and M. Carriero, "Electric and hybrid vehicle testing: BMWi3 performance assessment in realistic use scenarios," Publications Office of the European Union, 2018.

[50] Wikipedia, "On-board diagnostics," [Online]. Available: https://en.wikipedia.org/wiki/On-board_diagnostics.

[51] T. Huybrechts, Y. Vanommeslaeghe, D. Blontrock, G. Van Barel and P. Hellinckx, "Automatic Reverse Engineering of CAN Bus Data Using Machine Learning," 2018.

[52] J. Pavlovic, A. Tansini, G. Fontaras, B. Ciuffo, M. Otura Garcia, G. Trentadue, R. Suarez Bertoa and F. Millo, "The Impact of WLTP on the Official Fuel Consumption and Electric Range of Plug-in Hybrid Electric Vehicles in Europe," 2017.

[53] G. Paganelli, T. Guerra, S. Delprat, J. Santin, M. Delhom, and E. Combes,, "Simulation and assessment of power control strategies for a parallel hybrid car," *Journal of Automobile Engineering,* vol. 214, p. 705–717, 2000.

[54] L. Rolando, ""An Innovative Methodology for the Development of HEVs Energy Management System" PhD diss., Politecnico di Torino, 2012".

[55] C. Musardo, G. Rizzoni, Y. Guezennec, and B. Staccia, "A-ECMS: An adaptive algorithm for hybrid electric vehicle energy management," *European Journal of Control,* Vols. 11, no. 4-5, pp. 509-524, 2005.

[56] B. Gu and G. Rizzoni, "An adaptive algorithm for hybrid electric vehicle energy management based on driving pattern recognition," in *ASME International Mechanical Engineering Congress and Exposition*, 2006.

[57] S. Onori, L. Serrao and G. Rizzoni, "Equivalent Consumption Minimization Strategy," in *Hybrid Electric Vehicles Energy Management Strategies*, Springer, 2015, pp. 65 - 77.

References

[58] A. Sciarretta, M. Back and L. Guzzella, "Optimal Control of Parallel Hybrid Electric Vehicles," *IEEE Transactions on Control Systems,* vol. vol. 12, no. 3, p. 352–363, 2004.

[59] Oguz H. Dagci, ""Hybrid Electric Powertrain Design and Control" PhD diss., University of Michigan, 2018," University of Michigan, 2018.

[60] L. Guzzella and A. Sciarretta, Vehicle Propulsion Systems - Introduction to Modeling and Optimization (Second edition), Springer, 2005.

[61] F. Millo, L. Rolando and M. Andreata, "Numerical Simulation for Vehicle Powertrain Development," *Numerical Analysis - Theory and Application,* 2011.

[62] G. DiPierro, F. Millo, M. Scassa and A. Perazzo, "An Integrated Methodology for 0D Map-Based Powertrain Modelling Applied to a 48 V Mild-Hybrid Diesel Passenger Car," 2018.

[63] Martin Larsson, "Electric Motors for Vehicle Propulsion," Linköpings universitet, Linköping, 2014.

[64] Kwo Young, Caisheng Wang, Le Yi Wang, and Kai Strunz, "Electric Vehicle Battery Technologies," in *Electric Vehicle Integration into Modern Power Networks*, Springer, 2012, pp. 15-56.

[65] Dr. Gregory Plett, "Lecture notes and recordings for ECE4710/5710: Modeling, Simulation, and Identification of Battery Dynamics," University of Colorado Colorado Springs.

[66] S.-H. Lee, C.-Y. Park, J.-M. Kwon and B.-H. Kwon, "Hybrid-type Full-bridge DC/DC Converter with High Efficiency," *IEEE Transactions on Power Electronics,* vol. 30, no. 8, pp. 4156-4164, 2015.

[67] G. Fontaras, M. Rexeis, P. Dilara, S. Hausberger and K. Anagnostopoulos, "The Development of a Simulation Tool for Monitoring Heavy-Duty Vehicle CO_2 Emissions and Fuel Consumption in Europe," in *SAE 11th International Conference on Engines & Vehicles*, 2013.

Appendix A

Air drag evaluation – Constant speed test execution

Vehicle 1 – Interurban bus:

During the data post-processing phase, it was found that the torquemeters fitted on Vehicle 1 had a wrong calibration; the problem was discovered after the Air Drag tool first processed the original input data returning unrealistic values for CdA (very low value) and rolling resistance (very high value). Having checked all the other possible sources of error, the conclusion was that the torquemeters measured values were affected by a problem and a solution was investigated. The torquemeters measured values were compared with the experimental torque at wheels from multiple chassis dynamometer tests; this analysis returned the following evidence: the sensors sensitivity set with the calibration must have been wrong, bringing to the overestimation of torque in the lower and underestimation in the higher end of the sensor range. The data from the most representative cycles were used to correlate the theoretical torque from the chassis dynamometer (calculated with dyno load and actual vehicle speed) with the torquemeters measurement from the same tests, with the aim of developing a correction formula for the experimental data collected during the constant speed test (which could not be repeated since the vehicle had returned to the OEM). The correlation formula, obtained through appropriate data filtering to ensure robustness, is presented in Figure 71.
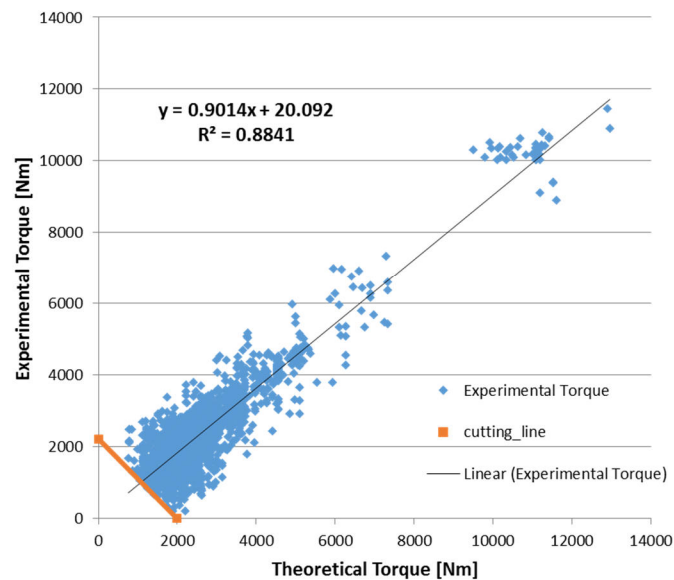

Figure 71. Interurban bus torque measurement correction

The correction formula obtained from the analysis is the following:

$$T_{corrected} = [(T_{left} + T_{right}) + q] * m$$
$$q = -20 \, [Nm]$$
$$m = \frac{1}{0.9} \, [-]$$

where $T_{corrected}$ is the total torque at wheels corrected to account for wrong the torquemeters calibration, T_{left} and T_{right} are the torque from left and right torquemeters obtained during the constant speed experiment and m and q are the correction parameters.

The formula was proved to be accurate by the VECTO simulation of the on-road tests performed in SiCO mode (power determination from torque at wheels), and Engineering mode (power determination from VECTO Air Drag road loads), which both improved the results after the correction. The approach adopted for ensuring that the robustness of the correction is presented in Figure 71.
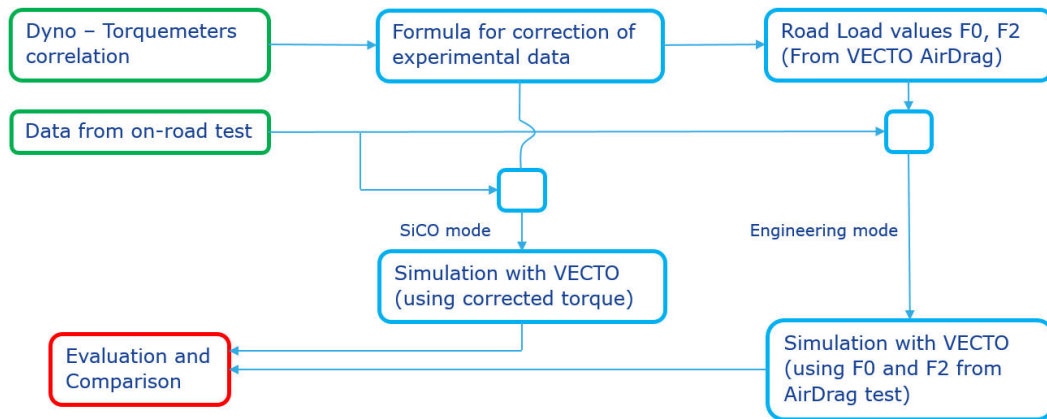

Figure 72. Approach for ensuring the robustness of torquemeters measurements correction

Vehicle 2 - Coach:

During the execution of the constant speed test for the Coach vehicle it became evident that the left torquemeter was suffering of a problem that eventually brought it to a complete mechanical failure later in the same day. Fortunately, it was possible to recover the data from the test performed in the morning, although a considerable drift in the measurement was already present. The torque measurements from the different phases of the test (warm-up, high-speed laps and low-speed sections) were averaged on the left and right wheels to understand what type of correction could be applied. The analysis showed a robust dependency of the drift from time; therefore, a linear time-based torque correction was applied considering the difference of the torquemeter reading between the two zeroing procedures. The result of the correction is presented in Figure 73, from which we see that the discrepancy between the left and right torque measurement was reduced. Additionally, weather conditions during the constant speed test were not ideal due to intermittent rain. Since this phenomenon was of light intensity, it was still possible to perform the test in proper conditions for the definition of vehicle resistance to motion and the calculation of the CdA value. Anyhow, those laps in which the rain changed the surface properties had to be discarded [40].
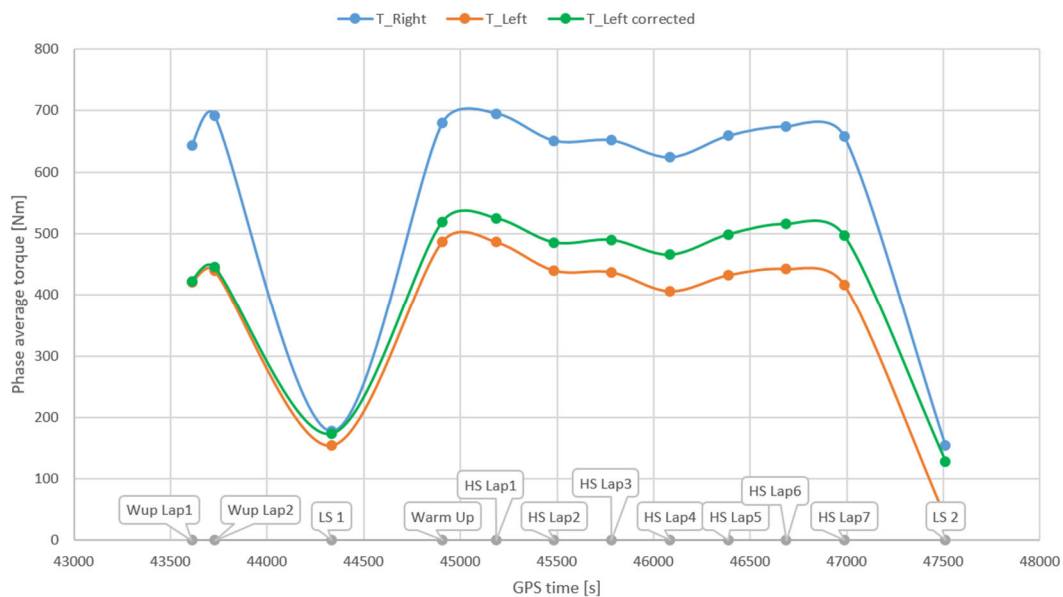

Figure 73. Coach torque measurement linear correction to account for instrument drift

Appendix B

HDV group	Traction configuration	Chassis configuration	Max. laden mass (tons)	Allocation of mission profile and vehicle configuration	
				Long haul	Regional Delivery
4	4x2	Rigid	>16	Rigid + Trailer	Rigid
5	4x2	Tractor	>16	Tractor + Semi-Trailer	Tractor + Semi-Trailer
9	6x2	Rigid	all weights	Rigid + Trailer	Rigid
10	6x2	Tractor	all weights	Tractor + Semi-Trailer	Tractor + Semi-Trailer

| Name	Unit	Description
E_roll	kWh	Energy for rolling resistance
E_air	kWh	Energy for air drag
E_brake	kWh	Energy wasted during braking
E_grad	kWh	Difference in potential energy
E_wheels	kWh	Energy at wheels
E_angle	kWh	Energy for angle drive losses
E_ds_axl	kWh	*Energy downstream the axle*
E_axl_loss	kWh	Energy for axle losses
E_us_axl	kWh	*Energy upstream the axle*
E_ret_loss	kWh	Energy for retarder losses
E_ds_gbx	kWh	*Energy downstream the gearbox*
E_gbx_loss	kWh	Energy for gearbox losses
E_clutch	kWh	Energy lost in the clutch
E_shift	kWh	Energy for gear shifts (AMT, AT)
E_tc_loss	kWh	Energy for torque converter losses
E_us_gbx	kWh	*Energy upstream the gearbox*
E_aux_sum	kWh	Sum of auxiliaries consumption
E_fcmap_neg	kWh	Energy for engine frictions
E_fcmap_pos	kWh	Positive energy produced at the engine
Declared CdA	m2	Cross-sectional area of the vehicle w/o trailer(s)
speed	km/h	Actual average vehicle speed during the cycle
Total vehicle mass	kg	Total mass of the vehicle including standard bodies
total vehicle RRC	-	Total RRC of the vehicle including standard bodies
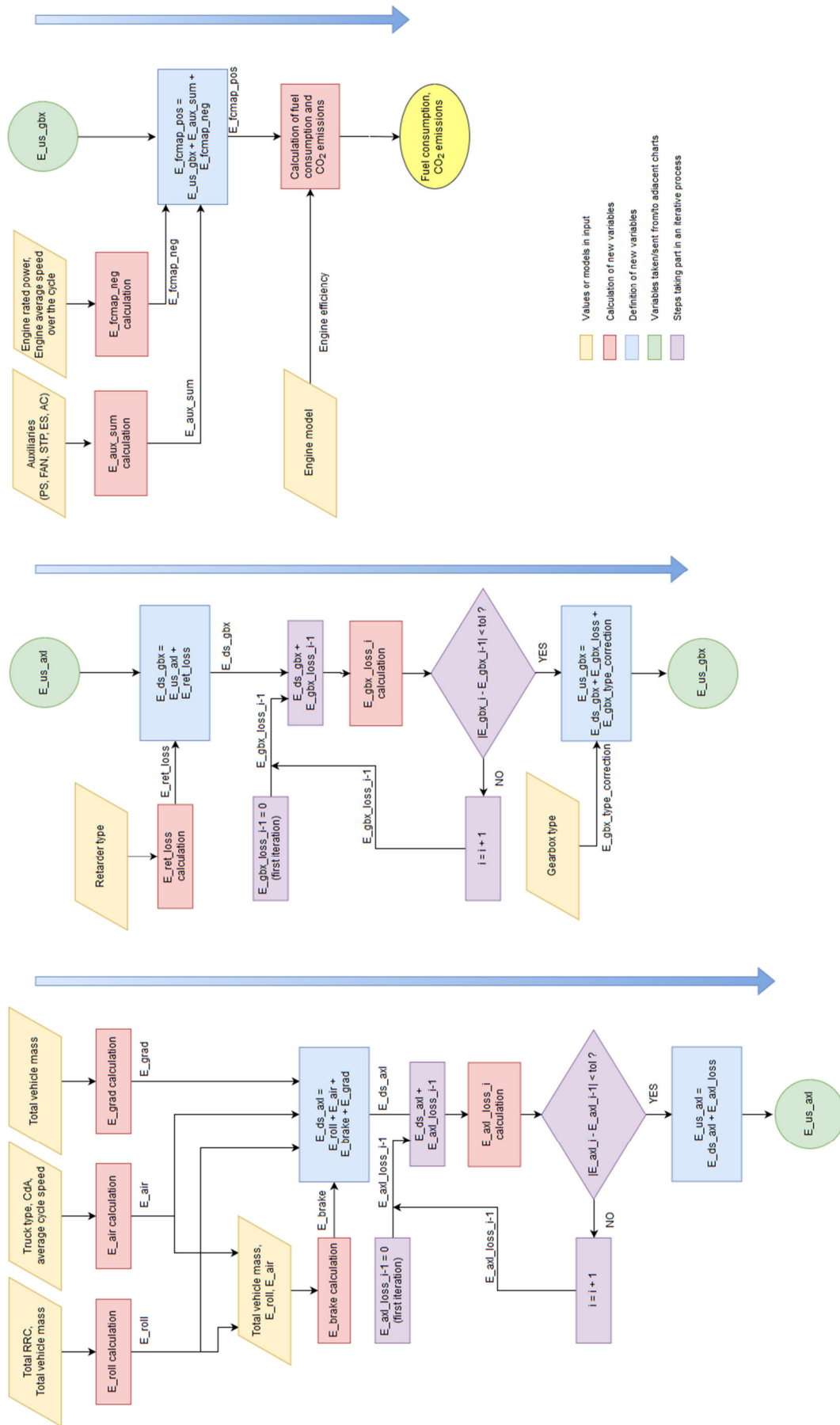
Figure 74. Workflow for the calculation of HDVs EC, FC and CO₂ emissions

Appendix C
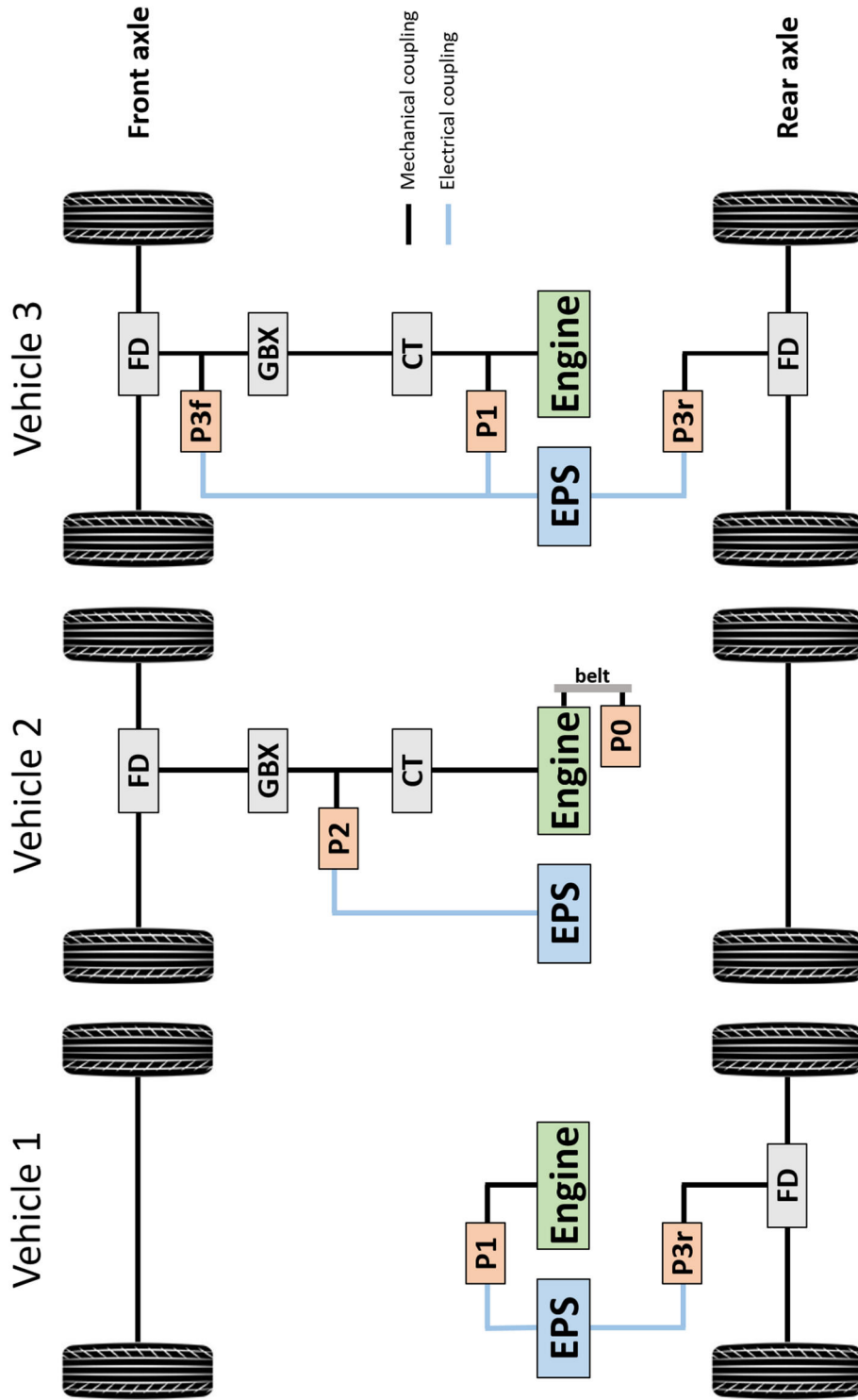

Figure 75. Driveline hybrid architectures of vehicles 1, 2 and 3
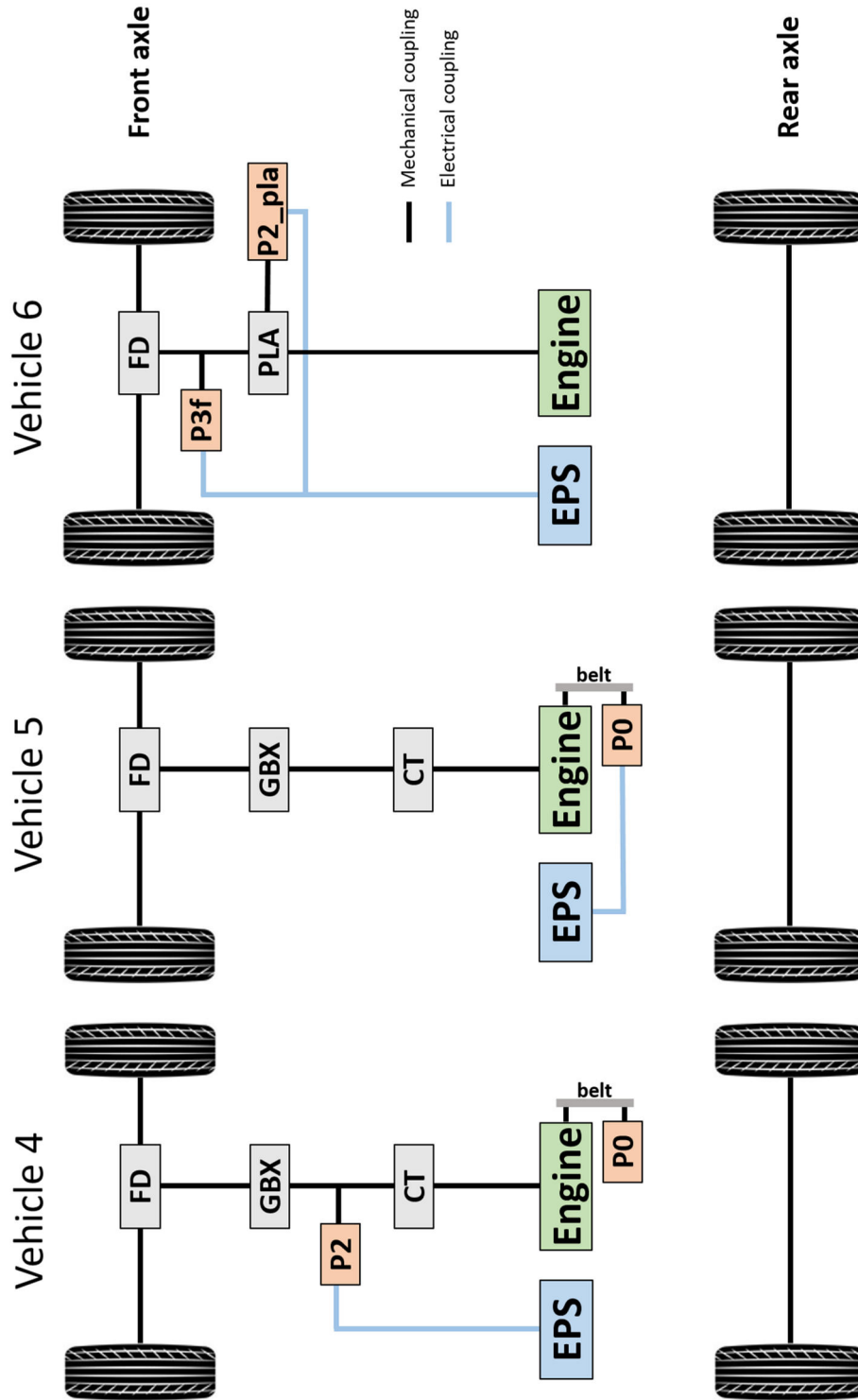
Figure 76. Driveline hybrid architectures of vehicles 4, 5 and 6

Appendix D

## ICE-off elapsed time criterion for warm-up trigger
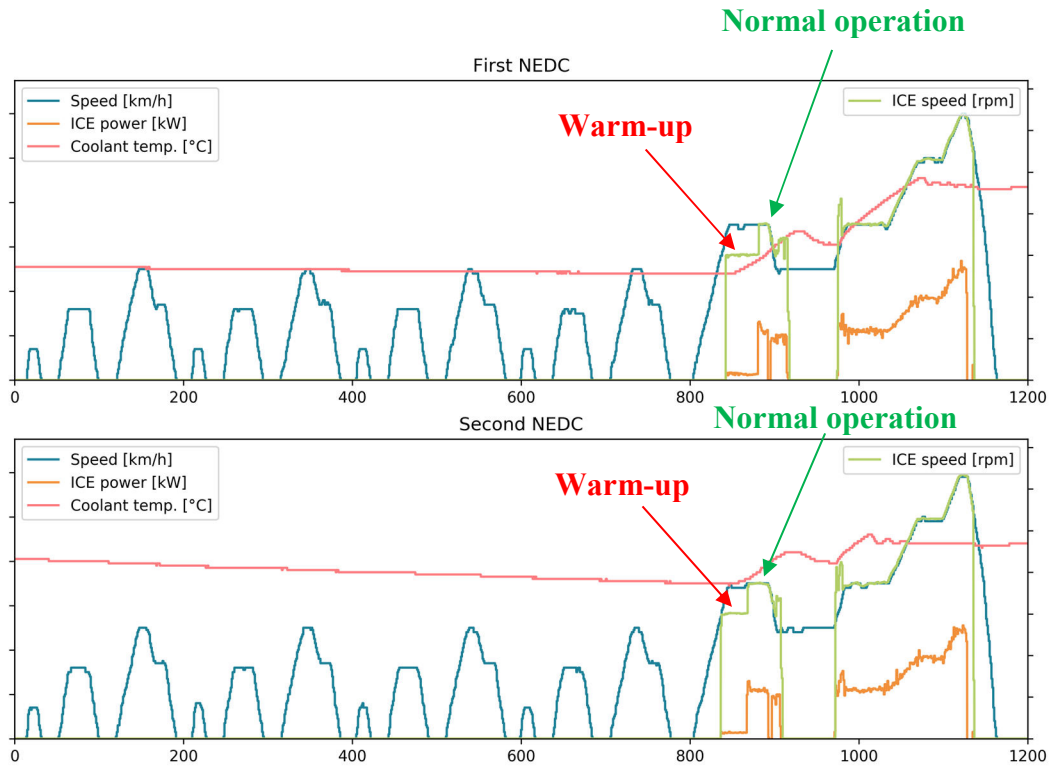
Figure 77. ICE-off elapsed time criterion for warm-up trigger

The experimental data here reported was obtained from the test campaign on vehicle 3 (plug-in). This test was specifically tailored to obtain the transition from CD to CS in a different point of the NEDC compared to that obtained following the official type-approval procedure; as a result, additional data about this behaviour was collected under different conditions. The figure shows that two warm-up procedures were triggered in two subsequent cycles. This is evident due to the lower rotational speed and power output the ICE keeps right after the activation, before switching to the normal operation that is obtained in a traditional CS test. Assuming that between the two tests a maximum of 600 seconds elapsed (10 minutes break allowed between two subsequent cycles according to the NEDC procedure), and considering that the ICE first started at second 850 in the second cycle, a period of 1000 s for the after-treatment cool-down was assumed to be reasonable.

ICE Manager logic

keep_ice_active can be obtained as follows:

> *supervisor_act* = (supervisor_state == 'CH') | (supervisor_state == 'EA')
> *warmup_act* = *warming_up*
> *limitations_act* = *vehicle_speed_ice_on* | *min_time_ice_on* | *ice_spinning_fast*
>
> *keep_ice_active* = *supervisor_act* | *warmup_act* | *limitations_act*

Battery SOC calculation and charge correction factor

For some of the vehicles, the SOC calculated with Eq.53 did not accurately replicate the SOC logged from the Battery Management System (BMS) of the vehicle. The hypothesis that the experimental current suffered of measurement bias was excluded, since the same problem is obtained using the battery current logged from the BMS. It was found that the deviations between the calculated SOC and the SOC from the BMS showed some degree of correlation with the battery operating conditions. One way to get a better matching is to use in Eq. 53 a charge correction factor (replacing η_c) that is function of the intensity of the current and possibly also the average battery temperature using lookup tables; the result obtained accordingly are presented in Figure 78 and Figure 79 for a full and a plug-in hybrid respectively. In the figures, the SOC from the BMS is compared with the Simple Coulomb Counting (SCC) method (Eq. 53 with $\eta_c = 1$) and two Improved Coulomb Counting (ICC) methods taking into consideration the battery operating conditions.
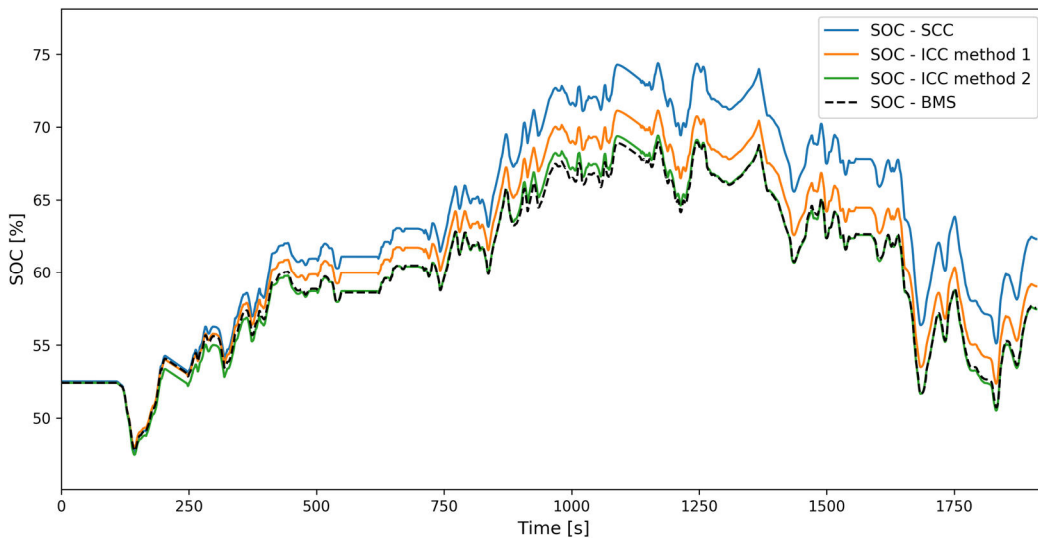

Figure 78. Full hybrid SOC comparison - BMS (black) vs Simple Coulomb Counting (blue) vs Improved Coulomb Counting method 1 (orange) and method 2 (green)
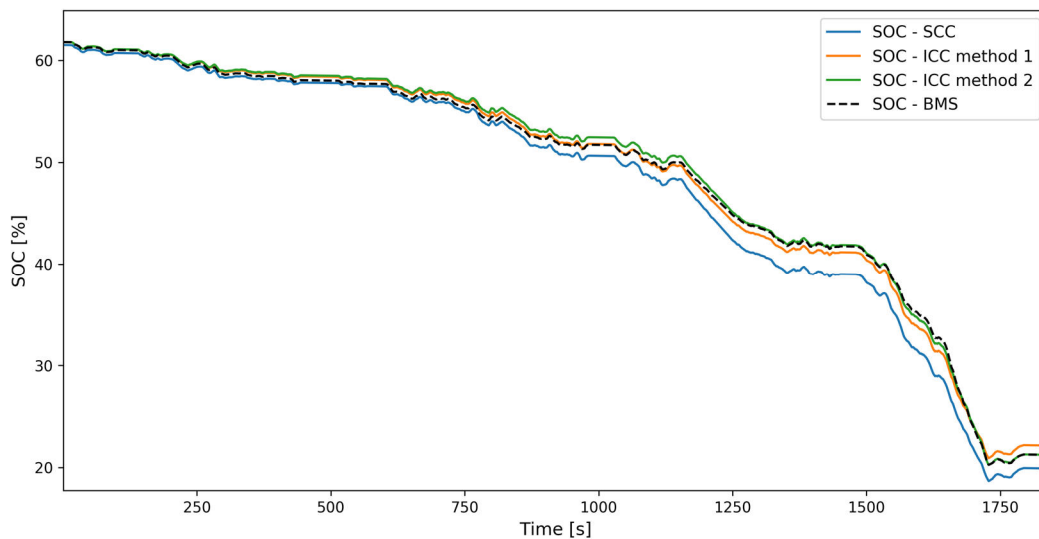
Figure 79. Plug-in hybrid SOC comparison - BMS (black) vs Simple Coulomb Counting (blue) vs Improved Coulomb Counting method 1 (orange) and method 2 (green)

ICC method 1 uses a charge correction factor that is solely function of the battery current output, whereas ICC method 2 also uses the battery average temperature.

The behaviour here analysed was only spotted on two vehicles, out of the six vehicles tested. Since these two vehicles share the same battery technology type, which differs from those of the other vehicles, it was assumed that this behaviour is limited to the specific battery technology type. The real battery capacity and the charge correction factor (either in the form of punctual factors or a lookup tables like the example above) can be derived from a rich set of experimental data providing battery current (experimental or logged), battery temperature and SOC values (logged from the vehicle).

The approach followed to produce the improved SOC estimations is under publication at the time this PhD thesis is being written. Further investigations will be carried out on this topic.